

# **Analysis of Configuration Singularities of Platform-type Robotic Manipulators**

by

**LO, Ka-Wah**

Systems Engineering and Engineering Management

Department



Submitted to the Chinese University of Hong Kong in partial  
fulfillment of the requirements for the degree of

**Master of Philosophy**

**June 1995**

Analysis of Configuration  
of Platform



TJ  
211  
L6  
1995  
wt

June 1995

# Table of Contents

<b>Acknowledgments</b>	i
<b>Abstract</b>	ii
<b>Notations</b>	iii
<b>List of Figures</b>	v
<b>List of Tables</b>	vii
<b>1. Introduction</b>	
1.1 Motivation.....	1
1.2 Literature Review .....	4
1.3 Objective.....	10
<b>2. Comparison of Different Approaches</b>	
2.1 Sample Manipulator.....	11
2.1.1 Force Decomposition Method .....	12
2.1.2 Forward Rate Kinematics Base Method .....	15
2.1.3 Grassmann Geometry Method.....	18
2.2 Comparison Criteria.....	20
2.2.1 Computational Complexity.....	20
2.2.2 Scope of Application .....	22
2.3 Summary.....	23
<b>3. Enumeration of Configuration Singularity</b>	
3.1 Novel 6 DOF.....	25
3.1.1 Result Analysis .....	31
3.2 A 3 DOF with Symmetric Base .....	33
3.2.1 Result Analysis .....	35
3.3 A 3 DOF with Non-Symmetric Base.....	36
3.3.1 Result Analysis .....	37
3.4 A New Model of 6-SPS Defined by Kong et al.....	40

3.5 A New Class of 6-SPS Platform-Type Parallel Manipulator .....	45
3.5.1 The Hexagonal Base .....	46
3.5.2 The Pentagonal Base.....	50
3.5.3 The Tetragonal Base .....	52
3.5.4 The Triangular Base .....	55
3.6 Summary.....	59
<b>4. Numerical Analysis</b>	
4.1 Parameter Analysis .....	60
4.1.1 One Unknown Variable .....	61
4.1.2 Two Unknown Variables.....	63
4.2 Critical Value of Ratio $R/q$ .....	69
4.3 Summary.....	72
<b>5. Conclusions and Future Work</b>	
5.1 Conclusions .....	73
5.2 Future Work.....	75
<b>References.....</b>	<b>76</b>
<b>Appendix.....</b>	<b>82</b>



# Acknowledgments

I would like to express my sincere gratitude to Dr. X. Shi, the thesis supervisor, for his dedicated supervision and continuous encouragement and assistance throughout the course of this project.

I would also like to thank all the technical staff of Hong Kong Polytechnic Industrial Center ( CNC Machine Shop ), for their assistance in making the mechanical model of a Stewart Platform.

Special thanks also go to the department office of Systems Engineering and Engineering Management and the technical team of the department. They always provided full support whenever I needed during my two years' study in the department.

# Abstract

The configuration singularity of a robotic manipulator will result in an unstable and non-rigid state which will in turn affect its accuracy and performance. There are several algorithms which are reasonably accurate and reliable for enumeration of configuration singularity for serial type robotic manipulators. However, only a few methods are available to identify the configuration singularity of parallel type robotic manipulators .

In this thesis, we compared three existing approaches, namely the Force Decomposition method, the Forward Rate Kinematics based method and the Grassmann Geometry method, for singularity analysis of parallel manipulators. We found that the Forward Rate Kinematics based method is the most efficient and simplest in terms of computational complexity. We applied this method to find the general expression of the configuration singularity for two classes of manipulators: Novel 6 DOF platform-type parallel manipulators and 3 Degree of Freedom (DOF) platform-type parallel manipulators with symmetric and non-symmetric bases. Moreover, this method was used to identify the configuration singularity of the class of 6-SPS platform-type parallel manipulators.

By examining the general expressions for the above cases, we found that the ratio of the radius of the base platform to the length of the sub-chain is a major factor affecting the existence of the configuration singularity. We suggested a method to determine the critical value of the ratio for platform-type parallel manipulators with symmetric base. This ratio provides a useful guideline for improving the design of the platform-type parallel manipulators.

# Notations

$\Phi_i$	Rotation Angle between the Local Coordinates and the Base Coordinate System
$\theta_{12}$	Active Joint Parameters, Specifying the Elbow Joint Angle between the Two Lengths $L_1$ & $L_2$ in a Novel 6 DOF Manipulator
$\theta_{i1}$	Passive Joint Parameters, Specifying the Angle between the Length $L_1$ & the Base Platform in a Novel 6 DOF Manipulator
$B_i$	Points Lie on the Base Platform
$B'_i$	Points Lie on the Base Platform
$P_i$	Points Lie on the Moving Platform
$P'_i$	Points Lie on the Moving Platform
$K_{ij}$	Coefficient of $\dot{\alpha}$ or $\dot{\beta}$ or $\dot{\theta}$
$d_i$	Side of the Base Platform
$q_i$	Active Joint Parameters
$q'_i$	Active Joint Parameters
$\alpha_i$	Passive Joint Parameters
$\alpha'_i$	Passive Joint Parameters
$\beta_i$	Passive Joint Parameters
$\beta'_i$	Passive Joint Parameters
$P_i$	Moving Platform Points Vector
$V_{pi}$	Moving Platform Points Velocities Vector
$V_o$	Linear Velocity of the End Effector
$\omega_o$	Angular Velocity of the End Effector
$M$	Vector Relating to the Three Points Position on the Moving Platform
$C$	Vector Relating to the Three Points Velocities on the Moving Platform
$J_{sj}^{ee}$	6x6 Matrix Relating Spherical Joint Forces to End-Effector Forces
$J_{act}^{sj}$	6x6 Matrix Relating Actuated Joint Torques to Spherical Joint Forces.
$\tau_{act}$	Vector of Actuated Joint Torques



$\hat{f}_{uli}$	Unit Vectors Along the Upper Link Axis and Elbow Axis
$\hat{f}_{ei}$	Unit Vectors Along the Upper Link Axis and Elbow Axis
$P_{ti}$	Point from the Center of the Top Plate to the Spherical Joint
	Connection point on the top plate
$f_{uli}$	Force Along the $i$ th Upper Link Axis
$f_{ei}$	Force Parallel to the $i$ th Elbow Axis
$R_{bi}$	Rotation Angle between the Local Coordinate & the Base Coordinate System
$R$	Radius of the Base Platform
$[T]$	Transformation Matrix
$[R_b^e]$	Rotation Matrix
$[P_b^e]$	Translation Vector
$[N]$	6 Dimensional Vector
$[K]$	3x3 Matrix for a Platform type Manipulator with Three Passive Joint Parameters.
$[J]$	Jacobian Matrix of the Manipulator

# List of Figures

- 1.1 A Manipulator in Architecture Singularity
- 1.2 Side Force Applied to a Manipulator in Architecture Singularity
- 1.3 A Manipulator in Configuration Singularity
- 2.1 Typical Structure of Novel 6 DOF Manipulator
- 2.2 Force and Torque Components
- 2.3 Geometry of the Novel 6 DOF Parallel Manipulator
- 2.4 A Singular Configuration of Novel 6 DOF Identified by Grassmann Geometry Method
- 3.1 Geometry of the Novel 6 DOF Platform-type Parallel Manipulator
- 3.2 Configuration Singularity of Novel 6-DOF Parallel Manipulator Identified by Equation (3.19)
- 3.3 Geometry of the 3 DOF Platform-type Parallel Manipulator
- 3.4 Configuration Singularity of 3 DOF Parallel Manipulator with Symmetric Base Identified by Equation (3.25)
- 3.5 Configuration Singularity of 3 DOF Parallel Manipulator with Non-Symmetric Base Identified by Equation (3.28)
- 3.6 Configuration Singularity of 3 DOF Parallel Manipulator with Non-Symmetric Base Identified by Equation (3.31)
- 3.7 A New Model of 6 SPS Defined by Kong et. al.
- 3.8 The Geometry of a New Model of 6 SPS Defined by Kong et. al.
- 3.9 The Geometry of the Base Platform of a New Model Defined by Kong et. al.
- 3.10 Configuration Singularity of the New Model Platform-type Parallel Manipulator Defined by Kong et. al. Identified by Equation (3.39)
- 3.11 The Geometry of the Class of 6 SPS Platform-type Parallel Manipulator with Hexagonal Base
- 3.12 The Geometry of the Hexagonal Base Platform



- 3.13 Configuration Singularity of Class 6 SPS Parallel Manipulator with Hexagonal Base Platform Identified by Equation (3.41)
- 3.14 The Geometry of the Pentagonal Base Platform
- 3.15 Configuration Singularity of Class 6 SPS Parallel Manipulator with Pentagonal Base Platform Identified by Equation (3.43)
- 3.16 The Geometry of the Tetragonal Base Platform
- 3.17 Configuration Singularity of Class 6 SPS Parallel Manipulator with Tetragonal Base Platform Identified by Equation (3.45)
- 3.18 The Geometry of the Triangular Base Platform
- 3.19 Configuration Singularity of Class 6 SPS Parallel Manipulator with Triangular Base Platform Identified by Equation (3.47)
- 4.1 - 4.16 Parameter Characteristics Curves

- 2.1 Comparison of Three Methods
- 4.1 The Reduced Singular Conditions of Five Sample Cases
- 4.2 Ratio  $R/q$  for Different Class of Platform-type Parallel Manipulators
- 4.3 Critical Values of Ratio  $R/q$  for the Class of 6 SPS Parallel Manipulators with Hexagonal Base Platform
- 4.4 Critical Value of Different Class of Platform-type Parallel Manipulator

# Chapter 1

## Introduction

In this chapter, we give a brief introduction to the parallel manipulator, singular configuration of the manipulator and its classification. Section two is the literature review. The objective of this thesis is presented at the end of this chapter.

### 1.1 Motivation

Typical serial type robots have traditionally been used as general-purpose positioning devices and are anthropomorphic open chain mechanisms which generally have the links actuated in series. The open chain manipulators usually have longer reach, larger workspace and more dexterous maneuverability. However, the cantilevered structure of the open chain mechanism is a serious disadvantage because of its low rigidity. In addition, each successive link and motor from the end-effector towards the base has to be large enough to support the weight of the preceding links and motors and to provide the required endpoint stiffness. This increases the mass and the size of the actuators and thus affects the dynamic performance of the robot, especially when it is used for high-speed or large-load operations. Furthermore, the actuator errors accumulate along the open chain mechanism and result in a large error at the endpoint of the robot. Therefore, serial type robot arms are not ideal for high-speed or high-precision operations.

On the other hand, platform-type parallel manipulator are structurally more rigid and capable of distributing the loads throughout the system. It is because all of the actuators can be fixed to the base and the moving parts are lighter than that of serial type. This advantage, together with the significantly improved endpoint stiffness due to the truss-like structure of the parallel manipulator, results in high



positioning accuracy and good dynamic performance. Therefore, parallel manipulators become ideal devices for applications that require high positional accuracy within a limited workspace. Recently, some effort has been directed towards the investigation of parallel manipulator such as the Stewart Platform [ST66] based closed kinematic chains.

When the manipulator is in a singular configuration, it will not be in a stable and rigid state which will in turn affect the accuracy and performance. Therefore determination of the singularity conditions for the manipulator is one of the most important problems in robot kinematics. For platform-type parallel manipulators, singularities can be classified into three categories. They are Architecture, Configuration and Formulation Singularities [MA91] respectively.

The architecture singularity usually spans over the whole workspace. The manipulator fails to balance the load on its moving plate and causes instabilities which leads to a very poor motion and force-transmission performance. Figure 1.1 shows that even all the extensible links are being locked in a fixed length, but the manipulator is still fail to balance the load on its moving plate. This indicates that the manipulator will not be able to withstand a small force in a direction of the arrow illustrated in Figure 1.2. It is very difficult to implement the control or singularity-avoidance strategies on the architecture singularity which can only be avoided by redesigning the mechanism of the manipulator.



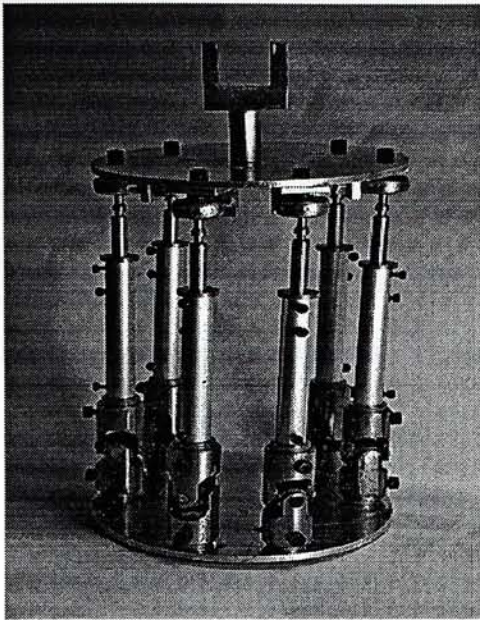


Figure 1.1 A Manipulator in Architecture Singularity

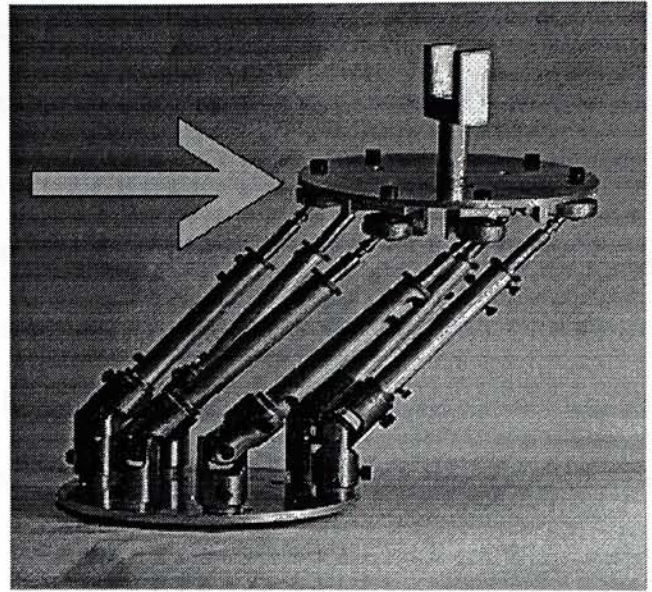


Figure 1.2 Side Force Applied to a Manipulator in Architecture Singularity

The configuration singularity is different from the architecture singularity. It is caused by a particular configuration of a manipulator during motion. This singularity is discrete and only depends on individual configurations. It directly affects motion planning and the control of manipulator during motion. An example is shown in Figure 1.3. Suitable algorithms to investigate the configuration singularity will be discussed in this thesis.

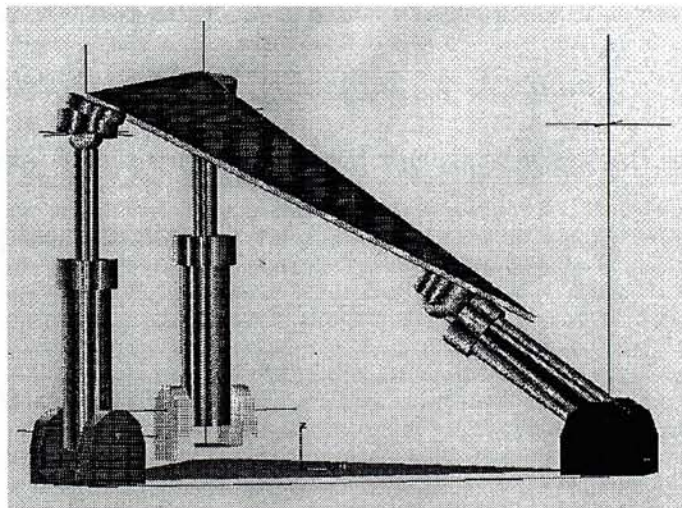


Figure 1.3 A Manipulator in Configuration Singularity

Formulation singularity is normally caused by the incorrect assumptions or failure of a kinematic model at a particular configuration of a manipulator [MA91].



Basically, the architecture singularity is the problem related to the design of robot and the formulation singularity is due to assumption errors in solving the kinematic model. Both of them can be avoided by carefully designing the robot. Unlike the above two singularities, it is not that straightforward in dealing with the configuration singularity. This type of singularity can only be detected through a detail study of a robot in motion. Therefore, the determination of the configuration singularity is important for the design of robotic manipulators, and is the main motive for this research work.

This thesis is divided into 5 chapters. In Chapter 1, the background and the objective of this thesis are given. In Chapter 2, we will discuss and compare three different approaches for identifying the configuration singularity in parallel manipulator and select the most appropriate one to be used in the following chapters. In Chapter 3, we identify and formulate the general expression of the configuration singularity for three classes of platform-type parallel manipulators. We also find a ratio which is a major factor affecting the existence of the configuration singularity. In Chapter 4, we further analyze the effect of the ratio to the existence of the configuration singularity and suggest a method to determine the critical value of the ratio. This ratio provides a useful guideline for designing improved platform-type parallel manipulators. The conclusions and the recommendation for future work are given in the last chapter, Chapter 5.

## **1.2 Literature Review**

In serial manipulators, the inverse kinematics is a central problem in robot control which has received a lot of attentions [AA79, DC80, LL88, PR86, RR73, RR89]. The first systematic study on the inverse kinematics problem was done by [PI68]. The work on the general solution of the problem for 6R manipulator includes

[DC80, RR73]. Tsai and Morgan [TM85] used a higher dimensional approach to the inverse kinematics problem. They also concluded that 16 is an upper bound on the number of the solutions. Raghavan and Roth [RR86] was the first to use the formulation introduced in [DC80] to prove that the problem of inverse kinematics has a maximum of 16 solutions. Lee and Liang [LL88] gave the exact solution in lower dimension by reducing the problem to a 16 degree polynomial. Raghavan and Roth [RR89] used elimination method to derive a 16 degree polynomial. Manseur and Doty [MD89] presented an example consisting of a manipulator and a pose (position and orientation) of the end-effector and it was found that the inverse kinematics problem has 16 real solutions and thereby, he established the fact that 16 is a tight bound on the number of solutions. Wanpler and Morgan et al. [TM85, WM91] presented that only continuation methods were able to solve the problem of different cases. According to Wanpler and Morgan [WM91], lower dimensional methods like the one in Raghavan and Roth [RR89] were impractical due to numerical problems. However, Manocha and Canny [MC92] presented an algorithm based on the results in Raghavan and Roth [RR89] for real time inverse kinematics solution for a general 6R manipulator. Fast algorithms of computing eigenvalues and eigenvectors of a matrix are available in [AU90, GU89].

These methods can be summarized as three different approaches in the inverse kinematics of serial manipulators. First, the algebraic formulations given in [DC80, LL88, PR86, RR89, RR90] can be used along with algorithms for finding roots of high degree polynomial. However, this approach is quite slow in practice (due to symbolic expansion) and suffers from numerical problems in the context of floating point arithmetic. This is mainly due to the fact that the problem of computing roots of high degree polynomials can be numerically ill-conditioned [WI59]. Moreover, the formulations in [LL88, RR89, RR90] are for generic manipulators and cannot be applied to manipulators with special geometries.



The second approach is based on homotopy method and used to solve a system of polynomial equations [TM85, WM91]. The third approach is based on linear algebra formulation of the problem [MC92]. In particular, the algebraic formulation, given in Raghavan and Roth [RR89], is used along with matrix computation. As opposed to deriving a high degree polynomial, the problem of inverse kinematics is reduced to computing the eigendecomposition of a numeric matrix. It has been applied to general 6R manipulator in Manocha and Canny [MC92] and involves symbolic preprocessing, numeric substitution and matrix computations.

As for platform-type parallel manipulators, progress has been reported in the literature on kinematics, dynamics as well as control strategies [BE88, FI86, HU78, HU83, ME90, SU89, WN89, YL87]. Hunt [HU78] suggested that the manipulation capability of parallel mechanism be utilized in robots and he [HU83] later listed a number of possible structures of parallel mechanisms suitable for robotic applications. Yang and Lee [YL87] discussed the feasibility of applying such a mechanical device in order to obtain close form solution in robotics.

The forward kinematics of platform-type parallel manipulator is to find the pose of the moving platform by given a set of link lengths. The first platform-type parallel manipulator was designed as an aircraft simulator and is usually called the " Stewart Platform " [ST66] ( Two bodies connected by 6 links with a variable length. In fact it was first proposed by Gough as stated in Stewart's paper ). Fichter [FI86] performed a detailed theoretical and experimental investigation of a Stewart Platform type manipulator. Stewart Platform with triangular moving platform has been studied and it is found out that the problem has at most 16 solutions [ME89], as its forward kinematics can be reduced to a sixteen th order polynomial [CD88]. If the articulation points have different location, there will be at most 40 solutions when either the base or the moving platform is planar [LA92] and this is also true for most parallel manipulators [LA93, RV92].

On the other hand, determination of singularity condition for serial manipulators has long been a topic for researchers in robotics, and a large number of publications related to this problem can be found in the literature [AL88, FS90, HU83, GO81, PA81, PS83, SD82, WH88]. Moreover, the kinematic and static performances of manipulators had been shown to be directly affected by the numerical conditioning of the corresponding Jacobian matrices [PS83]. Yoshikawa [YO85] proposed the concept of manipulability that can be applied to both redundant and non-redundant manipulators. Klein and Blaho [KB87] proposed the minimum singular value of Jacobian as a measure of distance to a singular configuration of the manipulator. Wenger et al. [BM84, WE84] proposed the adoption of closed-loop inverse kinematic schemes based on the use of the Jacobian transpose instead of the Jacobian inverse. The Jacobian transpose approach has been developed by Chiacchio and Siciliano [CS88] to improve the performance close to singular configuration. Wampler [WA86] used damped least-squares methods to obtain a modified Jacobian that is nonsingular in the whole workspace, and an approximate inverse kinematic solution was found. Whitney [WH72] proposed to use nonsingular blocks of the Jacobian matrix to calculate an approximate solution at singular configurations.

Burdick [BU91] investigated the singularities of 3R regional manipulators. Pai and Leu [PL89] introduced the notion of generic manipulator singularities. Application of damped least-squares solutions [LH74] to robot control, which can be easily formulated by using Singular Value Decomposition (SVD), has been proposed as one of the most efficient ways of robot motion synthesis near singularities [NH86]. Maciejewski and Klein [MK89] presented that the numerical complexity was reduced by about 5-6 times by applying his proposed method. Klein and Blaho [KB92] presented that the numerical complexity was reduced by about 10 times by deriving symbolic expressions through SVD with the result of two 3x3 Jacobian submatrices of 6 DOF robot of the PUMA configuration with no shoulder offset. The problem of position error created by the damped least-squares solution had been considered in



[NH86]. Pai and Leu [PL91] presented that the generalized coordinates of the robot were discretized just like that in a finite-element method and a unique solution was gained on the basis of a 2nd order Taylor-series expansion of the co-ordinate differences near singularities. He also considered the complex expansion of the joint co-ordinates of the robot near the boundaries of the work-space of the arm.

For platform-type parallel manipulators, Ma and Angeles [MA91] classified singularities into three categories, namely, the Architecture, Configuration and Formulation singularities. They also discussed the details of architecture singularity of a 6 DOF parallel manipulator. Gorla [GO81], by applying the above method, derived singularity conditions for manipulators with relatively simple geometries. Merlet [ME89] proposed a new method based on Grassmann Line Geometry. It can be performed on a special parallel manipulator. Special configurations fall into two categories : uncertainty configurations and stationary configurations [LD85]. Sugimoto and Duffy [SD82] presented a detailed analysis of singularities (uncertainty configurations) of all single-loop mechanisms using the reciprocal screw concept. Hunt [HU83], applying the principle of reciprocity of screws, pointed out that a parallel manipulator gains, rather than loses, one or more degree of freedom in singular configurations. Waldron [WH88] further analyzed such properties of dualities between serial and parallel manipulators. Ahmad and Luo [AL88] analyzed the singularity states of manipulators using the inverse kinematic relationships. Fichter [FI86] determined a few singular configurations for a 6 DOF parallel manipulator through experiments. Litvin and Tan [LT89], based on certain parameters of motion, proposed a general approach for the determination of singularities in motion and displacement functions of manipulators and linkages.

The most straightforward method for singularity determination is to equate the  $6 \times 6$  determinant of the Jacobian matrix to zero [PA81]. The analysis was done by expressing the Jacobian in end-effector space using vector quantities [WH72].



Previous algorithms for analyzing singular configurations were usually derived from Jacobian which was based on the joint space relationship (i.e., describing singularity conditions in terms of joint angles) [LC86, SD88]. Lipkin and Pohl [LP88] presented a method for enumerating all singular configurations for a given manipulator by using vector quantities to express the Jacobian in end-effector space. Cleary and Uebel [CU94] proposed a force decomposition approach to compute the Jacobian matrix for a Novel 6 DOF parallel manipulator. By using a Cartesian vector approach, a great deal of insight into the singularity problem was gained, and therefore it was possible to further identify degeneracies of the primary singular configurations. Additionally, the concepts of active and passive joints were elaborated by Hunt [HU85], and a theorem regarding the relationship between invariant screw systems and passive joints was similarly expanded. Fenton and Shi [FS92a] presented a method for identifying singular configuration causing instabilities in a platform-type parallel manipulator. This method was based on the forward instantaneous kinematic formulation and the principle of reciprocity of screws.

It should be noted that broad knowledge of kinematic and singularity condition is important in manipulator design, analysis, trajectory planning, and control. Furthermore, when determining the kinematics and singularity condition for serial type manipulators in robotics, there exist several algorithms which are reasonably accurate and reliable. On the contrary, only a few algorithms available for dealing with the problem of kinematics as well as singularity condition of parallel type robotic manipulators. Therefore, a general and robust method to enumerate the configuration singularities of platform-type parallel manipulator is required and the development of such an algorithm becomes the primary objective of this research.

### **1.3 Objective**

The objectives of my study are as follows:

- 1) To compare existing methods for singularity analysis of parallel manipulators and to find out the effective method based on certain criteria ;
- 2) To apply this method to identify the configuration singularity and formulate its general expression for a number of cases which are of significance in application but have not been studied before ;
- 3) To analyze the above results and find out the major factors causing the configuration singularity.
- 4) To analyze the relationship between the factors and the existence of the configuration singularity and to establish a guideline for avoiding configuration singularity in the design stage.

## Chapter 2

### Comparison of Different Approaches

As stated in Chapter 1, the problem of identifying the configuration singularity of 6 DOF platform-type parallel manipulator with prismatic joints had been studied in depth by various researchers [FS92a, MA91, ME89, MM92]. However, the same problem in the platform-type parallel manipulator with elbow joints has not been explored. In view of the potential applications of this type of manipulator [CU94] and the importance of the singularity problem, we concentrate on selecting a suitable method to identify the problem on the 6 DOF platform-type parallel manipulator with elbow joints.

In this chapter, we first describe three methods for singularity analysis, namely: (1) the Force Decomposition method, (2) the Forward Rate Kinematics Based method, and (3) the Grassmann Geometry method. These three methods tackle the problem from different basis. The first method is derived from the Dynamics of a robot; the second from Kinematics; and the last from Geometry. We use the sample manipulator (Novel 6 DOF platform-type parallel manipulator) as the basis for the comparison of these three methods according to two selected criteria : Computational Complexity and Scope of Application.

#### 2.1 Sample Manipulator

In the following subsections, we will use a Novel 6 DOF platform-type parallel manipulator (Figure 2.1) to explain the three methods for identifying the configuration singularity. The sample manipulator consists of a base plate, a top plate and three connection legs. Each leg has a lower and an upper link which are connected by an elbow joint.



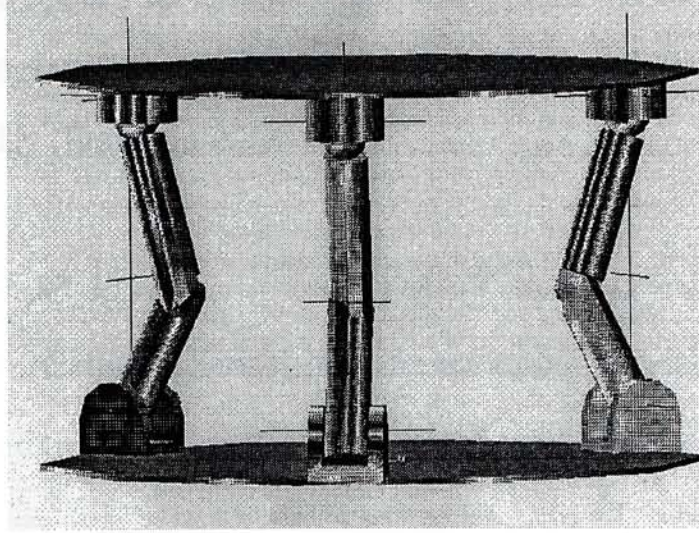


Figure 2.1 Typical Structure of Novel 6 DOF Manipulator

### 2.1.1 Force Decomposition Method

In general, for a parallel manipulator, the inverse kinematics usually has a closed form solution. To ensure a closed form solution for our sample case, inverse kinematics has been used, as shown Equation 2.1.

$$F_{ee} = J_p^T \tau_{act} \quad (2.1)$$

where  $F_{ee}$  is a 6-vector matrix of end-effector forces (forces and torques)

$$F_{ee} = [ f_x, f_y, f_z, m_x, m_y, m_z ]^T$$

$J_p^T$  is a 6x6 matrix with non-linear expressions as its elements,

and  $\tau_{act}$  is a 6-vector matrix of actuated joint torques

$$\tau_{act} = [ \tau_{pitch1}, \tau_{roll1}, \tau_{pitch2}, \tau_{roll2}, \tau_{pitch3}, \tau_{roll3} ]$$

The Jacobian,  $J_p^T$ , relates the joint torques to the end-effector forces. Since it consists of non-linear expressions, the computation is complex and the roots are hard to find. According to Cleary, K. et al. [CU94], a Jacobian can be formulated and calculated using Force Decomposition approach. Since an elbow joint is a passive joint, the spherical joint connected to it can support neither moments nor a force perpendicular to the elbow axis and the upper link axis. Due to this, the force of the





Similarly, the actuated joint torques are mapped to the spherical joint forces by:

$$F_{sj} = J_{act}^{sj} \tau_{act} \quad (2.4)$$

In the derivation of the Jacobian,  $J_{act}^{sj}$ , the legs are assumed to be independent and they can be treated separately. As shown in Figure 2.2, the actuated joint on each leg consists of pitch and roll axes. The pitch axis is tangential to the base circle, and the roll axis is collinear with the lower link axis. As a result, the roll joint torque and the pitch joint torque can be further derived to produce Equations (2.5) and (2.6) respectively.

$$\tau_{rolli} = L_2 \text{Sin}\theta_{3i} f_{ei} \quad (2.5)$$

$$\tau_{pitchi} = L_1 \text{Cos}\theta_{2i} \text{Sin}\theta_{3i} f_{uli} - \text{Sin}\theta_{2i} (L_1 + L_2 \text{Cos}\theta_{3i}) f_{ei} \quad (2.6)$$

for  $i=1$  to 3

where  $L_1$  is the length of the lower link and  $L_2$  is the length of the upper link

Let us rewrite Equation (2.5) and (2.6) in a matrix form:

$$\begin{bmatrix} \tau_{pitchi} \\ \tau_{rolli} \end{bmatrix} = \begin{bmatrix} L_1 \text{Cos}\theta_{2i} \text{Sin}\theta_{3i} & -\text{Sin}\theta_{2i} (L_1 + L_2 \text{Cos}\theta_{3i}) \\ 0 & L_2 \text{Sin}\theta_{3i} \end{bmatrix} \begin{bmatrix} f_{uli} \\ f_{ei} \end{bmatrix} \quad (2.7)$$

or simply as:

$$\tau_{acti} = \left[ J_{sj}^{act} \right]_i F_{sji}$$

The combined matrix,  $J_{act}^{sj}$ , formed by  $\left[ J_{sj}^{act} \right]_i^T$  (for  $i=1$  to 3), is a 6x6 block diagonal matrix where each  $\left[ J_{sj}^{act} \right]_i$  is a 2x2 matrix with one zero element.



$$F_{sj} = \begin{bmatrix} [J_{act}^{sj}]_1 & 0 & 0 \\ 0 & [J_{act}^{sj}]_2 & 0 \\ 0 & 0 & [J_{act}^{sj}]_3 \end{bmatrix} \tau_{act}$$

The configuration singularity can be identified when the determinant of Jacobian is equal to zero. That is, if either the determinant of  $J_{sj}^{ee}$  or  $J_{act}^{sj}$  is equal to zero, the determinant of non-linear Jacobian is also zero. As a result, the singularity is identified. The determinant of Jacobian  $J_{act}^{sj}$  is zero only when  $\theta_{2i}$  takes the value of  $90^\circ$  or  $\theta_{3i}$  takes the value of  $0^\circ$  or  $180^\circ$ . But both cases are very unlikely. Therefore, the zero value usually comes from the determinant of Jacobian  $J_{sj}^{ee}$ .

### 2.1.2 Forward Rate Kinematics Based Method

The forward instantaneous kinematics of a platform-type parallel manipulator is defined as: " *given the velocity vector of the active joints in joint space and the geometric configuration of the manipulator, determine the corresponding generalized velocity of the end effector in task space* " [FS92a]. This approach uses the velocities of three non-collinear points which attached to the end-effector to define the velocity of the end-effector.

Referring to the sample manipulator described in the last section, the three non-collinear points are  $P_i$  (for  $i=1$  to 3) (Figure 2.3). Each leg has a lower link and a upper link, with link lengths  $L_1$  and  $L_2$  respectively.  $\theta_{i2}$  is the active joint parameter while  $\theta_{i1}$  the passive joint parameter.  $R_b$  is the radius of the base platform.  $R_{bi}$  is the rotation angle between the local coordinates and the base coordinate system.

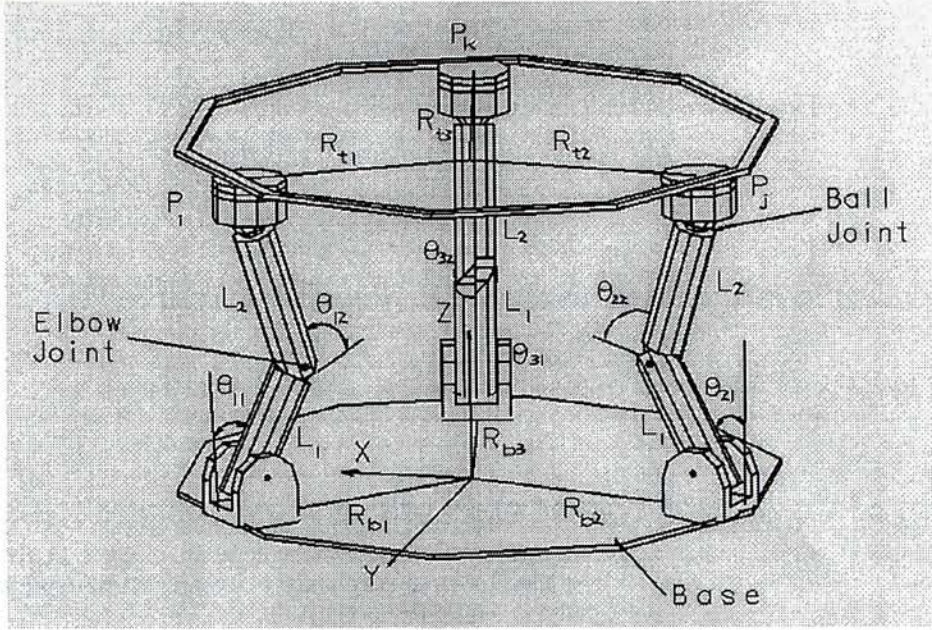


Figure 2.3 Geometry of the Novel 6 DOF Parallel Manipulator

According to the definition, with all the active joint velocities and geometrical configuration given, the coordinates of the three non-collinear points  $P_i$  (for  $i=1$  to 3) with respect to the base reference frame can be represented by point vectors:

$$P_i = B_i + w_i L_1 + w'_i L_2$$

where  $B_i$  is a constant vector fixed to the base platform and  $w_i$  and  $w'_i$  are the unit vectors representing the orientation of  $L_1$  and  $L_2$ .

$P_i$  can be rewritten in details as:

$$p_i = \begin{bmatrix} R_b \cos R_{bi} + L_1 \cos \theta_{i1} \cos R_{bi} + L_2 \cos \theta_{i2} \cos R_{bi} \\ R_b \sin R_{bi} + L_1 \cos \theta_{i1} \sin R_{bi} + L_2 \cos \theta_{i2} \sin R_{bi} \\ L_1 \sin \theta_{i1} + L_2 \sin \theta_{i2} \end{bmatrix} \quad (2.8)$$

By taking the derivative of Equation (2.8), the velocities of the three non-collinear points in the matrix form are:



$$v_{pi} = \begin{bmatrix} -L_1 \dot{\theta}_{i1} \sin \theta_{i1} \cos R_{bi} - L_2 \dot{\theta}_{i2} \sin \theta_{i2} \cos R_{bi} \\ -L_1 \dot{\theta}_{i1} \sin \theta_{i1} \sin R_{bi} - L_2 \dot{\theta}_{i2} \sin \theta_{i2} \sin R_{bi} \\ L_1 \dot{\theta}_{i1} \cos \theta_{i1} + L_2 \dot{\theta}_{i2} \cos \theta_{i2} \end{bmatrix} \quad (2.9)$$

The linear velocity of the end-effector,  $V_0$ , is given by the mean of these velocities:

$$V_0 = \frac{1}{3} \sum_{i=1}^3 V_{pi}$$

The three point velocities,  $V_{pi}$ , can also be expressed in terms of the linear velocity,  $V_0$ , and the angular velocity,  $\omega$ , of the end-effector:

$$V_{pi} = [R_b^e] [\omega] A_i + V_0 \quad (2.10)$$

where  $[R_b^e]$  is a 3x3 rotation matrix and  $A_i$  is a constant vector

The linear velocity  $V_0$  and the angular velocity  $\omega$  of the end-effector are in terms of the three unknown passive joints rate  $\dot{\theta}_{i1}$ . As stated in the principle of reciprocity of screw, "*for a given set of joint velocities, if the velocities of the end effector, which under normal circumstances can be specified using the forward kinematics, cannot be defined, singularity occurs.*" [FS92a]. This implies that the manipulator has a configuration singularity which occurs wherever  $\dot{\theta}_{i1}$  are undefined. The passive joint rate can be solved using the Kinematic Constraint of a 3-D Rigid Body Motion [FS92a]. By utilizing the kinematic constraints, three constrained equations can be found:

$$V_{Pi} \cdot (P_i - P_j) = V_{Pj} \cdot (P_i - P_j) \quad (2.11)$$

(for  $i \& j=1$  to  $3$ ,  $i \neq j$ )

Substitute Equations (2.8) and (2.9) into Equation (2.11), it can be written into a matrix form as follows :



$$\begin{bmatrix} K_{11} & K_{12} & 0 \\ 0 & K_{22} & K_{23} \\ K_{31} & 0 & K_{33} \end{bmatrix} \cdot \begin{bmatrix} \dot{\theta}_{11} \\ \dot{\theta}_{21} \\ \dot{\theta}_{31} \end{bmatrix} = \begin{bmatrix} N_1 \\ N_2 \\ N_3 \end{bmatrix} \quad (2.12)$$

or  $[K] \cdot [\theta] = [N]$

where  $K_{ji}$  and  $N_i$  are functions of joint parameters, and  $K_{ji}$  is the coefficient of  $\dot{\theta}_{ji}$

If Equation (2.12) is solved, the computation of  $V_{Pi}$ ,  $V_0$  and  $\omega$  will be straightforward. However, if the determinant of  $[K]$  is zero,  $[\dot{\theta}]$ ,  $V_{Pi}$ ,  $V_0$  and  $\omega$  will be undefined. This means that the configuration of the platform-type parallel manipulator is singular. On the other hand, the only requirement for applying this method is that the three selected points are not collinear.

### 2.1.3 Grassmann Geometry Method

This method is derived from the principle of Grassmann line geometry [ME89]. The set of lines are defined through six linearly independent vector and is therefore of rank 6. When the independent vector spanned by the lines associated to the robot links has a rank less than 6, a singular configuration exists. An important feature of the independent vectors of this geometry is that they can be described by simple geometric rules. Therefore, to find the singular configurations of parallel manipulators is equivalent to identifying the configurations in which the robot matches these rules.

Grassmann defined a set of rules for ranking the linear independent vectors according to their geometric characterization [ME89]. The linear independent vector is basically divided into 6 classes as follows:

Rank 0 - An empty set.

Rank 1 - A point which is a line in the 3D space.

Rank 2 - Pair of skew lines or lines which lie on a plane and pass through some point on that plane.

Rank 3 - Planes :

- (a) a regulus;
- (b) the union of two flat pencils having a line in common, but lying on distinct planes and with distinct centers;
- (c) all lines through a point;
- (d) all lines on a plane.

Rank 4 - Linear congruences :

- (a) a linear spread generated by four skew lines;
- (b) all the lines concurrent with two skew lines;
- (c) a one-parameter family of flat pencils, having one line in common and forming an independent;
- (d) all the lines on a plane or they pass through one point on that plane.

Rank 5 - Linear complexes :

- (a) non-singular : generated by five independent skew lines;
- (b) singular : all the lines meeting one given line.

Among the above rules, we have found that the rule 5b can be applied in the sample manipulator as all the links axes of the platform-type parallel manipulator are meeting in a line ( $B_3B_5$ ). So, according to the rules, the configuration shown in Figure 2.4 should be singular.



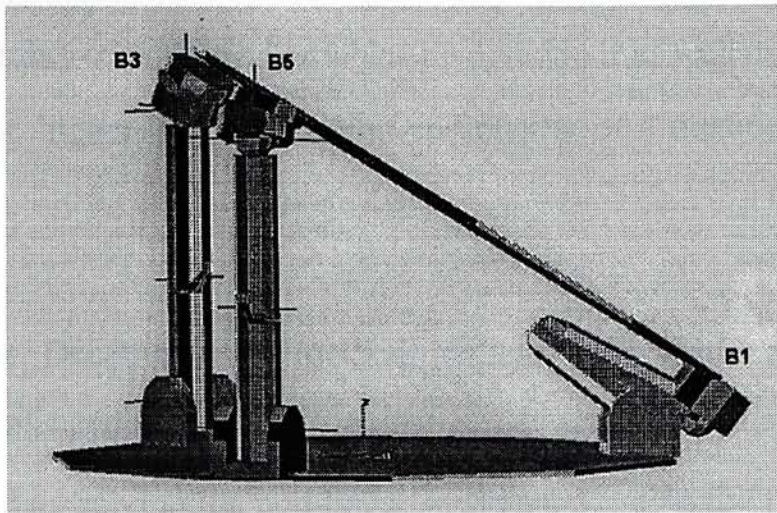


Figure 2.4 Singular Configuration of Novel 6 DOF Identified by Grassmann Geometry Method

From the mechanical analysis, the torque around the axis ( $B_3B_5$ ) exerted by the segments on the moving platform is always equal to zero. If we apply an external force on the moving platform such that the resulting torque around the axis ( $B_3B_5$ ) is not equal to zero, the moving platform cannot be in an equilibrium state. The configuration is not rigid [HU78]. It means that the platform-type parallel manipulator will be unstable at the singular configuration.

## 2.2 Comparison Criteria

We use the sample manipulator (i.e. Novel 6 DOF platform-type parallel manipulator) to compare the above three methods based on the following two criteria: Computational Complexity and Robustness.

### 2.2.1 Computational Complexity

Regarding a mathematical model, most researchers used the computational complexity as a direct measure of its efficiency [CH74, MK89, NH86, KB92, FS94]. In general, computational complexity is estimated in terms of the number of

equations, the number of unknown variables involved in it as well as the dimension of the matrices. The higher the computation complexity of a method is, the lower its efficiency.

The Force Decomposition method, reduces computational complexity by breaking the complicated non-linear Jacobian,  $J_p^T$ , down into two linear Jacobians,  $J_{sj}^{ee}$  and  $J_{act}^{sj}$ . Rather than solving the non-linear Jacobian,  $J_p^T$ , directly, it solves a number of linear equations (Equations 2.3, 2.5 and 2.6) instead. However, although the non-linear Jacobian is reduced, a set of six equations with six variables are required in the formulation of the 6x6 linear Jacobian  $J_{sj}^{ee}$ . Each element of  $J_{sj}^{ee}$  is a multiplication of several matrices. This is still a time consuming process as formulation of the Jacobian  $J_{sj}^{ee}$  involves 738 multiplications, 474 additions and 24 subtractions.

On the other hand, the Forward Rate Kinematics Base method generally involves a set of six linear equations with six passive joint variables. In some particular cases, only three variables (either three passive joint rates or three intermediate variables) are required and the solution can be obtained by solving a set of three linear equations [FS92b]. For instance, the sample manipulator, which is an elbow joint structure, involves only three linear equations with three passive joint variables. Thus, it is only required to solve the determinant of a 3x3 matrix with three zero elements. Furthermore, the formulation of matrix K which only involves 156 multiplications, 6 additions and 36 subtractions.

The Grassmann Geometry method is a rule based method for testing the singularity of a configuration. Although this method is simple implement, it is very difficult to find a singular configuration that satisfies the rules [ME89]. In fact, for a complicated structure, it is really difficult to identify a configuration which matches with rules like 3b, 4c and 4d.



### 2.2.2 Scope of Application

Currently, most of the methods are designed on an ad hoc basis (i.e. it is designed for solving a particular solution). Little consideration has been made on generalizing them [BU91, CU94, SO90]. This is certainly wasteful. A general method is one which is applicable to a wide range of problems. Such a method should always be given first hand consideration.

In this Section, the three methods will be compared by scope of application. Referring to the background study, the Forward Rate Kinematics Based method had been proved to be able to identify the Configuration Singularity of 6 DOF Stewart Platform [FS92a, FS92b, FS94]. It had been mentioned that the Grassmann Geometry method is not suitable for a complex manipulator whose geometry is difficult to analysis [ME89]. The result of comparison based on the sample manipulator is given in the following paragraphs.

The Force Decomposition method is limited application scope of the handcontrollers [CU94]. Another limitation is that it may not solve the singularity problem of a heavy duty robot with many legs. For instance, if the number of legs is increased to 4, the dimension of  $J_{sj}^{ee}$  increases to 6x8. The Jacobian then becomes a rectangular matrix and its determinant is almost impossible to find. This is because two force components at the spherical joint of each additional leg introduce two more columns to the Jacobian  $J_{sj}^{ee}$ . This gives rise to a non-square matrix. In short, the Force Decomposition method is only applicable to a simple and light work load structured manipulator.

The Forward Rate Kinematics Based method only uses the velocities of three non-collinear points which attached to the end-effector. Unlike the Force Decomposition Method, even if the number of legs is increased, the dimension of

matrix  $K$  (in Equation 2.12) will remain unchanged. Hence, this method can be generalized to cater for any elbow joint structured platform-type parallel manipulator (including 6 DOF Stewart platform [FS92a]).

The Grassmann Geometry method can only be applied to special parallel manipulators such as the example shown in Figure 2.4. For general parallel manipulators, it is difficult to find singular configurations that satisfy geometric rules Rank 0 to Rank 5 mentioned before.

### 2.3 Summary

Overall, the performance of the three methods in terms of the computational complexity and the Scope of Application is summarized in table 2.1.

Criteria / Methods	Force Decomposition	Forward Rate Kinematics Based	Grassmann Geometry
Computational Complexity	Solving a 6x6 Jacobian $J_{sj}^{ec}$ that involves 738 multiplications, 474 additions and 24 subtractions	Solving a 3x3 matrix $K$ that involves 156 multiplications, 6 additions and 36 subtractions.	No numerical form as it is a rule-based approach.
Scope of Application	Can be used in parallel manipulator with few legs only but not for other manipulator e.g. 6 DOF Stewart platform.	Can be used to analysis both few legs and other parallel manipulator e.g. 6 DOF Stewart platform	For special parallel manipulator and is not suitable for a complex manipulator whose geometry is difficult to analysis.

Table 2.1 Comparison of Three Methods



Among the three existing methods for identification of configuration singularity, the Forward Rate Kinematics Based method is most efficient. It is the best because of two reasons: (1) its computational complexity is the lowest, and (2) it can be applied to more general cases. Furthermore, it is noted that this method not only can tell whether the configuration is singular but also provide some useful hints for one to minimize or even eliminate the problem in the design of manipulator. This aspect will be further discussed in Chapter 3. Therefore, in this study, we used the Forward Rate Kinematics Based method to investigate the problem of configuration singularity in three types of platform-type parallel manipulator : namely, 3 DOF with symmetric and non-symmetric base, Novel 6 DOF, and class of 6 SPS.

# Chapter 3

## Enumeration of Configuration Singularity

In this chapter, we will firstly deduce the general expression of the configuration singularity of two classes of platform-type parallel manipulator, namely: Novel 6 DOF and 3 DOF with symmetric and non-symmetric base which have not been studied by other researchers. Numerical examples will be used to verify the general expressions derived in each case and we will also illustrate the physical meaning of each configuration singularity found. Secondly, the Forward Rate Kinematics Based method will be applied to the class of 6 SPS parallel manipulators to identify the configuration singularity. We will show that a relationship, between the radius of the base platform and the length of the upper and lower links, exists in each case. Such relationship is a major factor to consider for eliminating the configuration singularity in design stage. Further analysis to the relationship will be given in the next chapter.

### 3.1 Novel 6 DOF

The analysis of configuration singularity of 6 DOF platform-type parallel manipulator by using elbow joints has not been studied yet. Therefore, we would like to place some research effort on this class of manipulators. The Novel 6 DOF platform-type parallel manipulator is a good and typical example in this class. It consists of a base plate, a top plate (the moving platform) and three connection legs. Each leg has a lower and upper link which are connected by an elbow joint (Figure 3.1). We will deduce and simplify the general expression, which is expressed in terms of the passive and active joint variables, of the configuration singularity in the Novel 6 DOF platform-type parallel manipulator. A numerical examples will be used to verify the correctness of the general expression.



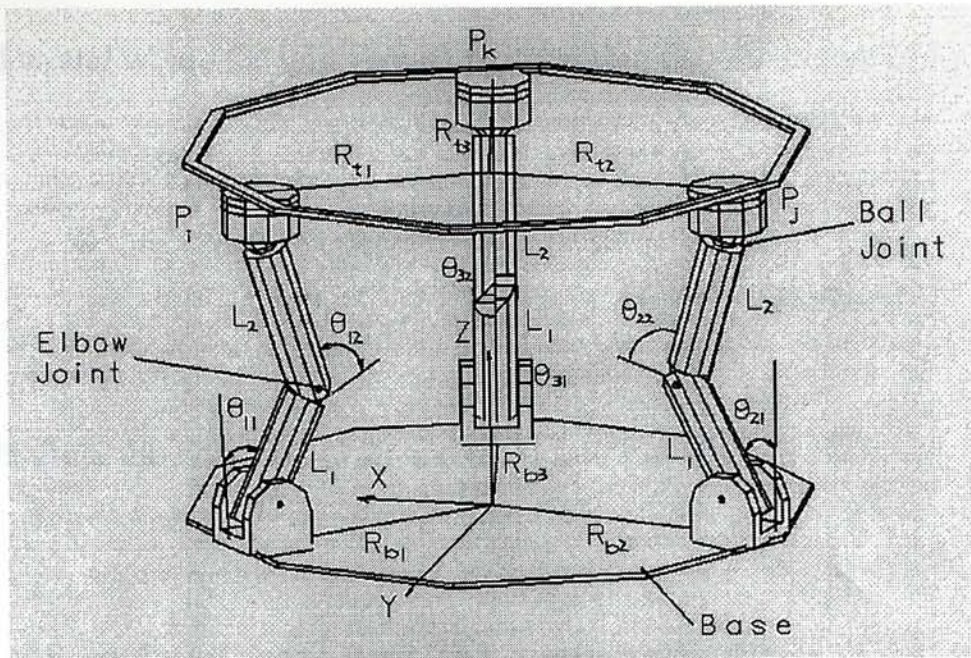


Figure 3.1 Geometry of the Novel 6 DOF Platform-type Parallel Manipulator

Referring to Figure 3.1, each leg has a lower link and a upper link, with lengths  $L_1$  and  $L_2$  respectively.  $\theta_{i2}$  is the active joint parameter while  $\theta_{i1}$  the passive joint parameter of leg  $i$ .  $R_b$  is the radius of the base platform.  $R_{bi}$  is the rotation angle between the local coordinates of leg  $i$  and the base coordinate system.  $P_i$  (for  $i=1$  to 3) (They are equivalent to  $P_i$ ,  $P_j$  and  $P_k$  respectively. This convention is used throughout this chapter.) is the connection point of the leg  $i$  and the moving platform. These three points are non-collinear .

Step 1: According to the definition of the Forward Rate Kinematics Based method, by giving the value of all the active joint velocities and geometrical configuration, the coordinates of the three non-collinear points  $P_i$  (for  $i=1$  to 3) with respect to the base reference frame can be represented by point vectors as follows:

$$P_i = B_i + w_i L_1 + w'_i L_2 \quad (3.1)$$

where  $B_i = \overline{OB_i}$  is a constant vector fixed to the base platform

$$B_i = \begin{bmatrix} R_b \cos R_{bi} \\ R_b \sin R_{bi} \\ 0 \end{bmatrix} \quad (3.2)$$

and  $w_i$  and  $w'_i$  are the unit vectors representing the orientation of  $L_1$  and  $L_2$ .

$$w_i = \begin{bmatrix} \cos\theta_{i1} \cos R_{bi} \\ \cos\theta_{i1} \sin R_{bi} \\ \sin\theta_{i1} \end{bmatrix} \quad \text{and} \quad w'_i = \begin{bmatrix} \cos\theta_{i2} \cos R_{bi} \\ \cos\theta_{i2} \sin R_{bi} \\ \sin\theta_{i2} \end{bmatrix} \quad (3.3)$$

Step 2: Substitute the Equation (3.2) and (3.3) into Equation (3.1),  $P_i$  can be rewritten as:

$$p_i = \begin{bmatrix} R_b \cos R_{bi} + L_1 \cos\theta_{i1} \cos R_{bi} + L_2 \cos\theta_{i2} \cos R_{bi} \\ R_b \sin R_{bi} + L_1 \cos\theta_{i1} \sin R_{bi} + L_2 \cos\theta_{i2} \sin R_{bi} \\ L_1 \sin\theta_{i1} + L_2 \sin\theta_{i2} \end{bmatrix} \quad (3.4)$$

Step 3: The velocity of  $P_i$  is the derivative of Equation (3.4) with respect to time, its matrix form is:

$$v_{pi} = \begin{bmatrix} -L_1 \dot{\theta}_{i1} \sin\theta_{i1} \cos R_{bi} - L_2 \dot{\theta}_{i2} \sin\theta_{i2} \cos R_{bi} \\ -L_1 \dot{\theta}_{i1} \sin\theta_{i1} \sin R_{bi} - L_2 \dot{\theta}_{i2} \sin\theta_{i2} \sin R_{bi} \\ L_1 \dot{\theta}_{i1} \cos\theta_{i1} + L_2 \dot{\theta}_{i2} \cos\theta_{i2} \end{bmatrix} \quad (3.5)$$

Step 4: The linear velocity of the end-effector,  $V_0$ , is the mean of velocity  $P_i$ :

$$V_0 = \frac{1}{3} \sum_{i=1}^3 v_{pi} \quad (3.6)$$

Step 5: The velocity of the three points,  $v_{pi}$ , can also be expressed in terms of the linear velocity,  $V_0$ , and the angular velocity,  $\omega$ , of the end-effector:

$$v_{pi} = [R_b^e] [\omega] A_i + V_0 \quad (3.7)$$

where  $[R_b^e]$  is a 3x3 rotation matrix and  $A_i$  is a constant vector

Step 6: The linear velocity  $V_0$  and the angular velocity  $\omega$  of the end-effector are expressed in terms of three unknown passive joints rate  $\dot{\theta}_{i1}$ . This implies that the singularity of the manipulator occurs whenever  $\dot{\theta}_{i1}$  is undefined. The passive joints



rate can be solved using the Kinematic Constraint of a 3-D Rigid Body Motion [FS92a]. By utilizing the kinematic constraints, three constrained equations can be found:

$$V_{P_i} \cdot (P_i - P_j) = V_{P_j} \cdot (P_i - P_j) \quad (3.8)$$

(for  $i \& j=1$  to  $3, i \neq j$ )

Step 7: In this case,  $R_b = R$ ,  $R_{b1} = 0$ ,  $R_{b2} = 2\pi/3$  and  $R_{b3} = 4\pi/3$ , by substituting these values and Equation (3.4) & (3.5) into Equation (3.8), the three constrained equations are expressed as follows :

$$\begin{bmatrix} 1.5R + L_1 \cos(\theta_{11}) + L_2 \cos(\theta_{12}) + \frac{L_1}{2} \cos(\theta_{21}) + \frac{L_2}{2} \cos(\theta_{22}) \\ -\frac{\sqrt{3}}{2} R - \frac{\sqrt{3}}{2} L_1 \cos(\theta_{21}) - \frac{\sqrt{3}}{2} L_2 \cos(\theta_{22}) \\ L_1 \sin(\theta_{11}) + L_2 \sin(\theta_{12}) - L_1 \sin(\theta_{21}) - L_2 \sin(\theta_{22}) \end{bmatrix}^T$$

$$\begin{bmatrix} -L_1 \dot{\theta}_{11} \sin(\theta_{11}) - L_2 \dot{\theta}_{12} \sin(\theta_{12}) - \frac{L_1}{2} \dot{\theta}_{21} \sin(\theta_{21}) - \frac{L_2}{2} \dot{\theta}_{22} \sin(\theta_{22}) \\ \frac{\sqrt{3}}{2} L_1 \dot{\theta}_{21} \sin(\theta_{21}) + \frac{\sqrt{3}}{2} L_2 \dot{\theta}_{22} \sin(\theta_{22}) \\ L_1 \dot{\theta}_{11} \cos(\theta_{11}) + L_2 \dot{\theta}_{12} \cos(\theta_{12}) - L_1 \dot{\theta}_{21} \cos(\theta_{21}) - L_2 \dot{\theta}_{22} \cos(\theta_{22}) \end{bmatrix} = 0 \quad (3.9)$$

$$\begin{bmatrix} -\frac{L_1}{2} \cos(\theta_{21}) + \frac{L_2}{2} \cos(\theta_{22}) + \frac{L_1}{2} \cos(\theta_{31}) + \frac{L_2}{2} \cos(\theta_{32}) \\ \sqrt{3}R + \frac{\sqrt{3}}{2} L_1 \cos(\theta_{21}) + \frac{\sqrt{3}}{2} L_2 \cos(\theta_{22}) + \frac{\sqrt{3}}{2} L_1 \cos(\theta_{31}) + \frac{\sqrt{3}}{2} L_2 \cos(\theta_{32}) \\ L_1 \sin(\theta_{21}) + L_2 \sin(\theta_{22}) - L_1 \sin(\theta_{31}) - L_2 \sin(\theta_{32}) \end{bmatrix}^T$$

$$\begin{bmatrix} \frac{L_1}{2} \dot{\theta}_{21} \sin(\theta_{21}) - \frac{L_2}{2} \dot{\theta}_{22} \sin(\theta_{22}) - \frac{L_1}{2} \dot{\theta}_{31} \sin(\theta_{31}) - \frac{L_2}{2} \dot{\theta}_{32} \sin(\theta_{32}) \\ -\frac{\sqrt{3}}{2} L_1 \dot{\theta}_{21} \sin(\theta_{21}) + \frac{\sqrt{3}}{2} L_2 \dot{\theta}_{22} \sin(\theta_{22}) - \frac{\sqrt{3}}{2} L_1 \dot{\theta}_{31} \sin(\theta_{31}) - \frac{\sqrt{3}}{2} L_2 \dot{\theta}_{32} \sin(\theta_{32}) \\ L_1 \dot{\theta}_{21} \cos(\theta_{21}) + L_2 \dot{\theta}_{22} \cos(\theta_{22}) - L_1 \dot{\theta}_{31} \cos(\theta_{31}) - L_2 \dot{\theta}_{32} \cos(\theta_{32}) \end{bmatrix} = 0 \quad (3.10)$$

$$\begin{bmatrix} -1.5R - L_1 \cos(\theta_{11}) - L_2 \cos(\theta_{12}) - \frac{L_1}{2} \cos(\theta_{31}) - \frac{L_2}{2} \cos(\theta_{32}) \\ -\frac{\sqrt{3}}{2} R - \frac{\sqrt{3}}{2} L_1 \cos(\theta_{31}) - \frac{\sqrt{3}}{2} L_2 \cos(\theta_{32}) \\ -L_1 \sin(\theta_{11}) - L_2 \sin(\theta_{12}) + L_1 \sin(\theta_{31}) + L_2 \sin(\theta_{32}) \end{bmatrix}^T$$

$$\begin{bmatrix} L_1 \dot{\theta}_{11} \sin(\theta_{11}) + L_2 \dot{\theta}_{12} \sin(\theta_{12}) + \frac{L_1}{2} \dot{\theta}_{31} \sin(\theta_{31}) + \frac{L_2}{2} \dot{\theta}_{32} \sin(\theta_{32}) \\ \frac{\sqrt{3}}{2} L_1 \dot{\theta}_{31} \sin(\theta_{31}) + \frac{\sqrt{3}}{2} L_2 \dot{\theta}_{32} \sin(\theta_{32}) \\ -L_1 \dot{\theta}_{11} \cos(\theta_{11}) - L_2 \dot{\theta}_{12} \cos(\theta_{12}) + L_1 \dot{\theta}_{31} \cos(\theta_{31}) + L_2 \dot{\theta}_{32} \cos(\theta_{32}) \end{bmatrix} = 0$$

(3.11)

Step 8: The Equation (3.9), (3.10) and (3.11) can be rewritten into a matrix form as:

$$\begin{bmatrix} K_{11} & K_{12} & 0 \\ 0 & K_{22} & K_{23} \\ K_{31} & 0 & K_{33} \end{bmatrix} \cdot \begin{bmatrix} \dot{\theta}_{11} \\ \dot{\theta}_{21} \\ \dot{\theta}_{31} \end{bmatrix} = \begin{bmatrix} N_1 \\ N_2 \\ N_3 \end{bmatrix} \quad (3.12)$$

or  $[K] \cdot [\theta] = [N]$

where  $K_{ji}$  and  $N_i$  are functions of joint parameters, and  $K_{ji}$  is the coefficient of  $\dot{\theta}_{i1}$

$$K_{11} = 1/2(-3 L_1 R \sin(\theta_{11}) - 2 L_1 L_2 \cos(\theta_{12}) \sin(\theta_{11}) - L_1^2 \cos(\theta_{21}) \sin(\theta_{11}) - L_1 L_2 \cos(\theta_{22}) \sin(\theta_{11}) + 2 L_1 L_2 \cos(\theta_{11}) \sin(\theta_{12}) - 2 L_1^2 \cos(\theta_{11}) \sin(\theta_{21}) - 2 L_1 L_2 \cos(\theta_{11}) \sin(\theta_{22}))$$

$$K_{12} = 1/2(-2 L_1^2 \cos(\theta_{21}) \sin(\theta_{11}) - 2 L_1 L_2 \cos(\theta_{21}) \sin(\theta_{12}) - 3 L_1 R \sin(\theta_{21}) - L_1^2 \cos(\theta_{11}) \sin(\theta_{21}) - L_1 L_2 \cos(\theta_{12}) \sin(\theta_{21}) - 2 L_1 L_2 \cos(\theta_{22}) \sin(\theta_{21}) + 2 L_1 L_2 \cos(\theta_{11}) \sin(\theta_{12}))$$

$$K_{22} = 1/2(-3 L_1 R \sin(\theta_{21}) - 2 L_1 L_2 \cos(\theta_{22}) \sin(\theta_{21}) - L_1^2 \cos(\theta_{31}) \sin(\theta_{21}) - L_1 L_2 \cos(\theta_{32}) \sin(\theta_{21}) + 2 L_1 L_2 \cos(\theta_{21}) \sin(\theta_{22}) - 2 L_1^2 \cos(\theta_{21}) \sin(\theta_{31}) - 2 L_1 L_2 \cos(\theta_{21}) \sin(\theta_{32}))$$



$$K_{23} = 1/2(-2 L_1^2 \cos(\theta_{31}) \sin(\theta_{21}) - 2 L_1 L_2 \cos(\theta_{31}) \sin(\theta_{22}) - 3 L_1 R \sin(\theta_{31}) - L_1^2 \cos(\theta_{21}) \sin(\theta_{31}) - L_1 L_2 \cos(\theta_{22}) \sin(\theta_{31}) - 2 L_1 L_2 \cos(\theta_{32}) \sin(\theta_{31}) + 2 L_1 L_2 \cos(\theta_{31}) \sin(\theta_{32}))$$

$$K_{31} = 1/2(-3 L_1 R \sin(\theta_{11}) - 2 L_1 L_2 \cos(\theta_{12}) \sin(\theta_{11}) - L_1^2 \cos(\theta_{31}) \sin(\theta_{11}) - L_1 L_2 \cos(\theta_{32}) \sin(\theta_{11}) + 2 L_1 L_2 \cos(\theta_{11}) \sin(\theta_{12}) - 2 L_1^2 \cos(\theta_{11}) \sin(\theta_{31}) - 2 L_1 L_2 \cos(\theta_{11}) \sin(\theta_{32}))$$

$$K_{33} = 1/2(-2 L_1^2 \cos(\theta_{31}) \sin(\theta_{11}) - 2 L_1 L_2 \cos(\theta_{31}) \sin(\theta_{12}) - 3 L_1 R \sin(\theta_{31}) - L_1^2 \cos(\theta_{11}) \sin(\theta_{31}) - L_1 L_2 \cos(\theta_{12}) \sin(\theta_{31}) - 2 L_1 L_2 \cos(\theta_{32}) \sin(\theta_{31}) + 2 L_1 L_2 \cos(\theta_{31}) \sin(\theta_{32}))$$

Step 9: The singularity of the manipulator occurs when  $[\dot{\theta}]$  is undefined, i.e.:

$$\text{Det } [K] = K_{11} K_{22} K_{33} + K_{31} K_{12} K_{23} = 0 \quad (3.13)$$

Step 10: Simplify the Equation (3.13) as:

$$(K_{11} K_{22} K_{33} + K_{31} K_{12} K_{23}) = f(1,2) * f(2,3) * f(3,1) + f(2,1) * f(3,2) * f(1,3) \quad (3.14)$$

where  $i, j = 1, 3$  and

$$f(\theta_{i2}, \theta_{i1}, R_{bi}, R_{bj}, \theta_{j1}, \theta_{j2}) = L_1 L_2 \sin(\theta_{i2} - \theta_{i1}) - L_1 R \sin(\theta_{i1}) + (\cos(R_{bi} - R_{bj}) \sin(\theta_{i1}) (L_1 R + L_1^2 \cos(\theta_{j1}) + L_1 L_2 \cos(\theta_{j2})) - L_1 \cos(\theta_{i1}) (L_1 \sin(\theta_{j1}) + L_2 \sin(\theta_{j2})))$$

Therefore, Equation (3.14) is the general expression of the configuration singularities existed in the Novel 6 DOF platform-type parallel manipulator.

### 3.1.1 Result Analysis

Now, we are going to use the following sample data set to verify whether the above general expression (Equation 3.14) is formulated correctly.

Step 11: Let the passive joint parameters  $\theta_{11} = \theta_{21} = \pi / 2$ , the active joint parameters  $\theta_{12} = \theta_{22} = \pi / 2$ , and  $\theta_{32} = \theta_{31} + 180^\circ$ , then the singularity condition can be reduced to:

$$\begin{aligned} & ((3L_1(L_1 + L_2)^2 R(3R - L_1 \cos\theta_{31} + L_2 \cos\theta_{32}) \cdot (-2L_1 \cos\theta_{31} - 2L_2 \cos\theta_{31} \\ & - 3R \sin\theta_{31} - 2L_2 \cos\theta_{32} \sin\theta_{31} + 2L_2 \cos\theta_{31} \sin\theta_{32}) / 2) = 0 \end{aligned} \quad (3.15)$$

Step 12: Since  $L_1$  and  $L_2$  are greater than zero, Equation (3.15) can be further split into Equations (3.16) and (3.17) :

$$(3R - L_1 \cos\theta_{31} + L_2 \cos\theta_{32}) = 0 \quad (3.16)$$

$$-2L_1 \cos\theta_{31} - 2L_2 \cos\theta_{31} - 3R \sin\theta_{31} - 2L_2 \cos\theta_{32} \sin\theta_{31} + 2L_2 \cos\theta_{31} \sin\theta_{32} = 0 \quad (3.17)$$

Step 13: Equation (3.16) shows the relationship between the sum of the lengths of upper and lower links and the base radius. Since  $\theta_{32} = \theta_{31} + 180^\circ$ , then  $\cos\theta_{32}$  is equal to  $-\cos\theta_{31}$  and Equation (3.16) can be simplified as:

$$R / (L_1 + L_2) = \cos\theta_{31} / 3$$

The maximum value of  $\cos\theta_{31}$  is 1, so:

$$R / (L_1 + L_2) \leq 1 / 3$$

It means that the configuration singularity can be avoided when designing the manipulator if the following condition (Equation 3.18) is satisfied.

$$R / (L_1 + L_2) \geq 1 / 3 \quad (3.18)$$

Step 14: Equation (3.18) only indicates the relationship between the base radius and the length of links in order to eliminate the configuration singularity. It does not give the value of the unknown passive joint parameter for configuration singularity. So,



this parameter will be solved from Equation (3.17) which shows the kinematic configurations of the manipulator. It is simplified as:

$$\tan \theta_{31} = (L_1 + L_2) / 1.5 R_b \quad (3.19)$$

Step 15: The configuration singularity identified by Equation (3.19) is shown in Figure 3.2. The  $k$ th elbow joint axis is collinear with the line between points  $P_k$  and  $P_a$ .  $P_a$  is the middle point between points  $P_i$  and  $P_j$  for a symmetric manipulator. This means that the end-effector of the manipulator gains one more degree of freedom and loses its stability when a force acts perpendicular to the  $k$ th elbow joint (ball joint). This configuration singularity is the same as the one found by using the Grassmann Geometry method described in Chapter two (Figure 2.4).

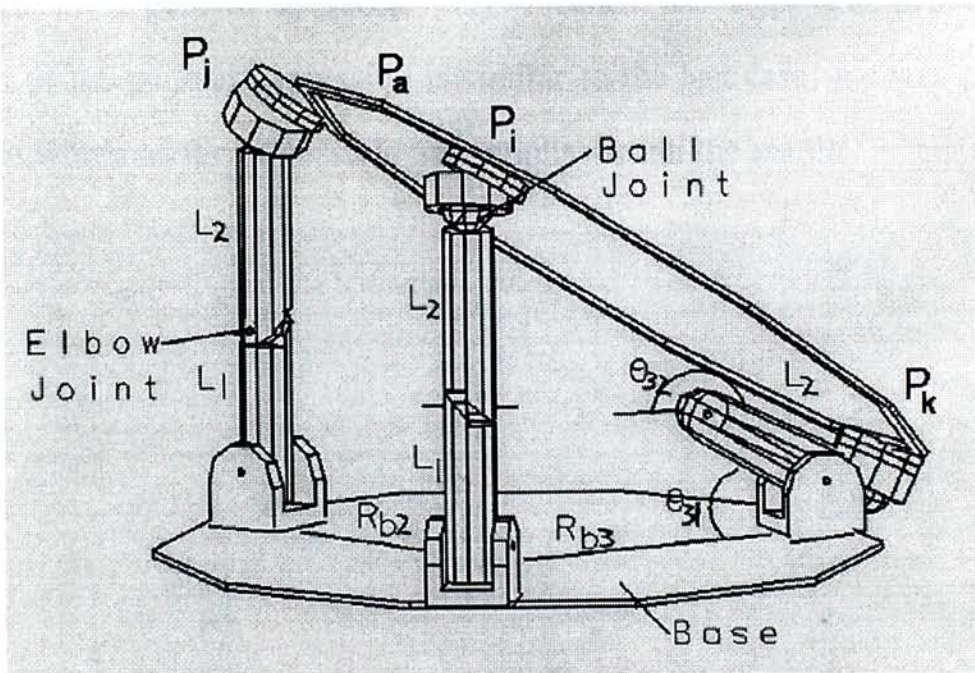


Figure 3.2 Configuration Singularity of Novel 6-DOF Parallel Manipulator Identified by Equation. (3.19)

As a result, the derived general expression (Equation 3.14) is able to identify the configuration singularity for the Novel 6 DOF platform-type parallel manipulator with elbow joints. It efficiently and accurately determines the configuration singularity of the manipulator. On the other hand, it also indicates a way (Equation



2.18) to avoid the configuration singularity in the design stage. This will save the time and effort to compensate the problem of configuration singularity.

### 3.2 A 3 DOF with Symmetric Base

In this section, the Forward Rate Kinematics Based method will be applied to a 3 DOF platform-type parallel manipulator with prismatic joints and symmetric base. The Forward Rate Kinematics Based method had been proved to work on any 3 DOF platform-type parallel manipulator with symmetric base (e.g. Equilateral Triangle Base) [FS92a]. Therefore, we would like to put the effort to rearrange the formulations in a general symbolic way. Since the steps of formulation and verification of the general expression is similar to the last case, we will avoid those burdensome words as far as possible and emphasize on the result.

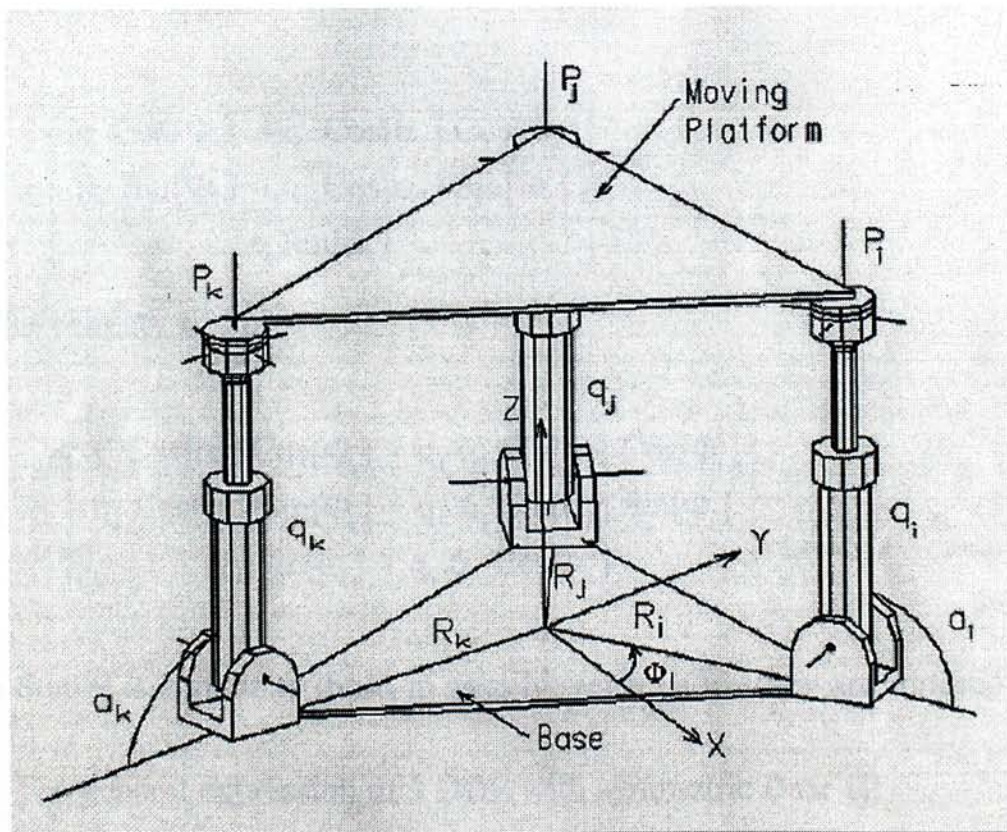


Figure 3.3 Geometry of the 3 DOF Platform-type Parallel Manipulator



The 3 DOF platform-type parallel manipulator (Figure 3.3) with prismatic joint consists of three kinematic sub-chains, each having an actuated sliding joint, noted as  $q_1$ ,  $q_2$  and  $q_3$ . The three passive joint variables used in this analysis are  $\alpha_1$ ,  $\alpha_2$  and  $\alpha_3$  respectively.  $R$  is the radius of the base platform and  $R_i$  is the radius to leg  $i$ . The values of  $R_i$  are  $R_1 = R_2 = R_3 = R$ .  $\Phi_i$  is the rotation angle between the local coordinates of leg  $i$  and the base coordinate system,  $\Phi_1 = 0$ ,  $\Phi_2 = 2\pi/3$ ,  $\Phi_3 = 4\pi/3$ .

Step 1: The coordinates of the three non-collinear points  $P_i$  (for  $i=1$  to 3) with respect to the base reference frame can be represented by point vectors:

$$P_i = B_i + w_i q_i \quad (3.21)$$

where  $B_i$  is a constant vector fixed to the base platform and  $w_i$  is the unit vectors representing the orientation of  $q_i$ .

Step 2:  $P_i$  in detail expression:

$$P_i = \begin{bmatrix} R_i \cos[\Phi_i] + q_i \cos[\alpha_i] \cos[\Phi_i] \\ R_i \sin[\Phi_i] + q_i \cos[\alpha_i] \sin[\Phi_i] \\ q_i \sin[\alpha_i] \end{bmatrix} \quad (3.22)$$

Step 3: The velocity of  $P_i$ :

$$V_{P_i} = \begin{bmatrix} \dot{q}_i \cos[\alpha_i] \cos[\Phi_i] - q_i \dot{\alpha}_i \sin[\alpha_i] \cos[\Phi_i] \\ \dot{q}_i \cos[\alpha_i] \sin[\Phi_i] - q_i \dot{\alpha}_i \sin[\alpha_i] \sin[\Phi_i] \\ \dot{q}_i \sin[\alpha_i] - q_i \dot{\alpha}_i \cos[\alpha_i] \end{bmatrix} \quad (3.23)$$

Step 4 to Step 9 is similar to those in case Novel 6 DOF, they are omitted here.

Step 10: The general expression of 3 DOF with symmetric Base is:

$$\begin{aligned} & (k_{11} k_{22} k_{33} + k_{31} k_{12} k_{23}) \\ & = f(1,2) * f(2,3) * f(3,1) + g(1,2) * g(2,3) * g(3,1) \end{aligned} \quad (3.24)$$

where  $i,j = 1,3$  and

$$\begin{aligned}
& f(R_i, \alpha_i, \Phi_i, q_j, \alpha_j, \Phi_j) \\
& = -R_i \sin \alpha_i - q_j \cos \alpha_i \sin \alpha_j + (R_j + q_j \cos \alpha_j) \sin \alpha_i \cos(\Phi_i - \Phi_j) \\
& g(R_j, \alpha_j, \Phi_j, q_i, \alpha_i, \Phi_i) \\
& = -R_j \sin \alpha_j - q_i \cos \alpha_j \sin \alpha_i + (R_i + q_i \cos \alpha_i) \sin \alpha_j \cos(\Phi_i - \Phi_j)
\end{aligned}$$

### 3.2.1 Result Analysis

Step 11- Step 15: Let the passive joint parameter  $\alpha_1 = 90^\circ$  and  $\alpha_2, \alpha_3$  as unknown variables. Let's assume  $\alpha_2 = \alpha_3$ , then the length of  $q_2$  is equal to the length of  $q_3$ . We will obtain the following equations:

$$\begin{aligned}
\text{Det [k]} &= (1.5 R \sin[\alpha_3] + q_1 \cos[\alpha_3]) (R q_3 \sin[\alpha_3] \cos[\alpha_3] + 3 R^2 \sin[\alpha_3]) \\
&= 0
\end{aligned}$$

$$(1.5 R \sin[\alpha_3] + q_1 \cos[\alpha_3]) = 0 \tag{3.25}$$

$$\tan [\alpha_3] = -\frac{q_1}{1.5 R}$$

Or

$$(R q_3 \sin[\alpha_3] \cos[\alpha_3] + 3 R^2 \sin[\alpha_3]) = 0$$

$$\frac{R}{q_3} \geq \frac{1}{3} \tag{3.26}$$

The configuration singularity found is shown in Figure 3.4.



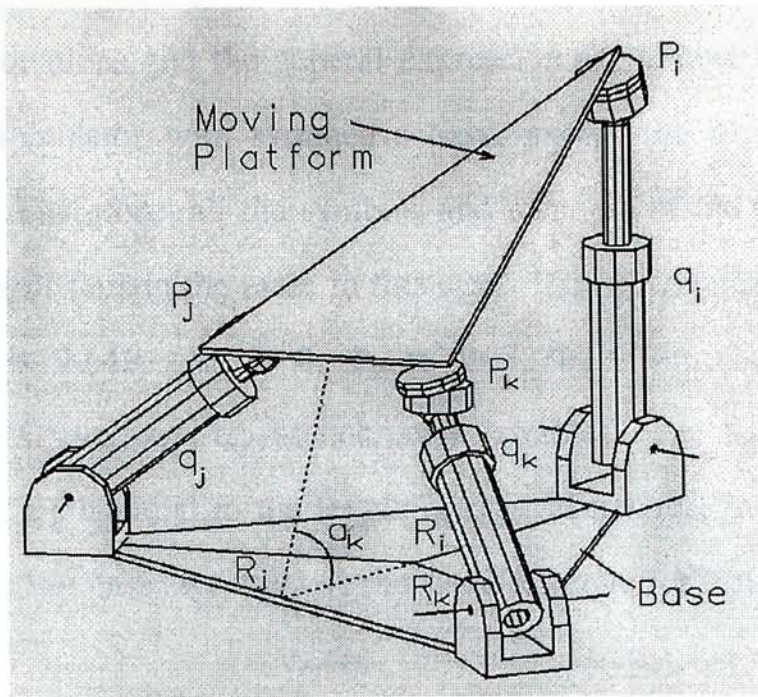


Figure 3.4 Configuration Singularity of 3 DOF Parallel Manipulator with Symmetric Base Identified by Equation.(3.25)

The solution of this example, which is solved from the general expression (Equation 3.24), is the same as the example mentioned by Shi et al. [FS92a]. The only difference is that this example consists of two unknown passive joint parameters while Shi's example involved only one. That means the general expression is able to give correct solutions for whatever example data. This can prove that the general expression is accurate enough to identify the configuration singularity of 3 DOF platform-type parallel manipulator with symmetric base (e.g. Equilateral Triangle Base). Similar to the last case, the general expression returns a ratio  $R/q_3$  which gives an idea to avoid configuration singularity.

### 3.3 A 3 DOF with Non-Symmetric Base

A 3 DOF platform-type parallel manipulator with non-symmetric base (e.g. right-angled triangle base) is a variety of the one with symmetric base. The only difference is the shape of the base platform. Actually, the formulation of the coordinates and velocities of the non-collinear points, velocity of the end-effector,

the constrained equations and the general expression are almost the same as the 3 DOF parallel manipulator with symmetric base, except the parameters will take different values. Therefore, all the symbols and meaning of the passive and active joint parameters will remain the same in this case. The new values of  $R_i$  are:  $R_1 = R_2 = R$  and  $R_3 = \sqrt{0.4}R$ .  $\Phi_1 = 0$ ,  $\Phi_2 = 2\pi/3$ ,  $\Phi_3 = 4\pi/3$ . The passive joint parameter  $\alpha_3 = 90^\circ$  and  $\alpha_1, \alpha_2$  as unknown variables. Let's assume  $\alpha_1 = \alpha_2$ , then the length of  $q_1$  is equal to the length of  $q_2$ . Moreover, in order to compare the result with the last case, we will use the same example for testing.

The determinant of matrix  $K$  and the general expression is the same as the Equation (3.24).

### 3.3.1 Result Analysis

By substituting all known values into the general expression equation (3.24), we have :

$$(q_2 \text{Cos}\alpha_2 + 2.26492 R) \cdot (q_3 R \text{Sin}\alpha_2 \text{Cos}\alpha_2 + 1.31623 R^2 (\text{Sin}\alpha_2)^2) = 0 \tag{3.27}$$

Then :

$$(q_3 R \text{Sin}\alpha_2 \text{Cos}\alpha_2 + 1.31623 R^2 (\text{Sin}\alpha_2)^2) = 0$$

$$(q_3 \text{Cos}\alpha_2 + 1.31623 R \text{Sin}\alpha_2) = 0$$

$$\tan\alpha_2 = \frac{q_3}{1.31623 R} \tag{3.28}$$

Or

$$(q_2 \text{Cos}\alpha_2 + 2.26492 R) = 0$$

$$\frac{R}{q_2} \geq 0.44 \tag{3.29}$$

The resulting configuration singularity is shown in Figure 3.5:



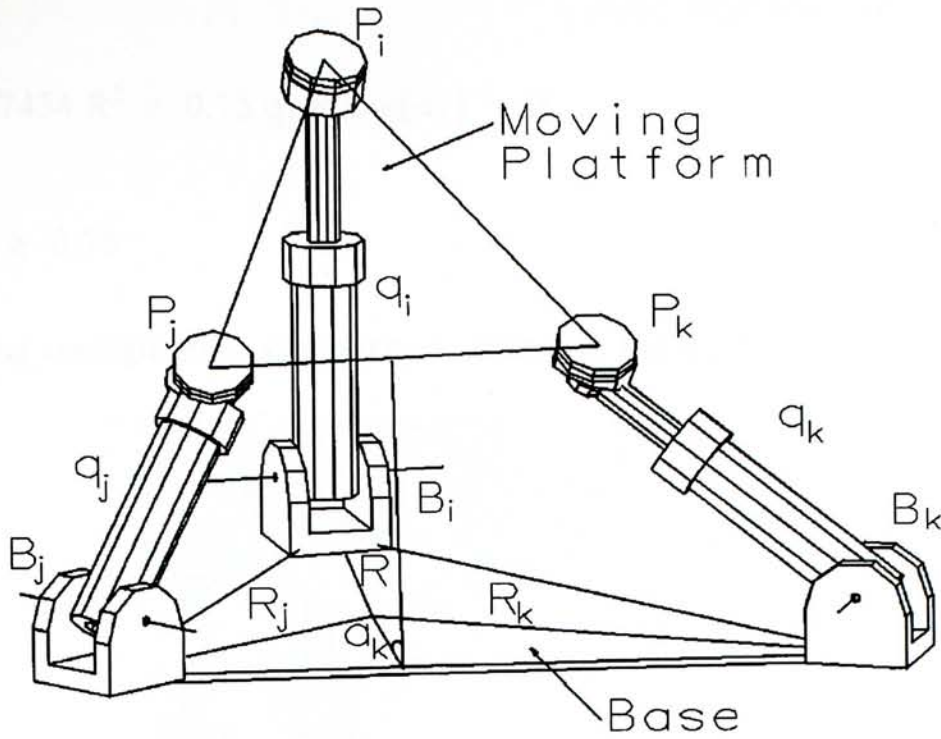


Figure 3.5 Configuration Singularity of 3 DOF Parallel Manipulator with Non-Symmetric Base Identified by Equation.(3.28)

Here is another example with one unknown variable  $\alpha_3$ . The new values of  $R_i$  are:  $R_1 = R_2 = R$  and  $R_3 = \sqrt{0.4}R$ .  $\Phi_1 = 0$ ,  $\Phi_2 = 2\pi/3$ ,  $\Phi_3 = 4\pi/3$ . The passive joint parameter  $\alpha_1 = \alpha_2 = 90^\circ$ . We have :

$$\begin{aligned}
 &= (q_1 \cos[\alpha_3] + q_2 \cos[\alpha_3] + 2.2649 R \sin[\alpha_3]) (1.97434 R^2 + 0.75 q_3 R \cos[\alpha_3]) \\
 &= 0
 \end{aligned}
 \tag{3.30}$$

Then :

$$(q_1 + \cos[\alpha_3] + q_2 \cos[\alpha_3] + 2.2649 R \sin[\alpha_3]) = 0$$

$$\tan[\alpha_3] = \frac{(q_1 + q_2)}{2.2649 R} \tag{3.31}$$

Or

$$(1.97434 R^2 + 0.75 q_3 R \cos[\alpha_3] = 0 \tag{3.32}$$

$$\frac{R}{q_3} \geq 0.38$$

The resulting configuration singularity is shown in Figure 3.6:

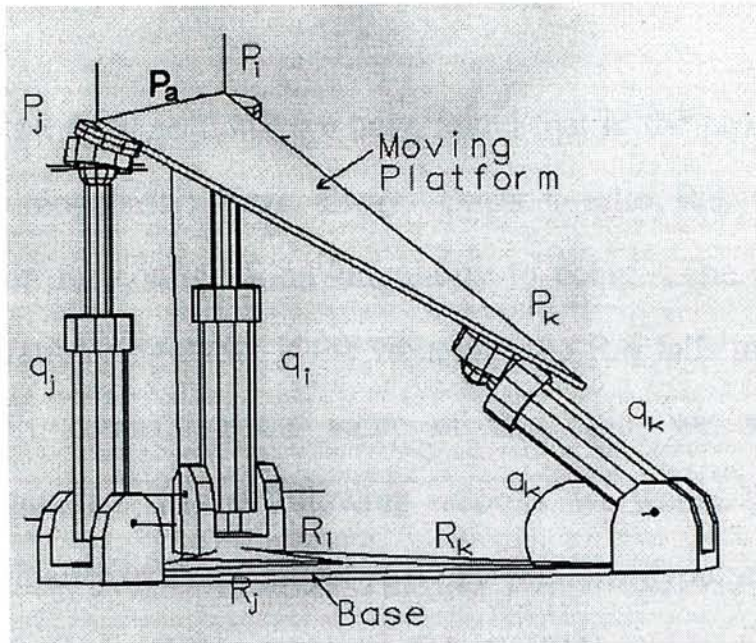


Figure 3.6 Configuration Singularity of 3 DOF Parallel Manipulator with Non-Symmetric Base Identified by Equation.(3.31)

From Figure 3.6, the prismatic joint axis is collinear with the point  $P_a$ , which could be any point on the moving platform. Comparing Figure 3.6 with Figure 3.5, we can see that for the second example, only one prismatic joint axis is collinear with point  $P_a$ . While for the first example, two prismatic joint axes are collinear with the point  $P_i$ . Therefore, if any prismatic joint axis is collinear with any point which is attached on the moving platform, then configuration singularity occurs. As a result, we can summarize that the Forward Rate Kinematics Based method is able to identify the configuration singularity of a 3 DOF platform-type parallel manipulator with symmetric or non-symmetric base.

Furthermore, the ratio of  $R$  to  $q_i$  is found again and its value are 0.44 (Equation 3.29) and 0.38 (Equation 3.32) which are different from  $1/3$  in the last two



cases. That means that the ratio exists for all parallel manipulators and it is not a constant. We will prove this idea by more case studies in the later sections.

### 3.4 A New Model of 6 SPS defined by Kong et al.

From the last three sections, we have found that in the process of identifying the configuration singularity, there always exists a ratio  $R/q$  which specified a necessary condition for configuration singularity to occur. The condition is: there may be a configuration singularity if the value of ratio  $R/q$  falls into a certain range. Then, by carefully controlling the value of this ratio, we may eliminate the configuration singularity. In the following sections, we would like to identify the configuration singularity in a new model of 6 SPS platform-type parallel manipulator, which is defined by Kong, X.W. and Yang, T.L. [KY94], and is shown in Figure 3.7. Since the general expression of the model is very complicated, we will not discuss in detail here. We will show that this ratio ( $R/q$ ) not only exists in the last three cases but also in the new model and its varieties. By generalizing this idea, the ratio can be used as a guideline for designing the manipulators.

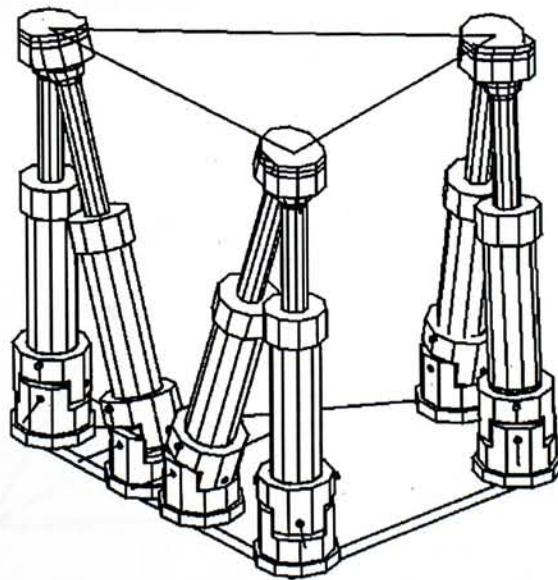


Figure 3.7 A New Model of 6 SPS Defined by Kong et al.

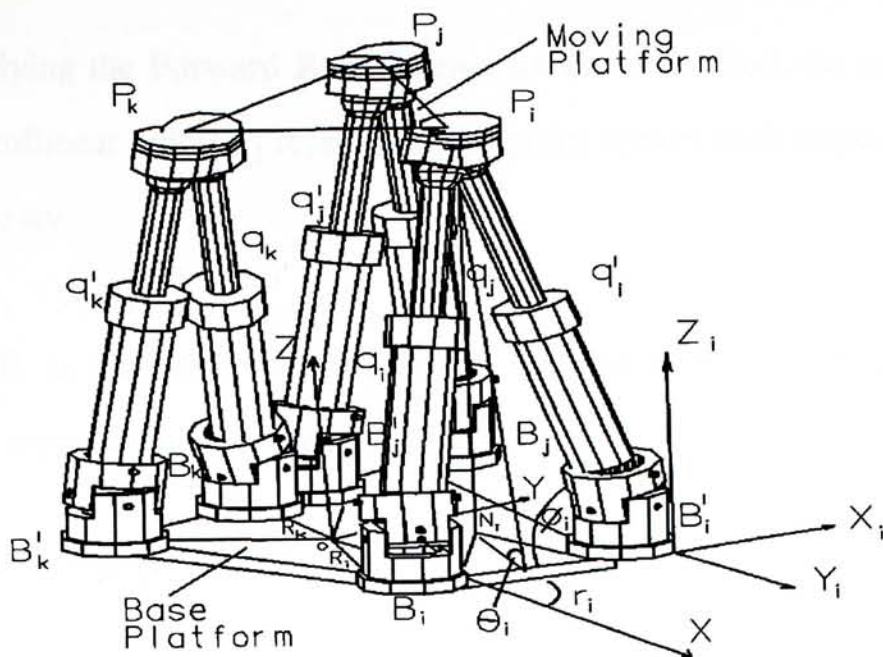


Figure 3.8 The Geometry of a New Model of 6 SPS Defined by Kong et al.

Figure 3.8 is the geometry of the new 6 SPS parallel manipulator. It consists of six kinematic sub-chains, each having an actuated sliding joint, between the base platform (Figure 3.9) and the top plate. Every two of them,  $q_i$  and  $q'_i$  (for  $i=1,3$ ), will join at one vertex point,  $P_i$ , on the triangular top plate. The three intermediate variables are  $\theta_i$ .  $R$  is the radius of the base platform and  $R_i$  is the length from the base center to the point  $B_i$ .  $\gamma_i$  is the rotation angle between the  $i$ th local coordinates and the base coordinate frame (the local coordinate frame is its  $x_i$  axis which is aligned with  $B'_i B_i$ ).  $\Phi_i$  is the rotation angle between the  $i$ th local coordinates and the base coordinate system.

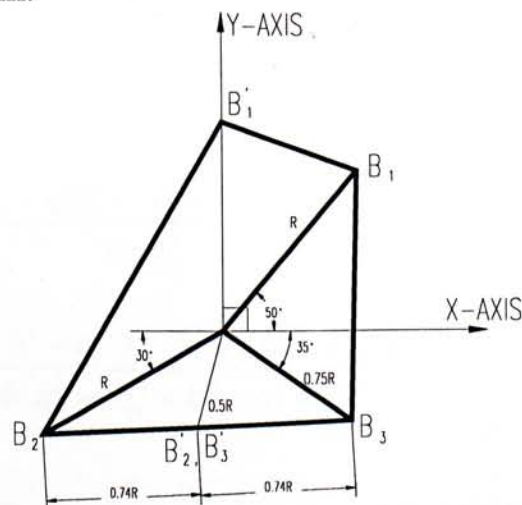


Figure 3.9 The Geometry of the Base Platform of a New Model Defined by Kong et al.



Step 1: By applying the Forward Rate Kinematics Based method, the coordinates of the three non-collinear points  $P_i$  represented by point vectors with respect to the base reference frame are:

$$P_i = B_i + w_i q_i \quad (3.33)$$

where  $B_i$  is a constant vector fixed to the base platform and  $w_i$  is the unit vectors representing the orientation of  $q_i$ .

Step 2: Rewrite  $P_i$  in details:

$$P_i = \begin{bmatrix} R_i \cos[\Phi_i] - q_i W_{1i} \cos[\gamma_i] - q_i W_{2i} \sin[\gamma_i] \cos[\theta_i] \\ R_i \sin[\Phi_i] - q_i W_{1i} \sin[\gamma_i] - q_i W_{2i} \cos[\gamma_i] \cos[\theta_i] \\ q_i W_{2i} \sin[\theta_i] \end{bmatrix} \quad (3.34)$$

where

$$W_{1i} = \cos\phi_i = \frac{q_i^2 + b_i^2 - q_i'^2}{2b_i q_i} \quad \text{and} \quad W_{2i} = \sin\phi_i = \left[ 1 - \left( \frac{q_i^2 + b_i^2 - q_i'^2}{2b_i q_i} \right)^2 \right]^{1/2}$$

Step 3: The velocity of the point is the derivative of Equation.(3.34) with respect to time,

$$V_{pi} = \begin{bmatrix} -\cos\gamma_i (\dot{q}_i W_{1i} + q_i \dot{W}_{1i}) - \sin\gamma_i (\dot{q}_i W_{2i} \cos\theta_i + q_i \dot{W}_{2i} \cos\theta_i - q_i W_{2i} \dot{\theta} \sin\theta_i) \\ -\sin\gamma_i (\dot{q}_i W_{1i} + q_i \dot{W}_{1i}) - \cos\gamma_i (\dot{q}_i W_{2i} \cos\theta_i + q_i \dot{W}_{2i} \cos\theta_i - q_i W_{2i} \dot{\theta} \sin\theta_i) \\ \dot{q}_i W_{2i} \sin\theta_i + q_i \dot{W}_{2i} \sin\theta_i + q_i W_{2i} \dot{\theta} \cos\theta_i \end{bmatrix} \quad (3.35)$$

where

$$\dot{W}_{1i} = \frac{2q_i(q_i \dot{q}_i - q_i' \dot{q}_i') - \dot{q}_i(q_i^2 + b_i^2 - q_i'^2)}{2b_i q_i^2} \quad \text{and}$$

$$\dot{W}_{2i} = \frac{\dot{q}_i(q_i^2 + b_i^2 - q_i'^2) - 2q_i(q_i \dot{q}_i - q_i' \dot{q}_i')}{2q_i [4b_i^2 q_i^2 - (q_i^2 + b_i^2 - q_i'^2)^2]^{1/2}}$$

Step 4 - Step 6 is similar to those in the case of Novel 6 DOF.

Step 7: In order to find the configuration singularity, let's make the following selections:

$$R_1 = R_2 = R \text{ and } R_3 = 0.75R.$$

$$\gamma_1 = 8\pi / 9, \gamma_2 = \pi / 2, \gamma_3 = \pi / 2$$

$$\Phi_1 = 5\pi / 18, \Phi_2 = 7\pi / 6, \Phi_3 = 65\pi / 36$$

$$b_1 (B_1 B_1') = 0.684R, b_2 (B_2 B_2') = 0.741R, b_3 (B_3 B_3') = 0.741R.$$

$$\theta_1 = \theta_2 = \pi / 2$$

$$\text{coefficient of } \dot{\theta}_j = K_{ij}, \text{ where } i, j = 1, 3$$

The matrix form of Equation (3.36) is:

$$\begin{bmatrix} K_{11} & K_{12} & 0 \\ 0 & K_{22} & K_{23} \\ K_{31} & 0 & K_{33} \end{bmatrix} \begin{bmatrix} \dot{\theta}_1 \\ \dot{\theta}_2 \\ \dot{\theta}_3 \end{bmatrix} = \begin{bmatrix} N_1 \\ N_2 \\ N_3 \end{bmatrix} \quad (3.36)$$

where

$$K_{11} = 2.5254 R \sin[\phi_1] \sin[\theta_1] - 0.4698 b_2 \sin[\phi_1] \sin[\theta_1] - 0.5 q_2 \sin[\phi_1] \sin[\phi_2] \cos[\theta_1]$$

$$K_{12} = 1.3784 R \sqrt{4 - (b_2^2 / q_2^2)} - 0.1710 q_1 \sqrt{4 - (b_2^2 / q_2^2)} \sin[\phi_1] \cos[\theta_1]$$

$$K_{22} = 1.7442 R \sqrt{4 - (b_2^2 / q_2^2)} - 0.25 b_3 \sqrt{4 - (b_2^2 / q_2^2)}$$

$$K_{23} = 0.0762 R \sqrt{4 - (b_3^2 / q_3^2)} + 0.25 b_2 \sqrt{4 - (b_3^2 / q_3^2)}$$

$$K_{31} = (1.4755 R + 0.1710 b_3) \sin[\phi_1] \sin[\theta_1] - 0.5 q_3 \sqrt{4 - (b_3^2 / q_3^2)} \sin[\phi_1] \cos[\theta_1]$$

$$K_{33} = 0.9182 R \sqrt{4 - (b_3^2 / q_3^2)} - 0.4698 q_1 \sqrt{4 - (b_3^2 / q_3^2)} \sin[\phi_1] \cos[\theta_1]$$

Step 8: The singularity condition is:

$$\text{Det [K]} = K_{11} K_{22} K_{33} + K_{31} K_{12} K_{23} = 0 \quad (3.37)$$

Step 9: Expressing the Equation(3.34) into:

$$(2.75686 R \sin[\phi_2] - 0.34202 q_1 \sin[\phi_1] \sin[\phi_2] \cos[\theta_1]) \times \\ (-q_3 \sin[\phi_1] \sin[\phi_3] \cos[\theta_1] + 1.602 R \sin[\phi_1] \sin[\theta_1]) = 0$$

Or

$$(1.93637 R \sin[\phi_3] - 0.939693 q_1 \sin[\phi_1] \sin[\phi_3] \cos[\theta_1]) \times \\ (-q_2 \sin[\phi_1] \sin[\phi_2] \cos[\theta_1] + 2.17772 R \sin[\phi_1] \sin[\theta_1]) = 0$$



Since  $R \neq 0$ , these condition can be rewritten as

$$\begin{aligned} 2.75686 R \sin[\phi_2] - 0.34202 q_1 \sin[\phi_1] \sin[\phi_2] \cos[\theta_1] &= 0 \\ 2.75686 R &= 0.34202 q_1 \sin[\phi_1] \cos[\theta_1] \end{aligned}$$

When  $\sin[\phi_1]$  and  $\cos[\theta_1] = 1$ , their maximum value,

$$R / q_1 \geq 0.124 \quad (3.38)$$

$$-q_3 \sin[\phi_1] \sin[\phi_3] \cos[\theta_1] + 1.602 R \sin[\phi_1] \sin[\theta_1] = 0$$

$$\tan[\theta_1] = \frac{q_3 \sin[\phi_3]}{1.602 R} \quad (3.39)$$

Alternatively, the condition can be written as :

$$\begin{aligned} 1.93637 R \sin[\phi_3] - 0.939693 q_1 \sin[\phi_1] \sin[\phi_3] \cos[\theta_1] &= 0 \\ 1.93637 R &= 0.939693 q_1 \sin[\phi_1] \cos[\theta_1] \end{aligned}$$

when  $\sin[\phi_1]$  and  $\cos[\theta_1] = 1$

$$R / q_1 \geq 0.5117 \quad (3.40)$$

$$-q_2 \sin[\phi_1] \sin[\phi_2] \cos[\theta_1] + 2.17772 R \sin[\phi_1] \sin[\theta_1] = 0$$

$$\tan[\theta_1] = \frac{q_2 \sin[\phi_2]}{2.17772 R} \quad (3.41)$$

The configuration singularity identified by equation (3.39) is shown in Figure 3.10. Therefore, the Forward Rate Kinematics Based method is able to identify the configuration singularity for the model defined by Kong et al. and the ratio of the base radius to the length of the kinematic sub-chains can also be determined.

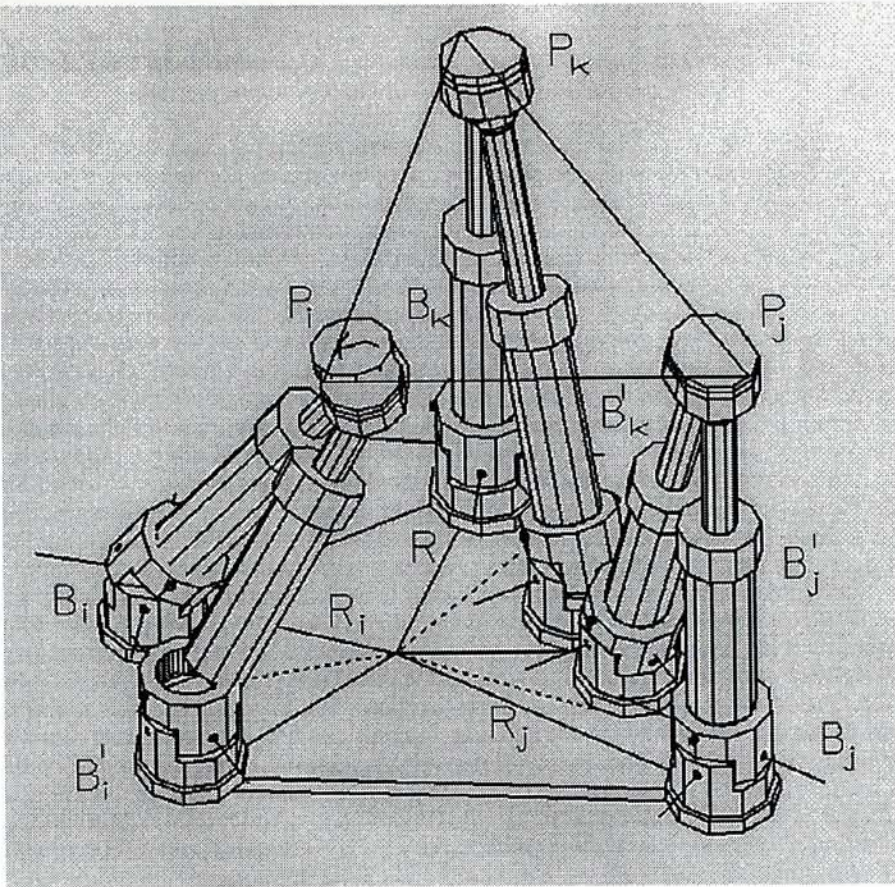


Figure 3.10 Configuration Singularity of the New Model Platform-type Parallel Manipulator Defined by Kong et al. Identified by Equations (3.39)

### 3.5 A New Class of 6-SPS Platform-Type Parallel Manipulator

Based on the ideal of the new model defined by Kong et al., we would like to modify the shape of the base platform of the model in order to observe whether the Forward Rate Kinematics Based method is able to identify the configuration singularity and the ratio  $R/q$  for each variety. The base platform of the model will be replaced by a hexagonal, pentagonal, tetragonal and triangular base respectively. Since the label and the meaning of the parameters and the first six steps in the process are the same for all varieties, we will start from step 7, assuming the value of the parameters.



### 3.5.1 The Hexagonal Base

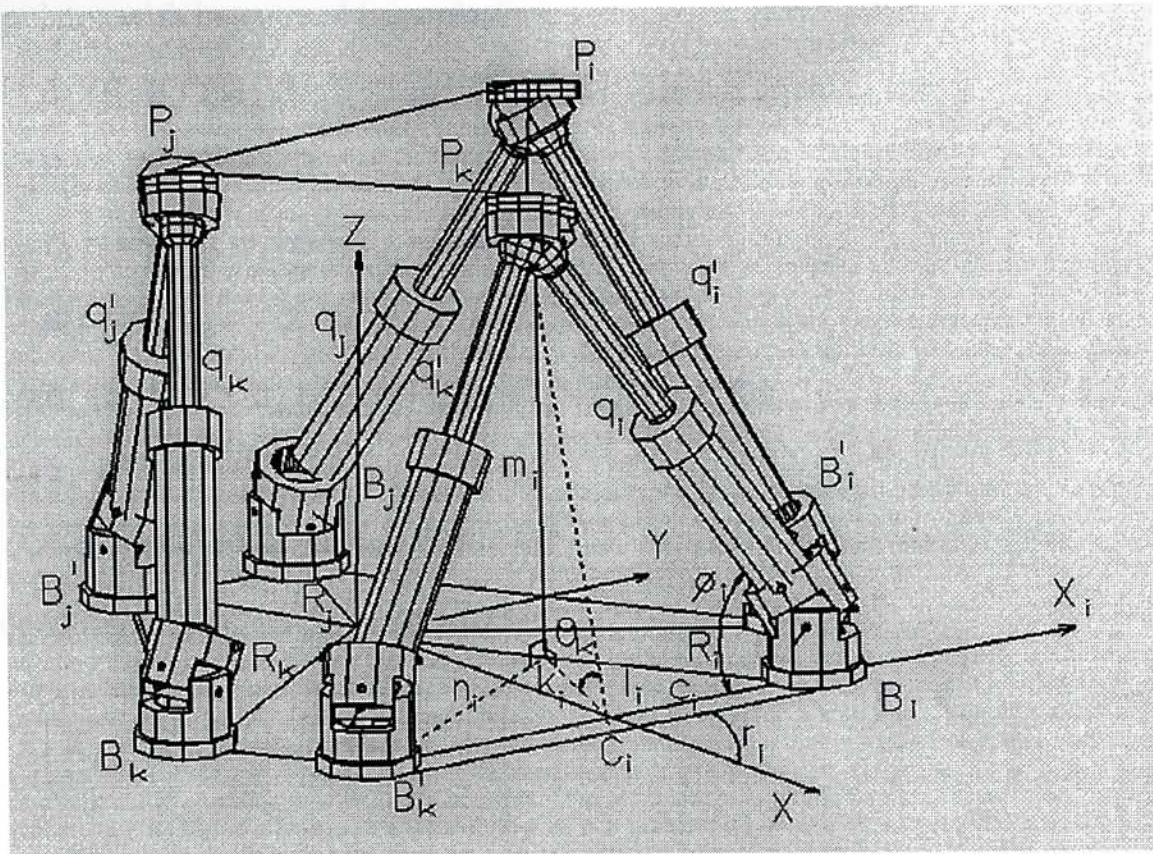


Figure 3.11 The Geometry of the Class of 6 SPS Platform-type Parallel Manipulator with Hexagonal Base

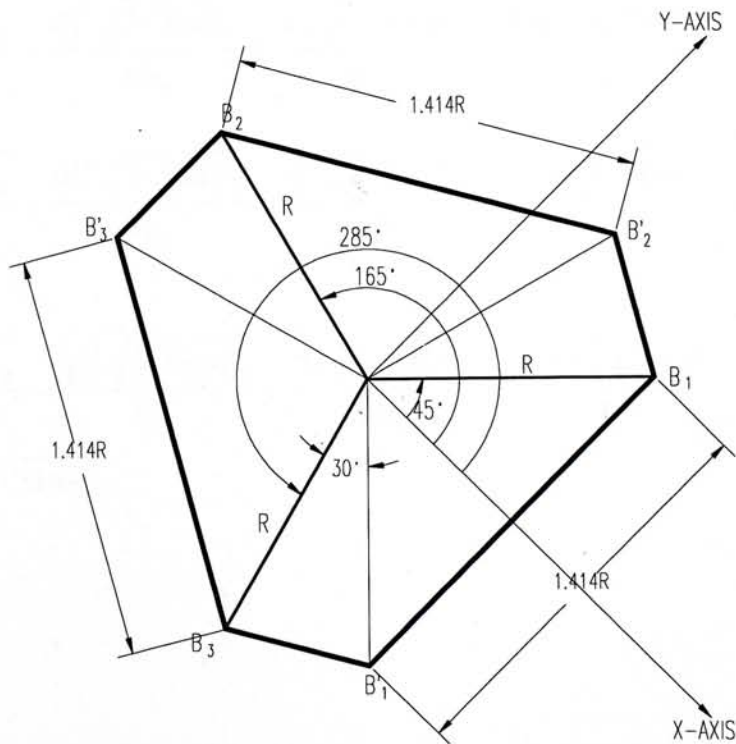


Figure 3.12 The Geometry of the Hexagonal Base Platform

Figure 3.11 and Figure 3.12 are the geometry of a new class of 6 SPS parallel manipulator with hexagonal base platform.

Let :  $d_1$  ( $B_1B_2'$ ),  $d_2$  ( $B_2B_3'$ ) and  $d_3$  ( $B_3B_1'$ ) are not equal to zero

$$R_1 = R_2 = R_3 = R.$$

$$\gamma_1 = \pi/2, \gamma_2 = 7\pi/6, \gamma_3 = 11\pi/6$$

$$\Phi_1 = 0, \Phi_2 = 2\pi/3, \Phi_3 = 4\pi/3$$

$$b_1 (B_1B_1') = b_2 (B_2B_2') = b_3 (B_3B_3') = 1.414R$$

$$\theta_1 = \theta_2 = \pi/2$$

$$\text{coefficient of } \dot{\theta}_j = K_{ij}, \text{ where } i,j=1,3$$

The constraint equations in matrix form:

$$\begin{bmatrix} K_{11} & K_{12} & 0 \\ 0 & K_{22} & K_{23} \\ K_{31} & 0 & K_{33} \end{bmatrix} \cdot \begin{bmatrix} \dot{\theta}_1 \\ \dot{\theta}_2 \\ \dot{\theta}_3 \end{bmatrix} = \begin{bmatrix} N_1 \\ N_2 \\ N_3 \end{bmatrix}$$

where

$$K_{11} = \frac{b_2 \sqrt{3 \cdot \text{Sin}\phi_1}}{4} - \frac{q_2'^2 \sqrt{3 \cdot \text{Sin}\phi_1}}{4b_2} + \frac{q_2^2 \sqrt{3 \cdot \text{Sin}\phi_1}}{4b_2} + \frac{R \sqrt{1.5} \sqrt{\text{Sin}\phi_1}}{2} + \frac{3R \sqrt{\text{Sin}\phi_1}}{2\sqrt{2}}$$

$$K_{12} = \frac{b_1 \sqrt{3 \cdot \text{Sin}\phi_2}}{4} + \frac{q_1'^2 \sqrt{3 \cdot \text{Sin}\phi_2}}{4b_1} - \frac{q_1^2 \sqrt{3 \cdot \text{Sin}\phi_2}}{4b_1} - \frac{R \sqrt{1.5} \sqrt{\text{Sin}\phi_2}}{2} + \frac{3R \sqrt{\text{Sin}\phi_2}}{2\sqrt{2}}$$

$$K_{22} = \frac{b_3 \sqrt{3 \cdot \text{Sin}\phi_2}}{4} - \frac{q_3'^2 \sqrt{3 \cdot \text{Sin}\phi_2}}{4b_3} + \frac{q_3^2 \sqrt{3 \cdot \text{Sin}\phi_2}}{4b_3} + \frac{R \sqrt{1.5} \sqrt{\text{Sin}\phi_2}}{2} + \frac{3R \sqrt{\text{Sin}\phi_2}}{2\sqrt{2}} \\ + q_3 \text{Cos}\theta_3 \sqrt{\text{Sin}\phi_2 \cdot \text{Sin}\phi_3}$$



$$K_{23} = q_2 \cos \theta_3 \sqrt{\sin \phi_2 \cdot \sin \phi_3} - \frac{b_2 \sin \theta_3 \sqrt{3 \cdot \sin \phi_3}}{4} + \frac{q_2'^2 \sin \theta_3 \sqrt{3 \cdot \sin \phi_3}}{4b_2} - \frac{q_2^2 \sin \theta_3 \sqrt{3 \cdot \sin \phi_3}}{4b_2}$$

$$- \frac{R \cdot \sin \theta_3 \sqrt{1.5} \sqrt{\sin \phi_3}}{2} + \frac{3R \cdot \sin \theta_3 \sqrt{\sin \phi_3}}{2\sqrt{2}}$$

$$K_{31} = \frac{-b_3 \sqrt{3 \cdot \sin \phi_1}}{4} + \frac{q_3'^2 \sqrt{3 \cdot \sin \phi_1}}{4b_3} - \frac{q_3^2 \sqrt{3 \cdot \sin \phi_1}}{4b_3} - \frac{R \sqrt{1.5} \sqrt{\sin \phi_1}}{2} + \frac{3R \sqrt{\sin \phi_1}}{2\sqrt{2}}$$

$$- \frac{q_3 \cos \theta_3 \sqrt{\sin \phi_1 \cdot \sin \phi_3}}{2}$$

$$K_{33} = q_1 \cos \theta_3 \sqrt{\sin \phi_1 \cdot \sin \phi_3} + \frac{b_1 \sin \theta_3 \sqrt{3 \cdot \sin \phi_3}}{4} - \frac{q_1'^2 \sin \theta_3 \sqrt{3 \cdot \sin \phi_3}}{4b_2} + \frac{q_1^2 \sin \theta_3 \sqrt{3 \cdot \sin \phi_3}}{4b_1}$$

$$+ \frac{R \cdot \sin \theta_3 \sqrt{1.5} \sqrt{\sin \phi_3}}{2} + \frac{3R \cdot \sin \theta_3 \sqrt{\sin \phi_3}}{2\sqrt{2}}$$

The singularity condition for the manipulator is:

$$\text{Det [K]} = K_{11} K_{22} K_{33} + K_{31} K_{12} K_{23} = 0 \quad (3.40)$$

$$(q_2 (2\sqrt{3} \cos \phi_2) - (3\sqrt{2} + \sqrt{6}) R) \cdot$$

$$4b_2 q_2 \sin \phi_2 \cdot \cos \theta_3 + 2\sqrt{3} \cdot b_2 \cdot q_2 \cos \phi_2 \sin \theta_3 + (3\sqrt{2} \cdot b_2 \cdot R + \sqrt{6} \cdot b_2 R) \sin \theta_3 = 0$$

Since  $R \neq 0$ , this condition can be rewritten as

$$\tan \theta_3 = \frac{q_2 \sin \phi_2}{1.673 R - 30.618} \quad (3.41)$$

$$\text{where } \cos \phi_2 = 35.355 / q_1$$

Configurations singularity identified by Equation.(3.41) is shown in Figure 3.13 in which the  $k$  and  $k'$  th prismatic joint axis is coplanar with the point  $P_a$  which is located at the moving platform. The end-effector of the manipulator gains one more degree of freedom and loses its stability when a force is perpendicularly applied to the  $k$ th joint (ball joint).

3.5.2 The second part of the singularity condition shows the relationship between the radius and the length of the sub-chain.

$$(q_2(2\sqrt{3} \cos\phi_2) - (3\sqrt{2} + \sqrt{6}) R) = 0$$

$$\text{where } \cos\phi_2 = 1$$

$$R / q_i \geq 0.517 \tag{3.42}$$

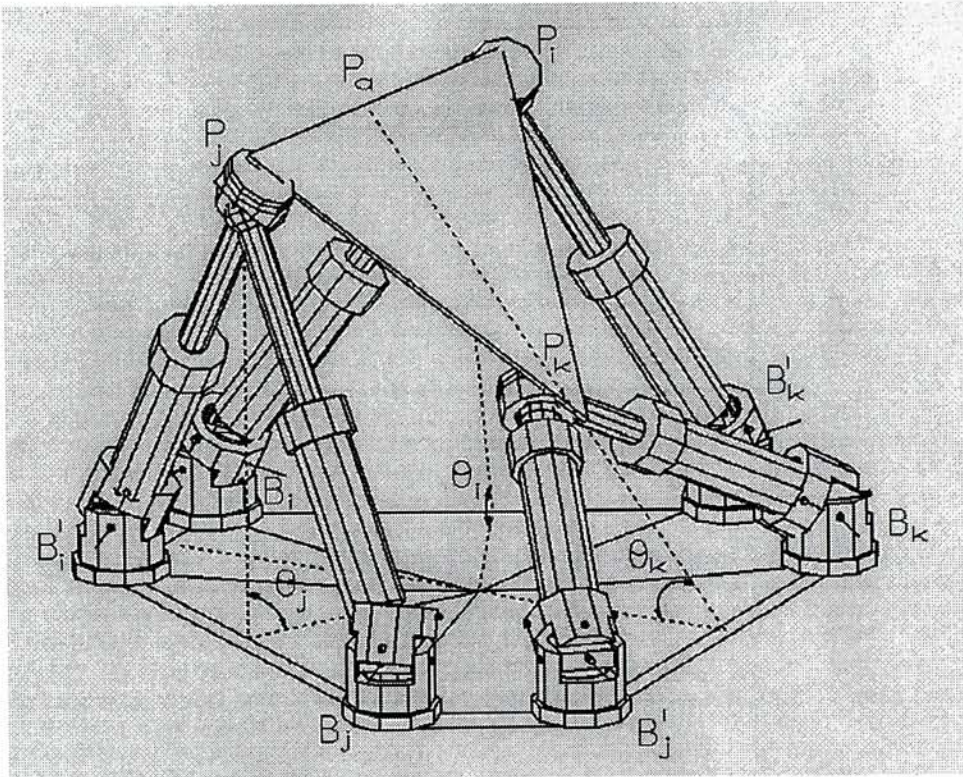


Figure 3.13 Configuration Singularity of Class 6 SPS Parallel Manipulator with Hexagonal Base Platform Identified by Equation (3.41)



### 3.5.2 The Pentagonal Base

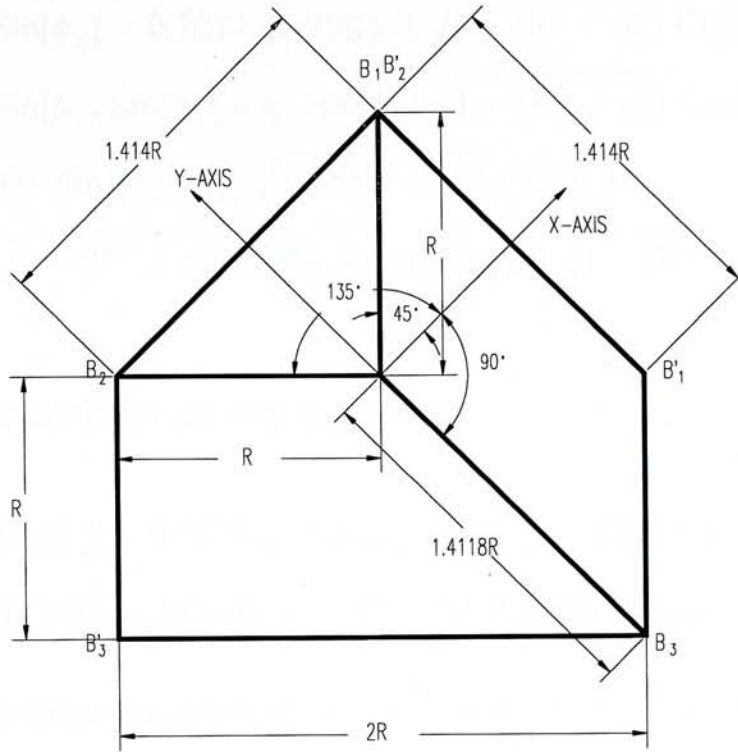


Figure 3.14 The Geometry of the Pentagonal Base Platform

Let :  $d_1 (B_1B_2') = 0$ ,  $d_2 (B_2B_3')$  and  $d_3 (B_3B_1')$  are not equal to zero

$$R_1 = R_2 = R, R_3 = 1.412R.$$

$$\gamma_1 = \pi/2, \gamma_2 = 0, \gamma_3 = \pi / 4$$

$$\Phi_1 = \pi / 4, \Phi_2 = 3\pi / 4, \Phi_3 = 3\pi / 2$$

$$b_1 (B_1B_1') = b_2 (B_2B_2') = 1.414R, b_3 (B_3B_3') = 2R$$

$$\theta_1 = \theta_2 = \pi / 2$$

$$\text{coefficient of } \dot{\theta}_j = K_{ij}, \text{ where } i,j=1,3$$

The constraint equations in matrix form is:

$$\begin{bmatrix} K_{11} & K_{12} & 0 \\ 0 & K_{22} & K_{23} \\ K_{31} & 0 & K_{33} \end{bmatrix} \begin{bmatrix} \dot{\theta}_1 \\ \dot{\theta}_2 \\ \dot{\theta}_3 \end{bmatrix} = \begin{bmatrix} N_1 \\ N_2 \\ N_3 \end{bmatrix}$$

where

$$K_{11} = 1.464 R \sin[\phi_1]$$

$$K_{12} = 1.464 R \sin[\phi_2]$$

$$K_{22} = 2.8266 R \sin[\phi_2] - 0.7071 q_3 \sin[\phi_2] \sqrt{1 - (R^2 / q_3^2)} \cos[\theta_3]$$

$$K_{23} = 1.9636 R \sin[\phi_3] \sin[\theta_3] - q_2 \sin[\phi_2] \sqrt{1 - (R^2 / q_3^2)} \cos[\theta_3]$$

$$K_{31} = 2 R + 0.7071 \sin[\phi_1] - q_3 \sqrt{1 - (R^2 / q_3^2)} \cos[\theta_3]$$

$$K_{33} = 1.9638 R \sqrt{1 - (R^2 / q_3^2)} \sin[\phi_3] - q_1 \sin[\phi_1] \sqrt{1 - (R^2 / q_3^2)} \cos[\theta_3]$$

The singularity condition for the manipulator is:

$$\begin{aligned} & ( 1.414 R \sin[\phi_1] - 0.7071 q_3 \sin[\phi_1] \sin[\phi_3] \cos[\theta_3] ) \times \\ & ( -q_2 \sin[\phi_2] \sin[\phi_3] \cos[\theta_3] + 1.96364 R \sin[\phi_3] \sin[\theta_1] ) = 0 \end{aligned}$$

Since  $R \neq 0$ , this configuration singularity and the relationship between  $R$  and  $q$  are:

$$1.414 R \sin[\phi_1] - 0.7071 q_3 \sin[\phi_1] \sin[\phi_3] \cos[\theta_3] = 0$$

$$1.414 R = 0.7071 q_3 \sin[\phi_3] \cos[\theta_3]$$

When  $\sin[\phi_3]$  and  $\cos[\theta_3] = 1$

$$\tan[\theta_3] = \frac{q_2 \sin[\phi_2]}{1.96364 R} \quad (3.43)$$

$$R / q_3 \geq 0.5 \quad (3.44)$$

The result is similar to the one with hexagonal base, and the configuration singularity is shown in Fig 3.15.



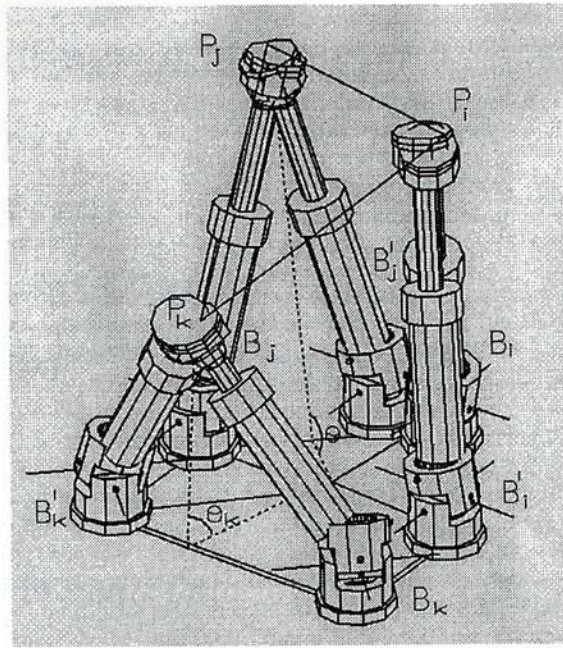


Figure 3.15 Configuration Singularity of Class 6 SPS Parallel Manipulator with Pentagonal Base Platform Identified by Equation (3.43)

### 3.5.3 The Tetragonal Base

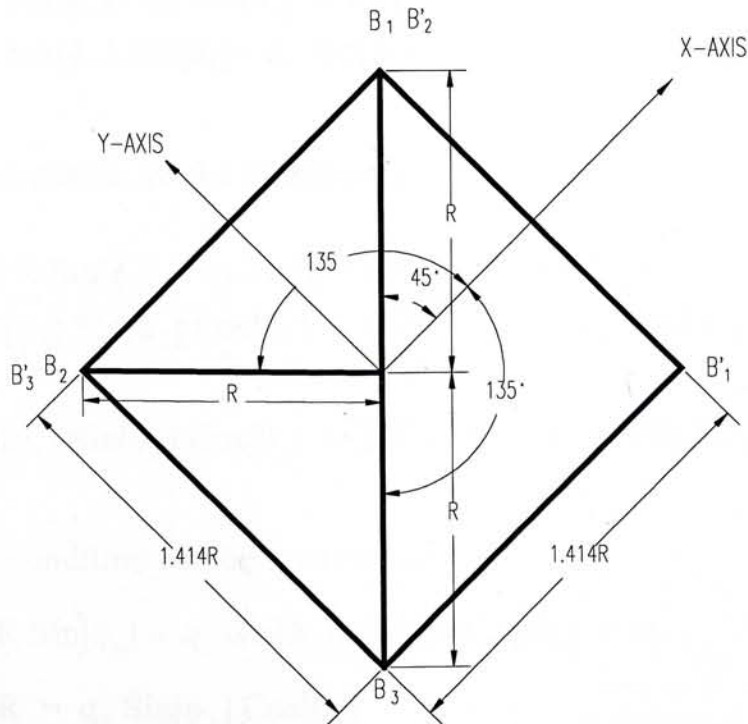


Figure 3.16 The Geometry of the Tetragonal Base Platform

Let :  $d_1 (B_1B_2') = d_2 (B_2B_3') = 0, d_3 (B_3B_1') \neq 0$

$$R_1 = R_2 = R_3 = R.$$

$$\gamma_1 = \pi/2, \gamma_2 = 0, \gamma_3 = 0$$

$$\Phi_1 = \pi / 4, \Phi_2 = 3\pi / 4, \Phi_3 = 5\pi / 4$$

$$b_1 (B_1B_1') = b_2 (B_2B_2') = b_3 (B_3B_3') = 1.414R$$

$$\theta_1 = \theta_2 = \pi / 2$$

coefficient of  $\dot{\theta}_j = K_{ij}$ , where  $i,j=1,3$

The constraint equations in matrix form:

$$\begin{bmatrix} K_{11} & K_{12} & 0 \\ 0 & K_{22} & K_{23} \\ K_{31} & 0 & K_{33} \end{bmatrix} \cdot \begin{bmatrix} \dot{\theta}_1 \\ \dot{\theta}_2 \\ \dot{\theta}_3 \end{bmatrix} = \begin{bmatrix} N_1 \\ N_2 \\ N_3 \end{bmatrix}$$

where

$$K_{11} = 1.4638 R \sin[\phi_1]$$

$$K_{12} = 1.4636 R \sin[\phi_2]$$

$$K_{22} = 2.2204 R \sin[\phi_2]$$

$$K_{23} = 0.7071 R \sin[\phi_3] \sin[\theta_3] - q_2 \sin[\phi_2] \sin[\phi_3] \cos[\theta_3]$$

$$K_{31} = 2.1708 R \sin[\phi_1] - q_3 \sin[\phi_1] \sin[\phi_3] \cos[\theta_3]$$

$$K_{33} = 2.1708 R \sin[\phi_3] \sin[\theta_3] - q_1 \sin[\phi_1] \sin[\phi_3] \cos[\theta_3]$$

The singularity condition for the manipulator is:

$$\begin{aligned} & ( 2.17082 R \sin[\phi_1] - q_3 \sin[\phi_1] \sin[\phi_3] \cos[\theta_3] ) \times \\ & ( -q_2 \sin[\phi_2] \sin[\phi_3] \cos[\theta_3] + 0.7071 R \sin[\phi_3] \sin[\theta_3] ) = 0 \end{aligned}$$

Or

$$( -q_1 \sin[\phi_1] \sin[\phi_3] \cos[\theta_3] + 2.17082 R \sin[\phi_3] \sin[\theta_3] ) = 0$$

Since  $R \neq 0$ , this condition can be rewritten as

$$2.17082 R \sin[\phi_1] - q_3 \sin[\phi_1] \sin[\phi_3] \cos[\theta_3] = 0$$

$$2.17082 R = q_3 \sin[\phi_3] \cos[\theta_3]$$

The configuration singularity and relationship between R and q are :

when  $\sin[\phi_3]$  and  $\cos[\theta_3] = 1$ :



3.5.4  $R/q_1 \geq 0.4607$  Base

$$-q_2 \sin[\phi_2] \sin[\phi_3] \cos[\theta_3] + 0.7071 R \sin[\phi_3] \sin[\theta_3] = 0$$

$$\tan[\theta_3] = \frac{q_2 \sin[\phi_2]}{0.7071 R} \quad (3.45)$$

Alternatively :

$$-q_1 \sin[\phi_1] \sin[\phi_3] \cos[\theta_3] + 2.17082 R \sin[\phi_3] \sin[\theta_3] = 0$$

$$\tan[\theta_3] = \frac{q_1 \sin[\phi_1]}{2.17082 R} \quad (3.46)$$

The configuration singularity, which is identified by Equation (3.45), is shown in Figure 3.17.

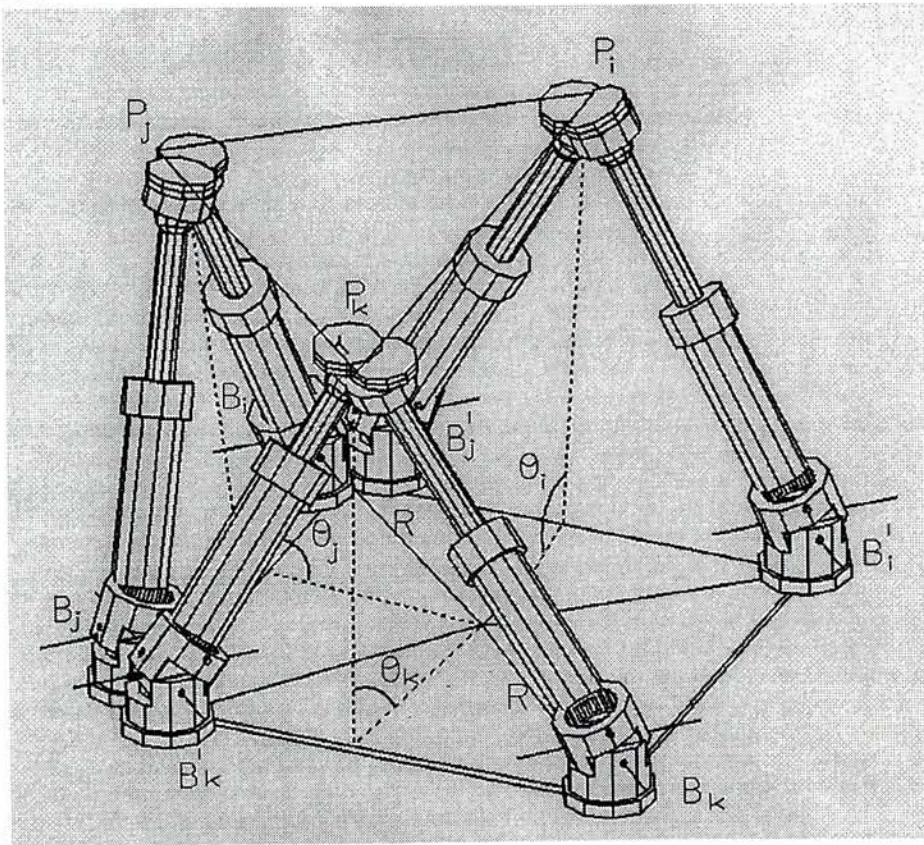


Figure 3.17 Configuration Singularity of Class 6 SPS Parallel Manipulator with Tetragonal Base Platform Identified by Equation (3.45)

### 3.5.4 The Triangular Base

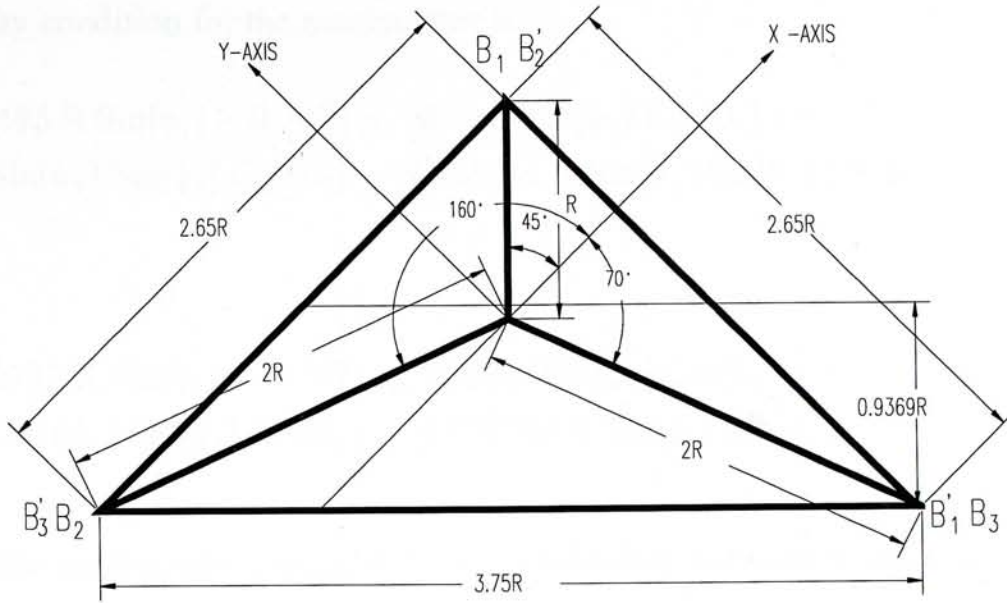


Figure 3.18 The Geometry of the Triangular Base Platform

Let :  $d_1 (B_1B_2') = d_2 (B_2B_3') = d_3 (B_3B_1') = 0$

$R_1 = R, R_2 = R_3 = 2.068R.$

$\gamma_1 = \pi/2, \gamma_2 = 0, \gamma_3 = \pi / 4$

$\Phi_1 = \pi / 4, \Phi_2 = 8\pi / 9, \Phi_3 = 29\pi / 18$

$b_1 (B_1B_1') = b_2 (B_2B_2') = 2.65R, b_3 (B_3B_3') = 3.748R$

$\theta_1 = \theta_2 = \pi / 2$

coefficient of  $\dot{\theta}_j = K_{ij},$  where  $i,j=1,3$

The constraint equations in matrix form is:

$$\begin{bmatrix} K_{11} & K_{12} & 0 \\ 0 & K_{22} & K_{23} \\ K_{31} & 0 & K_{33} \end{bmatrix} \cdot \begin{bmatrix} \dot{\theta}_1 \\ \dot{\theta}_2 \\ \dot{\theta}_3 \end{bmatrix} = \begin{bmatrix} N_1 \\ N_2 \\ N_3 \end{bmatrix}$$

where

$K_{11} = 1.3273 R \text{ Sin}[\phi_1]$

$K_{12} = 1.3273 R \text{ Sin}[\phi_2]$

$K_{22} = 1.3273 R \text{ Sin}[\phi_2] - 0.7071 q_3 \text{ Sin}[\phi_2] \text{ Sin}[\phi_3] \text{ Cos}[\theta_3]$

$K_{23} = 0.9369 R \text{ Sin}[\phi_3] \text{ Sin}[\theta_3] - q_2 \text{ Sin}[\phi_2] \text{ Sin}[\phi_3] \text{ Cos}[\theta_3]$

$K_{31} = 1.3250 R \text{ Sin}[\phi_1] - 0.7071 q_3 \text{ Sin}[\phi_1] \text{ Sin}[\phi_3] \text{ Cos}[\theta_3]$



$$K_{33} = 0.9379 R \sin[\phi_3] \sin[\theta_3] - q_1 \sin[\phi_1] \sin[\phi_3] \cos[\theta_3]$$

The singularity condition for the manipulator is:

$$(1.32495 R \sin[\phi_1] - 0.7071 q_3 \sin[\phi_1] \sin[\phi_3] \cos[\theta_3]) \times (-q_2 \sin[\phi_2] \sin[\phi_3] \cos[\theta_3] + 0.936916 R \sin[\phi_3] \sin[\theta_3]) = 0$$

Or

$$(1.32732 R \sin[\phi_2] - 0.7071 q_3 \sin[\phi_2] \sin[\phi_3] \cos[\theta_3]) \times (-q_1 \sin[\phi_1] \sin[\phi_3] \cos[\theta_3] + 0.937903 R \sin[\phi_3] \sin[\theta_3]) = 0$$

Since  $R \neq 0$ , the configuration singularity and relationship between  $R$  and  $q$  are:

$$\begin{aligned} 1.32495 R \sin[\phi_1] - 0.7071 q_3 \sin[\phi_1] \sin[\phi_3] \cos[\theta_3] &= 0 \\ 1.32495 R &= 0.7071 q_3 \sin[\phi_3] \cos[\theta_3] \end{aligned}$$

When  $\sin[\phi_3]$  and  $\cos[\theta_3] = 1$

$$\tan[\theta_3] = \frac{q_2 \sin[\phi_2]}{0.936916 R} \quad (3.47)$$

$$R / q_1 \geq 0.5337$$

Alternatives:

$$\begin{aligned} 1.32762 R \sin[\phi_2] - 0.7071 q_3 \sin[\phi_2] \sin[\phi_3] \cos[\theta_3] &= 0 \\ 1.32732 R &= 0.7071 q_3 \sin[\phi_3] \cos[\theta_3] \end{aligned}$$

When  $\sin[\phi_3]$  and  $\cos[\theta_3] = 1$

$$\tan[\theta_3] = \frac{q_1 \sin[\phi_1]}{0.937903 R} \quad (3.48)$$

$$R / q_1 \geq 0.5327$$

The configuration singularity is identified by equation (3.47) and is shown in Figure 3.19.

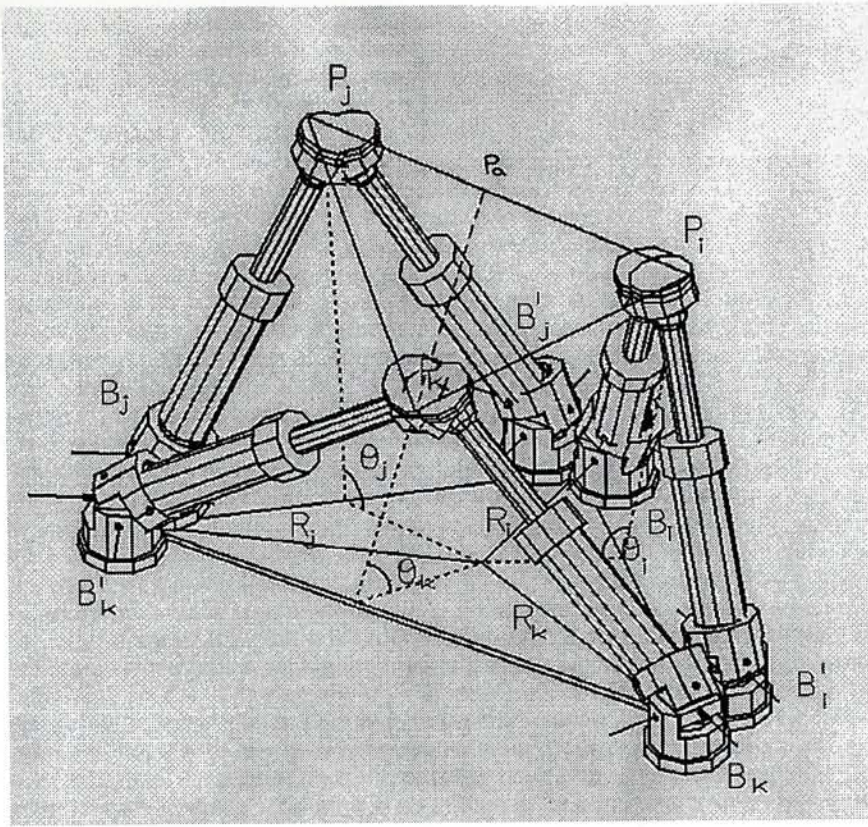


Figure 3.19 Configuration Singularity of Class 6 SPS Parallel Manipulator with Triangular Base Platform Identified by Equation. (3.47)

It shows that even the shape of the base platform is different from each other, we can still use the same formulation of position and velocities matrices to find out the general expression to identify the configuration singularity and calculate the value of the ratio  $R/q$ . It should be pointed out that all different shapes of the base platform mentioned previously belong to the same class of 6-SPS platform-type parallel manipulator. The formulation of the general expression for that class 6-SPS are based on the two matrices : the position matrix  $P_i$  and velocities matrix  $V_{P_i}$ . Their general forms are shown as follows : ( where  $i = 1,3$ )

$$P_i = \begin{bmatrix} R_i \cos[\Phi_i] - q_i W_{1i} \cos[\gamma_i] - q_i W_{2i} \sin[\gamma_i] \cos[\theta_i] \\ R_i \sin[\Phi_i] - q_i W_{1i} \sin[\gamma_i] - q_i W_{2i} \cos[\gamma_i] \cos[\theta_i] \\ q_i W_{2i} \sin[\theta_i] \end{bmatrix}$$

where

$$W_{1i} = \cos\phi_i = \frac{q_i^2 + b_i^2 - q_i'^2}{2b_i q_i} \quad \text{and}$$



3.6 Summary

$$W_{2i} = \text{Sin}\phi_i = \left[ 1 - \left( \frac{q_i^2 + b_i^2 - q_i'^2}{2b_i q_i} \right)^2 \right]^{1/2}$$

By grouping the terms in the velocity Jacobian matrix, the forward rate kinematics based method can be used to identify the configuration singularity in this class of 6-SPS platform-type parallel manipulator. The velocity Jacobian matrix is given by

$$V_{pi} = \begin{bmatrix} -\text{Cos}\gamma_i (\dot{q}_i W_{1i} + q_i \dot{W}_{1i}) - \text{Sin}\gamma_i (\dot{q}_i W_{2i} \text{Cos}\theta_i + q_i \dot{W}_{2i} \text{Cos}\theta_i - q_i W_{2i} \dot{\theta} \text{Sin}\theta_i) \\ -\text{Sin}\gamma_i (\dot{q}_i W_{1i} + q_i \dot{W}_{1i}) - \text{Cos}\gamma_i (\dot{q}_i W_{2i} \text{Cos}\theta_i + q_i \dot{W}_{2i} \text{Cos}\theta_i - q_i W_{2i} \dot{\theta} \text{Sin}\theta_i) \\ \dot{q}_i W_{2i} \text{Sin}\theta_i + q_i \dot{W}_{2i} \text{Sin}\theta_i + q_i W_{2i} \dot{\theta} \text{Cos}\theta_i \end{bmatrix}$$

where

$$\dot{W}_{1i} = \frac{2q_i(q_i \dot{q}_i - q_i' \dot{q}_i') - \dot{q}_i(q_i^2 + b_i^2 - q_i'^2)}{2b_i q_i^2} \quad \text{and}$$

$$\dot{W}_{2i} = \frac{\dot{q}_i(q_i^2 + b_i^2 - q_i'^2) - 2q_i(q_i \dot{q}_i - q_i' \dot{q}_i')}{2q_i [4b_i^2 q_i^2 - (q_i^2 + b_i^2 - q_i'^2)^2]^{1/2}}$$

In other words, it is demonstrated that the general expression for identifying configuration singularity in this class of 6-SPS platform-type parallel manipulator can be formed by using the Forward Rate Kinematics based Method.

## Chapter 4

### 3.6 Summary

By grouping the results from section 3.1 to section 3.5, we observed that the Forward Rate Kinematics Based method is able to identify the configuration singularity for different cases. It can also be used to deduce a simple general expression of configuration singularity for certain cases. Moreover, the method helps us to show that there exists a ratio, a major factor affecting configuration singularity for platform-type parallel manipulator. From the reduced singularity condition (e.g. Equation 3.15), one can see that configuration singularity may exist if the value of the ratio is smaller than a certain bounded constant. That means, if the value of the ratio does not fall below the critical value, by carefully determine the length of links and the base radius in the design stage, then the configuration singularity would be eliminated. Therefore this ratio can be used as a guideline for designing the improved platform-type parallel manipulators.



# Chapter 4

## Numerical Analysis

In chapter three, it is shown that the Forward Rate Kinematics Based method is able to identify configuration singularity of platform-type parallel manipulators. In addition, the method also returns the ratio  $R/q$  which is very useful in the control of configuration singularity. In this chapter, we will further analyze the relationship between the parameters involved in identifying the configuration singularity by using the class of 6 SPS parallel manipulator with hexagonal base platform. We will also suggest a method to determine the critical value of the ratio  $R/q$  for certain cases discussed in the last chapter.

### 4.1 Parameter Analysis

The 6 SPS parallel manipulator with hexagonal base platform, which had been mentioned in Section 3.5.1 (Figure 3.8 and 3.9), has the following parameters:

- $d_1, d_2$  and  $d_3$  are not equal to zero,
- $\Phi_1 = 0, \Phi_2 = 2\pi / 3, \Phi_3 = 4\pi / 3,$
- $\gamma_1 = \pi / 2, \gamma_2 = 7\pi / 6, \gamma_3 = 11\pi / 6,$
- $R_1 = R_2 = R_3 = R$
- $b_1 = b_2 = b_3 = 1.414R,$
- $\theta_1, \theta_2$  and  $\theta_3$  are three intermediate variables required to be solved for the configuration singularity. We will assign arbitrary values to one or two of them in order to simplify the process. The possible range of  $\theta_i$  is  $0^\circ - 180^\circ$ .

By using the Forward Rate Kinematics Based method, we can determine the singularity condition:

$$\text{Det [K]} = K_{11} K_{22} K_{33} + K_{31} K_{12} K_{23} = 0$$

#### 4.1.1 One Unknown Variable (Assign numerical values to $\theta_1$ and $\theta_2$ )

Substituting the parameters in the assumptions and let the value of  $\theta_1 = \theta_2 = \pi / 2$ , the following reduced expressions of singularity conditions can be obtained :

$$\frac{R}{q_2} = \frac{2\sqrt{3} \text{Cos}[\phi_2]}{(3\sqrt{2} + \sqrt{6})} \quad (4.1)$$

$$\text{Cos}[\theta_3] = \frac{(3\sqrt{2} + \sqrt{6}) R - 2\sqrt{3} q_3 \text{Cos}[\phi_3]}{2 q_3 \text{Sin}[\phi_3]} \quad (4.2)$$

$$\text{Tan}[\theta_3] = \frac{4 \text{Sin}[\phi_1]}{(3\sqrt{2} + \sqrt{6}) (R / q_1) - 2\sqrt{3} \text{Cos}[\phi_1]} \quad (4.3)$$

Equation (4.1) shows the relationship between the ratio  $R/q_i$  and the angle  $\phi_2$ . The curve in Figure 4-1 illustrates the conditions in which the configuration singularity may occurs. Since both  $R$  and  $q_i$  are greater than zero, the valley portion of the curve does not actually exists. The maximum value of the ratio is 0.518. This means that there is no configuration singularity if the ratio is greater than 0.518. This maximum value is called the critical value of ratio  $R/q$ .

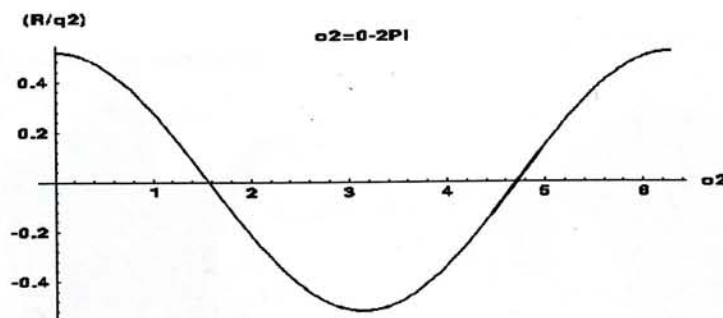


Figure 4-1



Equation (4.2) is plotted in Figure (4-2a) - (4-2c) with different values of  $q$ . It can be observed that the opportunity of the configuration singularity is increased as the value of  $q$  increased when the radius is fixed. By varying the values of both  $R$  and  $q$ , Figure 4-3 (Equation 4.3), shows that the curve of the singularity is inversely proportional to the value of the ratio  $R/q$ . The number of configuration singularity tends to zero as the value of ratio  $R/q$  increased.

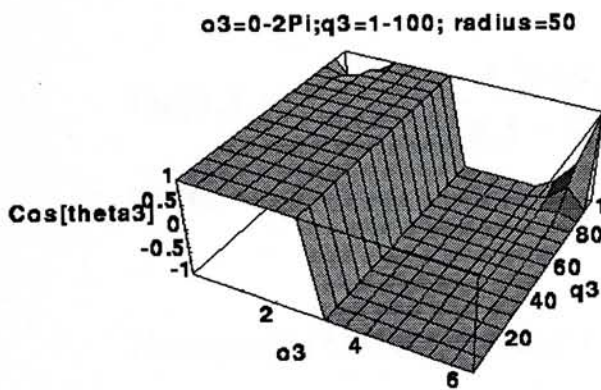


Figure 4-2a

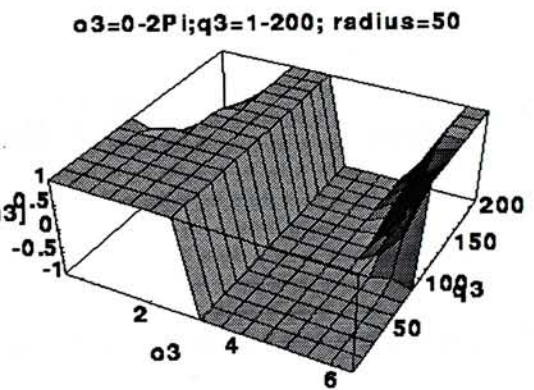


Figure 4-2b

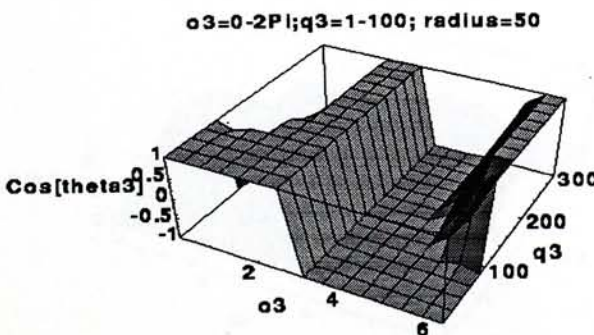


Figure 4-2c

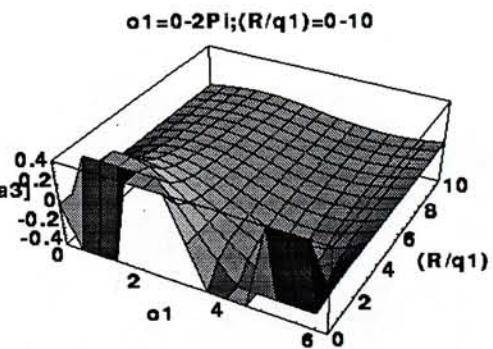


Figure 4-3

### 4.1.2 Two Unknown Variables (Assign numerical value to $\theta_1$ )

Let  $\theta_1 = \pi / 2$  and keep  $\theta_2$  and  $\theta_3$  as unknown variables, the reduced expressions of singularity conditions are:

$$\frac{R}{q_2} = \frac{(\sin[\phi_2] \sin[\theta_2 - \theta_3] - 2\sqrt{3} \sin[\theta_3] \cos[\phi_2]) + Y_3}{(3\sqrt{2} - \sqrt{6}) \sin[\theta_3]} \quad (4.4)$$

where  $Y_3 = 3 \sin[\phi_2] \sin[\theta_2 + \theta_3]$

$$\tan[\theta_2] = \frac{4 \sin[\phi_1]}{2\sqrt{3} \cos[\phi_1] + (3\sqrt{2} - \sqrt{6}) (R/q_1)} \quad (4.5)$$

$$\tan[\theta_3] = \frac{4 \sin[\phi_2] \sin[\theta_2]}{2(\sqrt{3} \cos[\phi_2] - \sin[\phi_2] \cos[\theta_2]) + Y_4} \quad (4.6)$$

where  $Y_4 = (3\sqrt{2} - \sqrt{6}) (R/q_2)$

The equations (4.4), (4.5) and (4.6) are displayed in Figures (4-4a) - (4-4c), (4-5) and (4-6a) - (4-6f). The ratio is bounded by a maximum value (1.934), and there is no singularity outside this range. The curves of configuration singularity for  $\theta_2$  and  $\theta_3$  is approaching to zero again as the ratio increased. These properties are very similar to those in sub-section 4.1.1 which involved only one unknown variable.

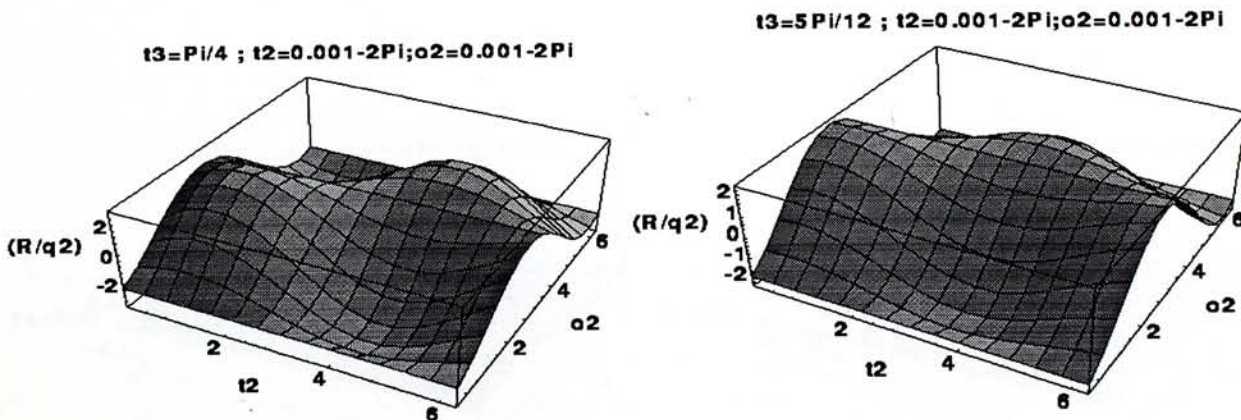


Figure 4-4a

Figure 4-4b



$t_3 = \pi/2 ; t_2 = 0.001 - 2\pi ; \alpha_2 = 0.001 - 2\pi$

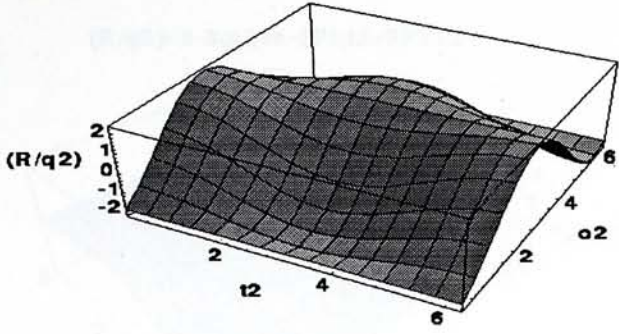


Figure 4-4c

$\alpha_1 = 0 - 2\pi ; (R/q_1) = 0 - 10$

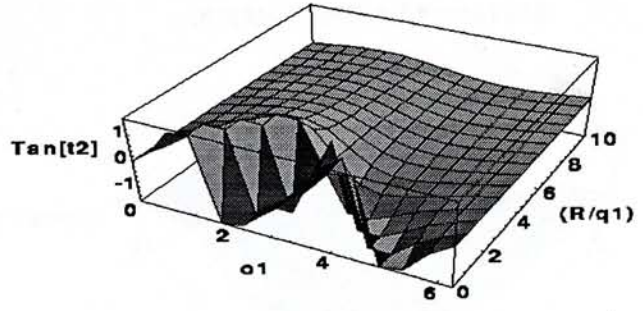


Figure 4-5

$\alpha_2 = 0 - 2\pi ; t_2 = 0 - 2\pi ; (R/q_2) = 0.4$

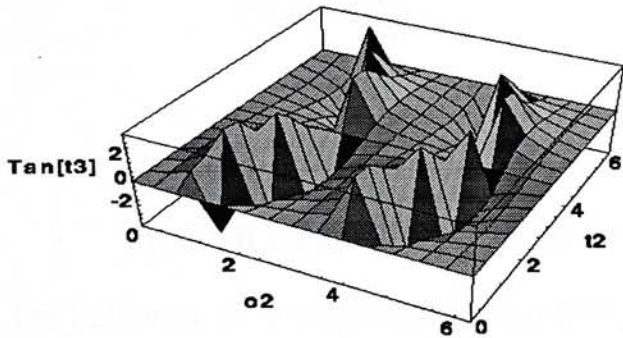


Figure 4-6a

$\alpha_2 = 0 - 2\pi ; t_2 = 0 - 2\pi ; (R/q_2) = 2$

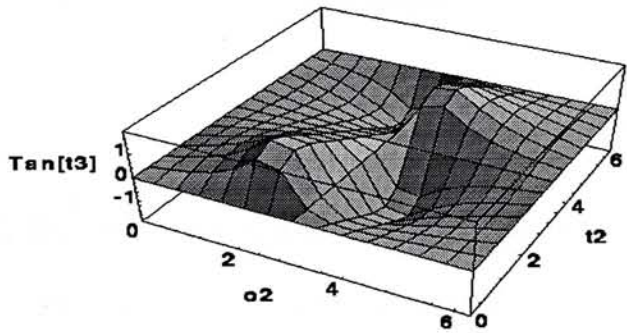


Figure 4-6b

$(R/q_2) = 0 - 3 ; t_2 = 0 - 2\pi ; \alpha_2 = \pi/12$

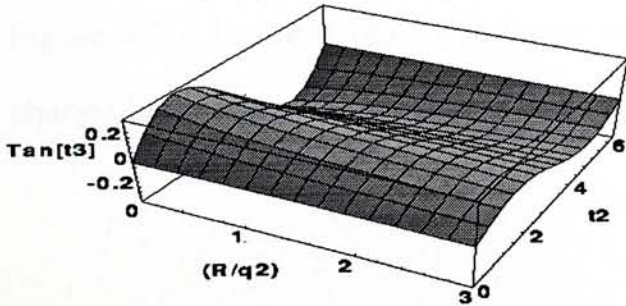


Figure 4-6c

$(R/q_2) = 0 - 3 ; t_2 = 0 - 2\pi ; \alpha_2 = 5\pi/12$

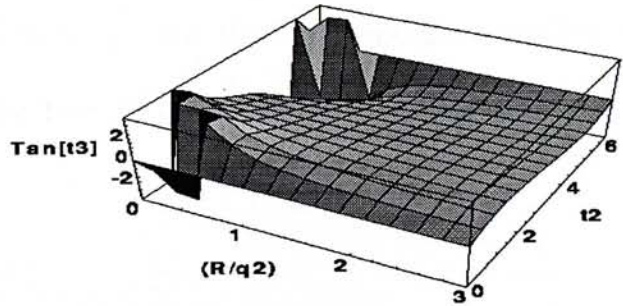


Figure 4-6d

Value of  $\theta_1$   
and  $\theta_2$

The Reduced Singularity Condition

Table 4.1

$\theta_1 = \pi/2$

$(R/q_2)=0-3; \theta_2=0-2\pi; t_2=5\pi/12$

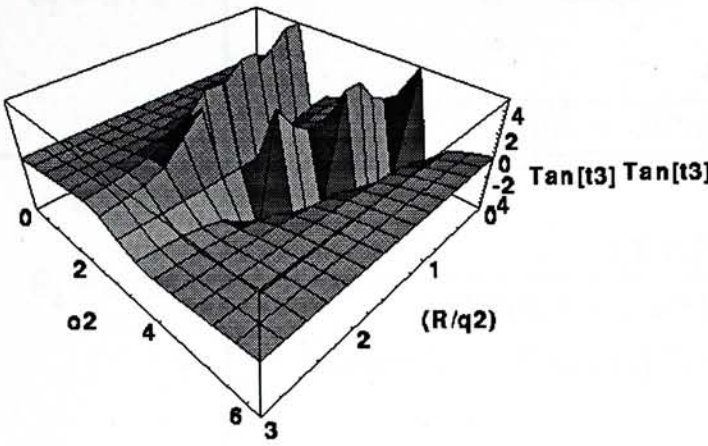


Figure 4-6e

$(R/q_2)=0-3; \theta_2=0-2\pi; t_2=\pi/12$

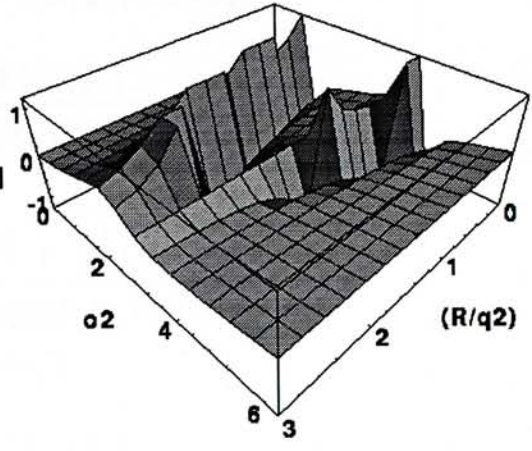


Figure 4-6f

From all these figures, we observe that the ratio  $R/q$  is an important factor to the behavior of configuration singularity. The existence of configuration singularity can be identified by the value of ratio  $R/q$ . And theoretically, configuration singularity can be avoided as the ratio is greater than a critical value.

Before switching to the computation of the ratio, let's have a look on the solutions obtained by assigning five different sets of values to  $\theta_1$  and  $\theta_2$  (Table 4.1, Figure 4.7 - Figure 4.16). The length of link,  $q_3$ , and the intermediate variable,  $\theta_3$ , change in the same step as  $\theta_1$  and  $\theta_2$  and the pace of  $q_3$  is greater than that of  $\theta_3$ .

Table 4.1

The Reduced Singularity Condition

Table 4.1



Value of $\theta_1$ and $\theta_2$	The Reduced Singular Conditions	Equation No.
$\theta_1 = \pi / 2$ $\theta_2 = \pi / 2$	$q_3 = \frac{(3\sqrt{2} + \sqrt{6}) R}{2(\sqrt{3} \text{Cos}[\phi_3] + \text{Sin}[\phi_3] \text{Cos}[\theta_3])}$	4.7
	$\text{Tan}[\theta_3] = \frac{4 \text{Sin}[\phi_1]}{(3\sqrt{2} + \sqrt{6}) (R/q_1) - 2\sqrt{3} \text{Cos}[\phi_1]}$	4.8
$\theta_1 = \pi / 2$ $\theta_2 = \pi / 3$	$q_3 = \frac{3 R (\sqrt{2} + \sqrt{6})}{6 \text{Cos}[\phi_3] + 2 \sqrt{3} \text{Sin}[\phi_3] \text{Cos}[\theta_3] + X_1}$ where $X_1 = 4 \text{Sin}[\phi_3] \text{Sin}[\theta_3]$	4.9
	$\text{Tan}[\theta_3] = \frac{4 \text{Sin}[\phi_1]}{(3\sqrt{2} + \sqrt{6}) (R/q_1) - 2\sqrt{3} \text{Cos}[\phi_1]}$	4.10
$\theta_1 = \pi / 2$ $\theta_2 = \pi / 4$	$q_3 = \frac{\sqrt{3} R}{\sqrt{6} \text{Cos}[\phi_3] + \sqrt{2} \text{Sin}[\phi_3] (\text{Cos}[\theta_3] + 2 \text{Sin}[\theta_3])}$	4.11
	$\text{Tan}[\theta_3] = \frac{4 \text{Sin}[\phi_1]}{(3\sqrt{2} + \sqrt{6}) (R/q_1) - 2\sqrt{3} \text{Cos}[\phi_1]}$	4.12
$\theta_1 = \pi / 2$ $\theta_2 = \pi / 12$	$q_3 = \frac{2 \sqrt{3} R}{(3\sqrt{2} - \sqrt{6}) \text{Cos}[\phi_3] - (\sqrt{2} - \sqrt{6}) \text{Sin}[\phi_3] Y_2 + X_2}$ where $X_2 = 2(\sqrt{2} + \sqrt{6}) \text{Sin}[\phi_3] \text{Sin}[\theta_3]$ and $Y_2 = \text{Cos}[\theta_3]$	4.13
	$\text{Tan}[\theta_3] = \frac{4 \text{Sin}[\phi_1]}{(3\sqrt{2} + \sqrt{6}) (R/q_1) - 2\sqrt{3} \text{Cos}[\phi_1]}$	4.14
$\theta_1 = 5\pi / 12$ $\theta_2 = 5\pi / 12$	$q_3 = \frac{2 (3 + 2\sqrt{3}) R}{(3\sqrt{2} + \sqrt{6}) \text{Cos}[\phi_3] + (\sqrt{2} + \sqrt{6}) \text{Sin}[\phi_3] Z_1 - Z}$ where $Z = 2(\sqrt{2} - \sqrt{6}) \text{Sin}[\phi_3] \text{Sin}[\theta_3]$ and $Z_1 = \text{Cos}[\theta_3]$	4.15
	$\text{Tan}[\theta_3] = \frac{2 (\sqrt{2} + \sqrt{6}) \text{Sin}[\phi_1]}{2 (3\sqrt{2} + \sqrt{6}) (R/q_1) - 4\sqrt{3} \text{Cos}[\phi_1] + Z_2}$ where $Z_2 = 2 (\sqrt{2} - \sqrt{6}) \text{Sin}[\phi_1]$	4.16

Table 4.1 The Reduced Singular Conditions of Five Sample Cases.

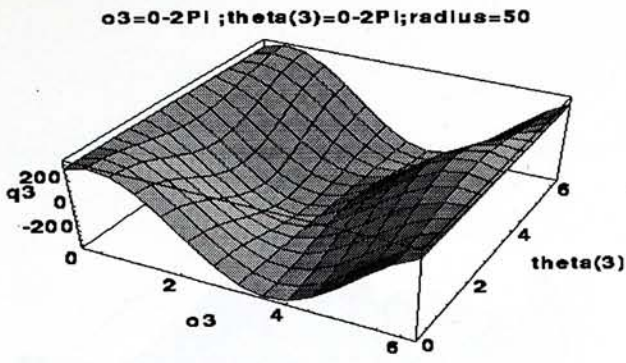


Figure 4-7

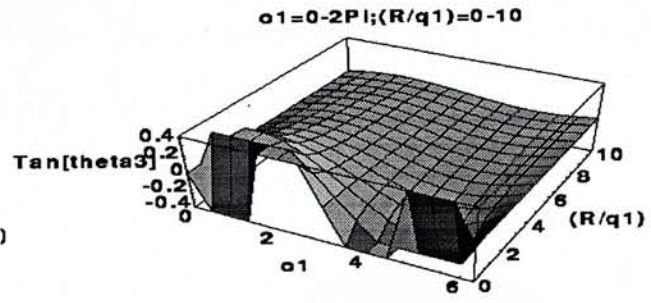


Figure 4-8

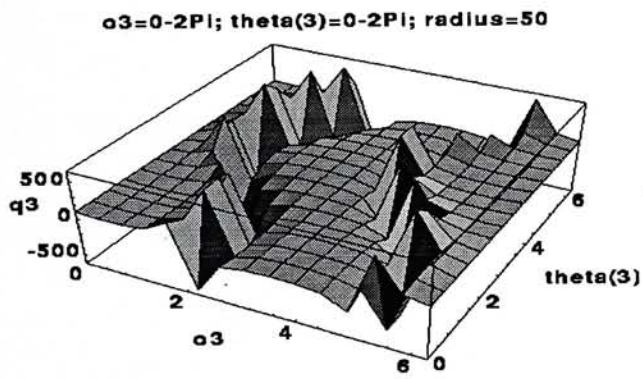


Figure 4-9

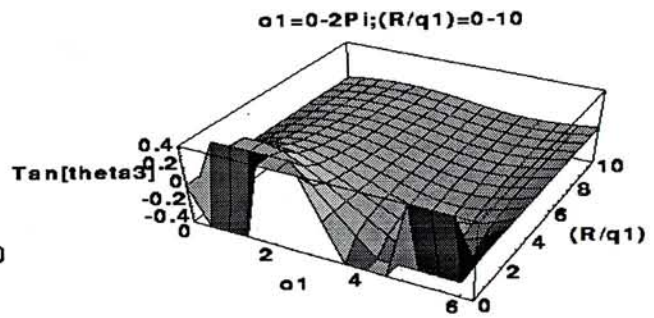


Figure 4-10

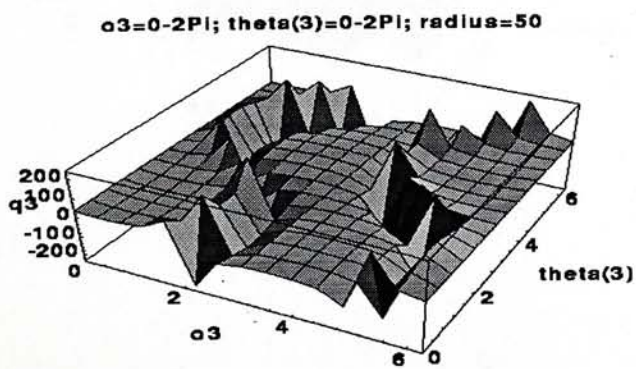


Figure 4-11

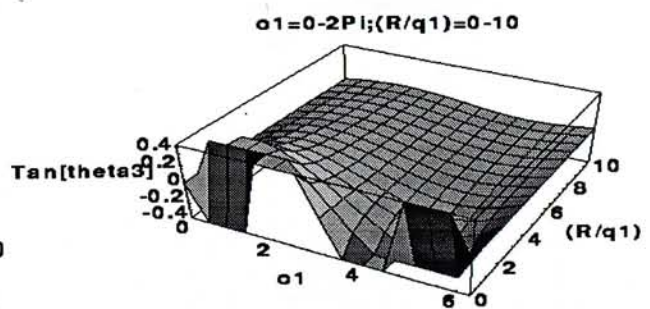


Figure 4-12



## 4.2 Critical Value of Ratio $R/q_1$

$\alpha_3=0-2\pi$ ;  $\theta_3=0-2\pi$ ; radius=50

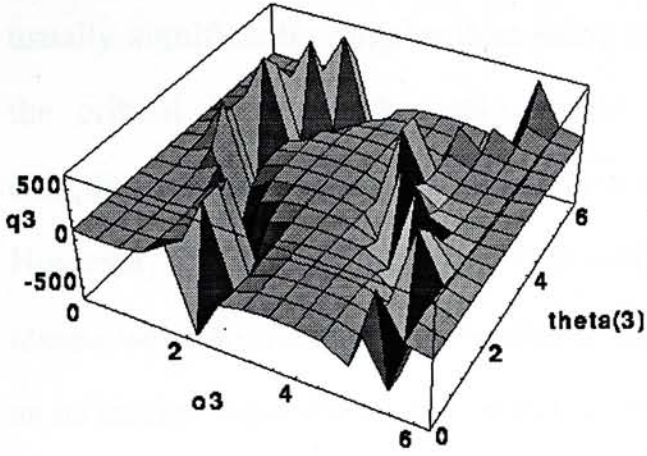


Figure 4-13

$\alpha_1=0-2\pi$ ;  $(R/q_1)=0-10$

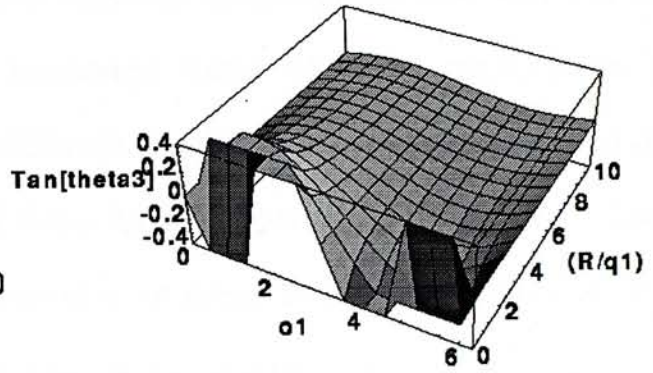


Figure 4-14

$\alpha_3=0-2\pi$ ;  $\theta_3=0-2\pi$ ; radius=50

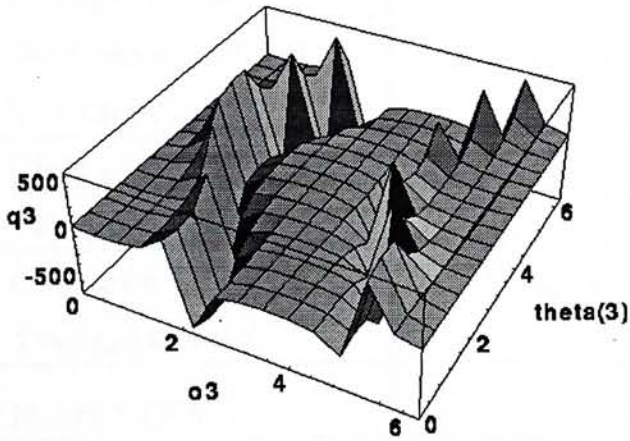


Figure 4-15

$\alpha_1=0-2\pi$ ;  $(R/q_1)=0-10$

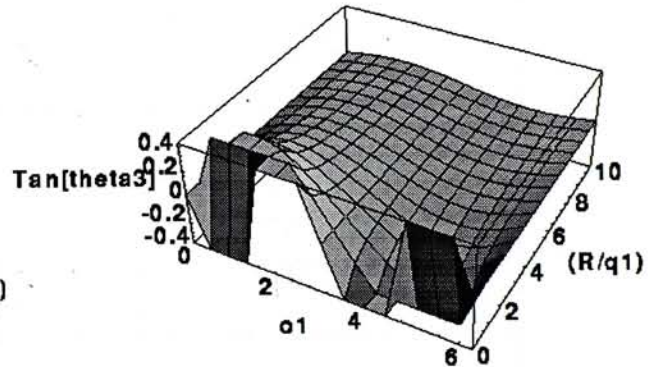


Figure 4-16

## 4.2 Critical Value of Ratio R/q

Table 4.2 shows the value of ratio R/q determined by using one or two unknown variables. The expressions of the ratio by using one unknown variable is usually significantly simpler than using two variables (Equation 4.1 and 4.4). Since the critical value of the ratio is the maximum value of these expressions, a complicated expression may result in a different number from a simple expression. However, the values in column two and three do not show any relationship. That means we cannot use this pair-value to determine an upper bound of the ratio as well as its critical value for the platform-type parallel manipulators.

Class of different platform type parallel Manipulator	Value of ratio R/q with one unknown intermediate variable	Value of ratio R/q with two unknown intermediate variables
Class of 6 SPS with Hexagonal Base	0.518	1.934
Class of 6 SPS with Pentagonal Base	0.500	0.500
New Model defined by Kong et al.	0.512	0.587
Class of 6 SPS with Tetragonal Base	0.461	0.461
Class of 6 SPS with Triangular Base	0.534	0.534
Novel 6 DOF	0.333	0.333
3 DOF with Symmetric Base	0.333	0.333
3 DOF with Non-Symmetric Base	0.380	0.440

Table 4.2 Ratio R/q for Different Class of Platform-type Parallel Manipulators



Table 4.3 lists the values obtained by using the same model and data set as Section 4.1

Value of $\theta_1$ and $\theta_2$	The Expression of R/q	Max. value of R/q
$\theta_1 = \pi / 2$ $\theta_2 = \pi / 2$	$\frac{R}{q_2} = \frac{2\sqrt{3} \text{Cos}[\phi_2]}{(3\sqrt{2} + \sqrt{6})}$	0.518
$\theta_1 = \pi / 2$ $\theta_2 = \pi / 3$	$\frac{R}{q_2} = \frac{2\sqrt{3} \text{Cos}[\phi_2] + \text{Sin}[\phi_2]}{(3\sqrt{2} + \sqrt{6})}$	0.518
$\theta_1 = \pi / 2$ $\theta_2 = \pi / 4$	$\frac{R}{q_2} = \frac{2\sqrt{3} \text{Cos}[\phi_2] + \sqrt{2} \text{Sin}[\phi_2]}{(3\sqrt{2} + \sqrt{6})}$	0.518
$\theta_1 = \pi / 2$ $\theta_2 = \pi / 12$	$\frac{R}{q_2} = \frac{4\sqrt{3} \text{Cos}[\phi_2] + (\sqrt{2} + \sqrt{6}) \text{Sin}[\phi_2]}{2(3\sqrt{2} + \sqrt{6})}$	0.518
$\theta_1 = 5\pi / 12$ $\theta_2 = 5\pi / 12$	$\frac{R}{q_2} = \frac{(2 \text{Cos}[\phi_2]) (3\sqrt{2} + \sqrt{6}) + 12 \text{Sin}[\phi_2]}{(12 + 8\sqrt{3})}$	0.518

Table 4.3 Critical Values of Ratio R/q for the Class of 6 SPS Parallel Manipulator with Hexagonal Base Platform

We observed from Table 4.3 that the critical value of the manipulator remains the same (0.518) for every pairs of  $\theta_1$  and  $\theta_2$ . Since the values of  $\theta_1$  and  $\theta_2$  are chosen randomly in their feasible range, i.e.  $0^\circ \leq \theta_i \leq 180^\circ$ , this number (0.518) can be considered as a general critical value of ratio R/q for this manipulator.

This method is only suitable for those manipulators with symmetric base platform (Table 4.4). For manipulators with non-symmetric base platform (e.g. the model defined by Kong et al. in Section 3.4), the maximum values of the ratio varies as the values of  $\theta_1$  and  $\theta_2$  change. Although the application of the method for determining the critical value for a manipulator is somewhat limited, (only to those

manipulators with symmetric base platform), it provides a useful means for the design of platform-type parallel manipulators, and the avoidance of configuration singularity.

Class of different platform type parallel Manipulator	Value of ratio R/q for $\theta_1 = \pi / 2$ $\theta_2 = \pi / 2$	Value of ratio R/q for another arbitrary value pair	Critical Value
Class of 6 SPS with Hexagonal Base	0.518	0.518	0.518
Class of 6 SPS with Pentagonal Base	0.500	0.500 ( $\theta_1 = \pi / 2$ ) ( $\theta_2 = 5\pi / 12$ )	0.500
New Model defined by Kong et al.	0.5120	1.105 ( $\theta_1 = \pi / 2$ ) ( $\theta_2 = \pi / 3$ )	--
Class of 6 SPS with Tetragonal Base	0.461	0.461 ( $\theta_1 = \pi / 2$ ) ( $\theta_2 = \pi / 3$ )	0.461
Class of 6 SPS with Triangular Base	0.534	0.534 ( $\theta_1 = 5\pi / 12$ ) ( $\theta_2 = \pi / 4$ )	0.534
Novel 6 DOF	0.333	0.333 ( $\theta_1 = \pi / 2$ ) ( $\theta_2 = \pi / 3$ )	0.333
3 DOF with Symmetric Base	0.333	0.333 ( $\theta_1 = \pi / 2$ ) ( $\theta_2 = \pi / 4$ )	0.333
3 DOF with Non-Symmetric Base	0.380	0.440 ( $\theta_1 = \pi / 2$ ) ( $\theta_2 = \pi / 3$ )	--

Table 4.4 Critical Value of Different Class of Platform-type Parallel Manipulators



### 4.3 Summary

In this chapter, we have illustrated and analyzed the effect of ratio  $R/q$  to the existence of the configuration singularity and the way to eliminate it. The ratio can be used as a useful guideline to avoid the configuration singularity in manipulator design. We also suggest a method to determine the critical value of the ratio for the platform-type parallel manipulator with symmetric base platform.

# Chapter 5

## Conclusions and Future Work

### 5.1 Conclusions

In this thesis, the Forward Rate Kinematics based method is applied to three cases : 3 DOF with Symmetric and Non-Symmetric Base, Novel 6 DOF and Class of 6-SPS, to enumerate the configuration singularity of platform-type parallel manipulators.

The basic architecture of the Forward Rate Kinematics Based method is a combination of the velocities of three non-collinear points on the moving platform (end-effector) and the principle of reciprocity of screws. Compared with the Force Decomposition method and the Grassmann Geometry method, this method was chosen for our work because it has the least computational complexity and is most general. The Force Decomposition method involves complicated computation and is only applicable to a simple structured manipulator with a fixed number of kinematic sub-chains. The Grassmann Geometry method is a rule-based method and is unsuitable for analyzing complex manipulators, whose geometry is often impossible to accurately describe by rules. On the other hand, the implementation of the Forward Rate Kinematics Based method is straightforward since it requires only a few passive joint variables. In addition, it can cater for a wide range of platform-type parallel manipulators.

The Forward Rate Kinematics Based method can be used to identify the configuration singularity for both of the new model defined by Kong et al. and the Class of 6 SPS parallel manipulators with different geometric bases (i.e. hexagonal, pentagonal, tetragonal and triangular bases). The formulations of the coordinates and



the velocities of the three non-collinear points are the same, independent of the shapes of the base platform. Moreover, it can be used to derive a simple general expression of configuration singularity for the Novel 6 DOF and 3 DOF platform-type parallel manipulators with a symmetric or non-symmetric base. The general expressions are very useful for further analysis of manipulator parameters (e.g. base radius  $R$ , length link  $q$ ). The work reported in this thesis is, in fact, first of its kind. To our knowledge, no one has ever applied the Forward Rate Kinematics Based method to the above manipulators which involved both elbow joint and prismatic joint structures. Furthermore, based on the enumeration analysis an useful guideline for improving the design of platform-type parallel manipulator is proposed. It is much easier and advantageous for the design engineer to know the configuration singularity early in the design stage. The rule of this guideline is handy and simple.

The result of the analysis revealed that a ratio ,  $R/q$ , of the base radius to the length link is a vital factor affecting the existence of the configuration singularity. For this reason, the relationship between the base radius  $R$  and the length link  $q$  was subjected to further investigation. It is found that theoretically, the configuration singularity can be eliminated when the ratio  $R/q$  is greater than a critical value. This value is different from case to case. We have suggested a simple method to evaluate the critical value for platform-type parallel manipulators with symmetric base by using one (out of three) unknown variable. The critical values for those types of manipulators are determined (see Table 4.4). These values can be used as an useful guideline for improving the design of platform-type parallel manipulators.

## 5.2 Future Works

Our work is by no means complete. To further improve the design of platform-type parallel manipulator, one could consider the following :

- ◆ The method, suggested in Chapter 4 for determining the critical value of ratio  $R/q$ , cannot be applied to the platform-type parallel manipulators with non-symmetric base. Therefore, some effort can be put on the design of a generic method applicable to all platform-type parallel manipulators.
- ◆ Another factor to avoid configuration singularity is the physical constraint which has not been studied in this thesis. Some future work can be done in the analysis of the relationship among the physical constraints, the workspace and the configuration singularity. This relationship will help us develop a simple way to avoid and to eliminate the configuration singularity without affecting the workspace of the manipulator.



## References

- [AL88] Ahmad, S. and Luo, S., ' Analysis of Kinematic Singularities for Robot Manipulators in Cartesian Coordinate Parameters ', Proc. of the IEEE Int. Con. on Robotics and Automation, 2:840-845, 1988.
- [AN86] Angeles, J., ' Automatic Computation of the Screw Parameters of Rigid Body Motion. Part I : Finite-Separated Positions ', ASME J. of Dynamic Systems, Measurement, and Control, 108(1) : 39-43, 1986.
- [BE88] Behi, F., ' Kinematic Analysis for a Six-Degrees-of-Freedom 3-PRRS Parallel Mechanism ', IEEE J. of Robotics and Automation, vol. 4, No. 5, pp.561-565, 1988.
- [BL86] Borrel P. and Liegeois A., ' A Study of Manipulator Inverse Kinematic Solutions with Application to Trajectory Planning and Workspace Determination ', Proc. IEEE Int. Conf. Rob. and Aut., pp.1180-1185, 1986.
- [BU88] Burdick, J. W., ' Kinematic Analysis and Design of Redundant Manipulators ', PhD Diss., Stanford University, 1988.
- [BU91] Burdick, J. W., ' A Classification of 3R Regional Manipulator Singularities and Geometries ', Proc. of the IEEE Int. Con. on Robotics and Automation, pp. 2670-2675, April, 1991
- [CA91] Cleary, K. and Arai, T., ' A Prototype Parallel Manipulator : Kinematics Construction, Software, Workspace Results and Singularity Analysis ', IEEE Int. Conf. on Robotics and Automation, pages 566-571, Sacramento, pp.11-14, April, 1991.
- [CD88] Charentus S., Diaz C. and Renaud M., ' Modular Serial Parallel Redudant Robot ', In IMACS, Cetraro, Italie, pp.18-21, September, 1988.
- [CU94] Cleary, K. and Uebel, M., ' Jacobian Formulation for a Novel 6-DOF Parallel Manipulator ', Proc. of the IEEE Int. Conf. on Robotics and Aut., 1994.
- [CW94] Chen, Y. C. and Walker, D., ' A Consistent Approach to the Instantaneous Kinematics of Redundant, Non-Redundant and in Parallel Manipulators ', Proc. of the IEEE Int. Conf. on Robotics and Automation, vol. 4, pp.2172-2179, 1994.
- [DC80] Duffy, J. and Crane, C., ' A Displacement Analysis of the General Spatial 7R Mechanism ', Mechanisms and Machine Theory, 15:153-169, 1980.
- [FG87] Fu, K.S., Gonzalez, R.C. and Lee, C.S.G., ' Robotics : Control, Sensing, Vision, and Intelligence ', Mcgraw Hill Int. Editions, 1987.



- [FI86] Fichter, E.F., ' A Stewart Platform-Based Manipulator : general theory and practical construction ', *The International J. of Robotics and Research*, 5(2):157-182, 1986.
- [FS90] Fenton, R.G. and Shi, X., ' A Laplace Expansion Principle Based Method for Identifying Singular Joint Geometries of 6 DOF Manipulator ', *Proc. of the ASME 1990 Mechanisms Conference, DE-Vol. 25:67-73, Sep., 1990.*
- [FS92a] Fenton, R.G. and Shi, X., ' Structural Instabilities in Platform-type Parallel Manipulators Due to Singular Configurations ', *ASME Robotics, Spatial Mechanisms, and Mechanical Systems, DE-vol. 45, 1992.*
- [FS92b] Fenton, R.G. and Shi, X., ' Solution to the Forward Instantaneous Kinematics for a General 6-DOF Stewart Platform ', *J. of Mech. and mach. Theory* Vol. 27, No. 3, pp.251-259, 1992.
- [FS92c] Fenton, R.G. and Shi, X., ' Comparison of Methods for Determining Screw Parameters of Finite Rigid Body Motion from Initial and Final Position Data ', *Tran. of the ASME J. of Mechanical Design*, Vol. 112, pp.472-479, 1992.
- [FS94] Fenton, R.G. and Shi, X., ' A Complete and General Solution to the Forward Kinematics Problem of Platform-type Robotic Manipulators ', *Proc. of the IEEE Int. Conf. on Robotics and Automation*, vol. 4, pp.3055-3062, 1994.
- [GO81] Gorla, B., ' Influence of the Control on the Structure of A Manipulator From A Kinematic Point of View ', *Proceedings of the 4th Symposium of Theory and Practice of Robots and manipulator, Zaborow, Poland*, pp.30-46, Sept., 1981.
- [GS92] Gosselin C., Sefrioui J. and Richard M.J., ' Solution polynomiale au problem de la cinematique directe des manipulators parallel plans 3DOF ', *Mechanism and Machine Theory*, 27(2): 107-119, March, 1992.
- [GV89] Golub, G.H. and Van Loan, C.F., ' *Matrix Computations* ', John Hopins Press, Baltimore, 1989.
- [HL93] Huang, M.Z., Ling, S.H. and Sheng, Y. ' A Study of Velocity Kinematics for Hybrid Manipulators with Parallel-Series Configurations ', *Proc. of IEEE, Int. Conf. on Robotics and Automation*, Vol. 1, pp.456-461, 1993.
- [HL94] Huang M. Z. and Ling S. H., ' Kinematics of a Class of Hybrid Robotic Mechanisms with Parallel and Series Modules ', *Proc. of the IEEE Int. Conf. on Robotics and Automation*, vol. 4, pp.2180-2185, 1994.
- [HP93] Hunt K.H. and Primrose E.J.F., ' Assembly Configurations of some In-Parallel Actuated Manipulators ', *Mechanism and Machine Theory*, 28(1): 31-42, January, 1993.



- [HU78] Hunt, K.H., ' Kinematic Geometry of Mechanisms ', Clarendon Press, Oxford, 1978.
- [HU83] Hunt, K. H., ' Structural Kinematics of In-Parallel-Actuated Robot Arms ', ASME J. of Mech. Trans. Automation in Design, 105:705-712, Dec., 1983.
- [HU87] Hunt, K. H., ' Robot Kinematics - A Compact Analytic Inverse Solution for Velocities ', ASME J. of Mech. Trans. Automation in Design, Vol.109, pp.42-49, March, 1987.
- [IP90] Innocenti C. and Parenti-Castelli V., ' Direct position analysis of the Stewart platform mechanism ', Mechanism and Machine Theory, 25(6): 611-621, 1990.
- [IP91] Innocenti C. and Parenti-Castelli V., ' A Novel Numerical Approach to the Closure of the 6-6 Stewart Platform Mechanism ', In ICAR, pages 851-855, Pise, pp.19-22, June, 1991.
- [IP93] Innocenti C. and Parenti-Castelli V., ' Echelon Form Solution of Direct Kinematics for the General Fully-Parallel Spherical Wrist ', Mechanism and Machine Theory, 28(4): 553-561, July, 1993.
- [KY94] Kong, X. W. and Yang, T. L., ' Generation and Forward Displacement Analyses of Two New Classes of Analytic 6-SPS Parallel Robots ', Reference No. 931282, 1994.
- [LA92] Lazard, D. ' Stewart platform and Grobner basis ', In ARK, pp.136-142, September, 1992.
- [LA93] Lazard, D. ' On the Representation of Rigid-Body Motions and its Application to Generalized Platform Manipulators ', In J. Angeles P. Kovacs, G. Hommel, editor, Computational Kinematics, pp.175-182, 1993.
- [LD85] Lipkin, H. and Duffy, J., ' A Vector Analysis of Robot Manipulators ', Recent Advances in Robotics, John Wiley & Sons, New York, 1985.
- [LD90] Lin, W., Duffy, J. and Griffis M., ' Forward Displacement Analysis of the 4-4 Stewart Platform ', In ASME Proc. of the 21 th Biennial Mechanisms Conf., pp.263-269, September, 1990.
- [LP88] Lipkin, K. and Pohl, E., ' Enumeration of Singular Configurations for Robotic Manipulators ', ASME Conf. on Trends and Developments in Mechanisms, Machines and Robotics, DE-Vol. 15-3, pp.283-290, 1988.
- [LS88] Lee, K.M. and Shah, D.K., ' Kinematic Analysis of a Three-Degrees-of-Freedom in Parallel Actuated Manipulator ', IEEE J. of Robotics and Automation, vol. 4, No. 3, pp.354-360, June, 1988.

- [LT89] Litvin, F.L. and Tan, J., ' Singularities in Motion and Displacement Functions of Constrained Mechanical System ', The Int. J. of Robotics Research, Vol. 8, No.2, pp.30-43, April, 1989.
- [MA91] Ma, O. and Angeles, J., ' Architecture Singularities of Platform Manipulators ', Proc. of the IEEE Int. Conf. on Robotics and Automation, 4:1542-1547, April, 1991.
- [MC92] Manocha, D. and Canny, J.F., ' Real Time Inverse Kinematics for General 6R Manipulators ', Technical Report ESRC92-2, RAMP 92-1. Engineering System Research Center, University of California, Berkeley, 1992.
- [MD84] Mohamod, M.G. and Duffy, J., ' Direct Determination of the Instantaneous Kinematics of Fully Parallel Robot Manipulator ', ASME Paper No.84-DET-114, 1984.
- [MD89] Manseur, R and Doty, K.L., ' A Robot Manipulator with 16 Real Inverse Kinematic Solution Set ', International Journal of Robotics Research, 8(5):75-79, 1989.
- [ME89] Merlet, J.P., ' Manipulators Paralleles, 4eme Partie : Mode D'assemblage et Cinematique Directesous Forme Polynomiale ', Research Report 1135, INRIA, December, 1989.
- [ME89] Merlet, J. P., ' Singular Configurations of Parallel Manipulators and Grassmann Geometry ', The International Journal of Robotics Research, Vol. 8, No.5, pp.45-56, October, 1989.
- [ME90] Merlet, J.P., ' Les Robots Paralleles ', Herm'es, Paris, 1990.
- [ME92] Merlet J.P., ' Direct Kinematics and Assenbly Modes of Parallel Manipulators ', International J. of Robotics Research, 11(2):150-162, April, 1992.
- [ME93] Megahed, M., ' Principles of Robot Modelling and Simulation ', John Wiley & Sons Ltd., 1993.
- [ME94] Merlet, J.P., ' Trajectory Verification of Parallel Manipulators in the Workspace', Proc. of the IEEE Int. Conf. on Robotics and Automation, vol. 4, pp.2166-2171, 1994.
- [ML94] Merlet, J.P. and Lazard, D., ' The (true) Stewart Platform has 12 Configurations ', Proc. of the IEEE Int. Conf. on Robotics and Automation, vol. 4, pp.2160-2165, 1994.
- [MM92] Merlet, J.P. and Mouly, N., ' Singular Configurations and Direct Kinematics of a New Parallel Manipulator ', Proc. of the IEEE Int. Con. on Robotics and Automation, pp. 338-343, May, 1992.



- [NA92] Nair P. ' On the Kinematics Geometry of Parallel Robot Manipulators ', Master's thesis, University du Maryland, College Park, 1992.
- [PA81] Paul, R.P., ' Robot Manipulators : Mathematics, Programming and Control ', MIT Press, Cambridge, 1981.
- [PI68] Pieper, D., ' The Kinematics of Manipulators under Computer Control ', PhD thesis, Stanford University, 1968.
- [PI92] Parenti-Castelli V. and Innocenti C. ' Forward Displacement Analysis of Parallel Mechanisms : Closed-form Solution of PRR-3S and PPR-3S Structures ', J. of Mechanical Design, 114 : 68-73, March, 1992.
- [PL89] Pai, D.K. and Leu, M.C., ' Generic Singularities of Robot Manipulators ', Proc. IEEE Int. Conf. Robotics and Aut., Scottsdale, pp.738-744, 1989.
- [PR86] Primrose, E.J.F., ' One the Input-Output Equation of the General 7R-Mechanism ', Mechanisms and Machine Theory, 21:509-510, 1986.
- [RR73] Roth, B., Rastegar, J. and Scheinman, V. ' On the Design of Computer Controlled Manipulators ' On the Theory and Practice of Robots and Manipulators, pp.93-113. First CISM IFToMM Symposium, 1973.
- [RV92] Ronga F. and Vust T., ' Stewart Platforms without Computer? ' Preprint, 1992.
- [SH92] Shahinpoor, M., ' Kinematics of a Parallel-Serial (Hybrid) Manipulator ', Journal of Robotic Systems, 9(1), pp.17-36, 1992.
- [ST66] Stewart, D., ' A Platform with Six Degree of Freedom ', Proc. Inst. Mech. Engrs, 180(15), pp. 371-186, 1965-66.
- [SD82] Sugimoto, K., Duffy, J. and Hunt, K.H., ' Special Configurations of Spatial Mechanisms and Robot Arms ', Mechanism and Machine Theory, Vol.17 No.2, pp.119-132 , 1982.
- [SD88] Soyulu, R. and Duffy, J., ' Hypersurfaces of Special Configurations of Serial Manipulators and Related Concepts Part II : Passive Joints, Configurations, Component Manifolds and Some Applications ', Journal of Robotic Systems, Vol. 5, pp.31-53, 1988.
- [SU89] Sugimoto, K., ' Computational Scheme for Dynamic Analysis of Parallel Manipulators ', Trans. of the ASME, J. of Mechanisms, Trans. and Auto. in Design, 111 : 29-33, March, 1989.
- [SV89] Spong, M.W. and Vidyasagar, M., ' Robot Dynamics and Control ' John Wiley and Sons, 1989.

- [TM85] Tsai, L.W. and Morgan, A.P., ' Solving the Kinematics of the most General Six and 5 DOF Manipulators by Continuation methods ' Tran. of the ASME, J. of Mecn., Transmissions and Automation in Design, 107:189-200, 1985.
- [WE92] Wenger, Ph., ' A New General Formalism for the Kinematic Analysis of All Nonredundant Manipulators ', Proc. of the IEEE Int. Con. on Robotics and Automation, pp. 442-447, May, 1992.
- [WH72] Whitney, D.E., ' The Mathematics of Coordinated Control of Prostheses and Manipulators ', ASME J. of Dynamic systems, Measurement, and Control, Vol. 94, pp.303-309, Dec., 1972.
- [WH88] Waldron, K. J. and Hunt, K.H., ' Serial-Parallel Dualities in Actively Coordinated Mechanism ', Proceedings of the Int. Symp. on Robotics Research, pp.175-181, 1988.
- [WI59] Wilkinson, J.H., 'The Evaluation of the Zeros of ill-conditioned Polynomials Part I and II ', Numer. Math., 1:50-166 and pp.167-180, 1959.
- [WM91] Wanpler, C. and Morgan, A.P., ' Solving the 6R Inverse Position Problem using a Generic-case Solution Methodology ', Mechanisms and Machine Theory, 26(1):91-106, 1991.
- [WN89] Waldron, K.J. and Nanua, P., ' Direct Kinematic Solution of a Stewart Platform', Proc. of the IEEE Int. Conf. on Robotics and Automation, 1:431-437, 1989.
- [WO87] Wolovich, A. William, ' Robotics :- Basic Analysis and Design ', Holt Rinehart & Winston, 1987.
- [YL84] Yang, D.C. and Lee, T.W. ' Feasibility Study of A Platform Type of Robotic Manipulators from A Kinematic Viewpoint ', Trans. ASME, J. Mech., Trans., and Auto. in Design, 106 : 191-198, 1984.
- [YL87] Yang, D.C. and Lee, T.W. ' Feasibility Study of A Platform Type of Robotic Manipulators from A Kinematic Viewpoint ', Proc. of the IEEE Int. Conf. on Robotics and Automation, 1 : 345-350, 1987.
- [YO85] Yoshikawa, T., ' Manipulability of Robotic Mechanisms ', Int. J. of Robotics Res., Vol. 4, No. 2, pp.3-9, 1985.
- [ZO92] Zomaya, Y. Albert, ' Modelling and Simulation of Robot Manipulators ', World Scientific Series in Robotics and Automated Systems, Oct., 1992.
- [ZS91] Zhang C.D. and Song S.M., ' Forward Kinematics of a Class of Parallel (Stewart) Platform with Closed-form Solutions ', IEEE Int. Conf. on Robotics and Automation, 2676-2681, Sacramento, pp.11-14, April , 1991.



# Appendix -- Listing of Programs and Drawings

## Novel 6 DOF Platform-Type Parallel Manipulator

- (1) Output Results of the General Form Equation
- (2) Input Program of an Example
- (3) Output Results of an Example

## 3 DOF Platform-Type Parallel Manipulator with Symmetric and Non-Symmetric Base

- (4) Input Program of Right Angled Triangular Base
- (5) Output Results of Right Angled Triangular Base
- (6) Input Program of Equilateral Triangular Base
- (7) Output Results of Equilateral Triangular Base
- (8) Input Program of Equilateral Triangular Base with different parameters
- (9) Output Results of Equilateral Triangular Base with different parameters
- (10) Input Program for Formulate the General Form Equation
- (11) Output Results of the General Form Equation

## A New Class of 6-SPS Platform-Type Parallel Manipulator

- (12) Input Program of New Model Defined by Kong et al.
- (13) Output Results of New Model Defined by Kong et al.
- (14) Input Program of Hexagonal Base
- (15) Output Results of Hexagonal Base
- (16) Input Program of Pentagonal Base
- (17) Output Results of Pentagonal Base
- (18) Input Program of Tetragonal Base
- (19) Output Results of Tetragonal Base
- (20) Input Program of Triangular Base
- (21) Output Results of Triangular Base

In Chapter 4

- (22) Input Program for Sample Case 1 to 5
- (23) Output Results of Sample Case 1 ( $\theta_1 = \pi/2$  ,  $\theta_2 = \pi/2$ )
- (24) Output Results of Sample Case 2 ( $\theta_1 = \pi/2$  ,  $\theta_2 = \pi/3$ )
- (25) Output Results of Sample Case 3 ( $\theta_1 = \pi/2$  ,  $\theta_2 = \pi/4$ )
- (26) Output Results of Sample Case 4 ( $\theta_1 = \pi/2$  ,  $\theta_2 = \pi/12$ )
- (27) Output Results of Sample Case 5 ( $\theta_1 = 5\pi/12$  ,  $\theta_2 = 5\pi/12$ )
  
- (28) Components Drawing of the Mechanical Model (Stewart Platform)





$$\begin{aligned}
& 11^*12^*\text{Cos}[03]^*\text{Cos}[rb3]^2*\text{Sin}[013] - 11^*12^*\text{Cos}[013]^*\text{Sin}[02] + \\
& 11^*12^*\text{Cos}[013]^*\text{Sin}[03] + 11^*r^*\text{Sin}[013]^*\text{Sin}[rb2]^*\text{Sin}[rb3] + \\
& 11^*\sqrt{2}^*\text{Cos}[012]^*\text{Sin}[013]^*\text{Sin}[rb2]^*\text{Sin}[rb3] + \\
& 11^*12^*\text{Cos}[02]^*\text{Sin}[013]^*\text{Sin}[rb2]^*\text{Sin}[rb3] - 11^*r^*\text{Sin}[013]^*\text{Sin}[rb3]^2 - \\
& 11^*\sqrt{2}^*\text{Cos}[013]^*\text{Sin}[013]^*\text{Sin}[rb3]^2 \}
\end{aligned}$$



\*\*\*\* (2) This is an Input Data and Equation File \*\*\*\*  
\*\*\*\* for a Novel 6 DOF Parallel Manipulator. \*\*\*\*

$$o11 = o12 = \text{Pi} / 2$$

$$o1 = o2 = \text{Pi} / 2$$

$$rb1 = 0$$

$$rb2 = 2 \text{ Pi} / 3$$

$$rb3 = 4 \text{ Pi} / 3$$

$$p1 = \left\{ \left\{ r \text{ Cos}[rb1] + l1 \text{ Cos}[o11] \text{ Cos}[rb1] + l2 \text{ Cos}[o1] \text{ Cos}[rb1] \right\}, \right. \\ \left. \left\{ r \text{ Sin}[rb1] + l1 \text{ Cos}[o11] \text{ Sin}[rb1] + l2 \text{ Cos}[o1] \text{ Sin}[rb1] \right\}, \right. \\ \left. \left\{ l1 \text{ Sin}[o11] + l2 \text{ Sin}[o1] \right\} \right\}$$

$$p2 = \left\{ \left\{ r \text{ Cos}[rb2] + l1 \text{ Cos}[o12] \text{ Cos}[rb2] + l2 \text{ Cos}[o2] \text{ Cos}[rb2] \right\}, \right. \\ \left. \left\{ r \text{ Sin}[rb2] + l1 \text{ Cos}[o12] \text{ Sin}[rb2] + l2 \text{ Cos}[o2] \text{ Sin}[rb2] \right\}, \right. \\ \left. \left\{ l1 \text{ Sin}[o12] + l2 \text{ Sin}[o2] \right\} \right\}$$

$$p3 = \left\{ \left\{ r \text{ Cos}[rb3] + l1 \text{ Cos}[o13] \text{ Cos}[rb3] + l2 \text{ Cos}[o3] \text{ Cos}[rb3] \right\}, \right. \\ \left. \left\{ r \text{ Sin}[rb3] + l1 \text{ Cos}[o13] \text{ Sin}[rb3] + l2 \text{ Cos}[o3] \text{ Sin}[rb3] \right\}, \right. \\ \left. \left\{ l1 \text{ Sin}[o13] + l2 \text{ Sin}[o3] \right\} \right\}$$

$$vp1 = \left\{ \left\{ -l1 \text{ d}[o11] \text{ Sin}[o11] \text{ Cos}[rb1] - l2 \text{ d}[o1] \text{ Sin}[o1] \text{ Cos}[rb1] \right\}, \right. \\ \left. \left\{ -l1 \text{ d}[o11] \text{ Sin}[o11] \text{ Sin}[rb1] - l2 \text{ d}[o1] \text{ Sin}[o1] \text{ Sin}[rb1] \right\}, \right. \\ \left. \left\{ l1 \text{ d}[o11] \text{ Cos}[o11] + l2 \text{ d}[o1] \text{ Cos}[o1] \right\} \right\}$$

$$vp2 = \left\{ \left\{ -l1 \text{ d}[o12] \text{ Sin}[o12] \text{ Cos}[rb2] - l2 \text{ d}[o2] \text{ Sin}[o2] \text{ Cos}[rb2] \right\}, \right. \\ \left. \left\{ -l1 \text{ d}[o12] \text{ Sin}[o12] \text{ Sin}[rb2] - l2 \text{ d}[o2] \text{ Sin}[o2] \text{ Sin}[rb2] \right\}, \right. \\ \left. \left\{ l1 \text{ d}[o12] \text{ Cos}[o12] + l2 \text{ d}[o2] \text{ Cos}[o2] \right\} \right\}$$

$$vp3 = \left\{ \left\{ -l1 \text{ d}[o13] \text{ Sin}[o13] \text{ Cos}[rb3] - l2 \text{ d}[o3] \text{ Sin}[o3] \text{ Cos}[rb3] \right\}, \right. \\ \left. \left\{ -l1 \text{ d}[o13] \text{ Sin}[o13] \text{ Sin}[rb3] - l2 \text{ d}[o3] \text{ Sin}[o3] \text{ Sin}[rb3] \right\}, \right. \\ \left. \left\{ l1 \text{ d}[o13] \text{ Cos}[o13] + l2 \text{ d}[o3] \text{ Cos}[o3] \right\} \right\}$$

$$m1 = (vp1 - vp2)$$

$$m2 = (p1 - p2)$$

$$e = (\text{Transpose}[m2]) \cdot (m1)$$

$$e1 = \text{Expand}[e]$$

$$\text{Factor}[e1]$$

$$k11 = \text{Coefficient}[e1, \text{d}[o11]]$$

$$k12 = \text{Coefficient}[e1, \text{d}[o12]]$$

$$m3 = (vp2 - vp3)$$

$$m4 = (p2 - p3)$$

$$f = (\text{Transpose}[m4]) \cdot (m3)$$

$$e2 = \text{Expand}[f]$$

$$\text{Factor}[e2]$$

$$k22 = \text{Coefficient}[e2, \text{d}[o12]]$$

$$k23 = \text{Coefficient}[e2, \text{d}[o13]]$$

```
m5 = (vp3 - vp1)
```

```
m6 = (p3 - p1)
```

```
g = (Transpose[m6]) . (m5)
```

```
e3 = Expand[g]
```

```
Factor[e3]
```

```
k31 = Coefficient[e3, d[o11]]
```

```
k33 = Coefficient[e3, d[o13]]
```

```
gf = (( k11 k22 k33 ) + ( k31 k12 k23))
```

```
Expand[gf]
```

```
Factor[gf]
```



\*\*\*\* (3) This is an Output Data and Equation File \*\*\*\*  
\*\*\*\* for a Novel 6 DOF Parallel Manipulator. \*\*\*\*

In[35] :=

In[35] :=

Out[35] =  $\left\{ \left\{ \left( 3 l_1 (l_1 + l_2)^2 r (3 r + l_1 \cos[\theta_{13}] + l_2 \cos[\theta_{03}]) \right. \right. \right.$

>  $\left. \left. \left( -2 l_1 \cos[\theta_{13}] - 2 l_2 \cos[\theta_{13}] - 3 r \sin[\theta_{13}] - \right. \right. \right.$

>  $\left. \left. \left. 2 l_2 \cos[\theta_{03}] \sin[\theta_{13}] + 2 l_2 \cos[\theta_{13}] \sin[\theta_{03}] \right) \right) / 2 \right\}$

>  $(3 r + l_1 \cos[\theta_{13}] + l_2 \cos[\theta_{03}]) = 0$

>  $3 r + l_1 \cos[\theta_{13}] - l_2 \cos[\theta_{13}] = 0$

> where  $\cos[\theta_{13}] = -1$

>  $r = (l_1 - l_2) / 3$

>

>  $-2 l_1 \cos[\theta_{13}] - 2 l_2 \cos[\theta_{13}] - 3 r \sin[\theta_{13}] - 2 l_2 \cos[\theta_{03}] \sin[\theta_{13}] + 2 l_2 \cos[\theta_{13}] \sin[\theta_{03}] = 0$

>  $(-2 l_1 - 2 l_2 - 2 l_2 \sin[\theta_{13}]) \cos[\theta_{13}] = (3 r + 2 l_2 \cos[180 + \theta_{13}]) \sin[\theta_{13}]$

>  $(-2 l_1 - 2 l_2) \cos[\theta_{13}] - (2 l_2 \sin[\theta_{13}] \cos[\theta_{13}]) = (3 r \sin[\theta_{13}]) - (2 l_2 \cos[\theta_{13}] \sin[\theta_{13}])$

>  $\tan[\theta_{13}] = (l_1 + l_2) / 1.5 r$

>

\*\*\*\* (4) Input Programme of Right Angled Triangular Base \*\*\*\*  
\*\*\*\* Platform in 3 DOF \*\*\*\*

r1 = r  
r2 = r  
r3 = Sqrt[0.4] r  
o1 = 0  
o2 = 2 Pi / 3  
o3 = 4 Pi / 3  
a1 = a2 = Pi / 2

p1 = {{r1 Cos[o1] + q1 Cos[a1] Cos[o1]},  
{r1 Sin[o1] + q1 Cos[a1] Sin[o1]},  
{q1 Sin[a1]}};

p2 = {{r2 Cos[o2] + q2 Cos[a2] Cos[o2]},  
{r2 Sin[o2] + q2 Cos[a2] Sin[o2]},  
{q2 Sin[a2]}};

p3 = {{r3 Cos[o3] + q3 Cos[a3] Cos[o3]},  
{r3 Sin[o3] + q3 Cos[a3] Sin[o3]},  
{q3 Sin[a3]}};

vp1 = {{dq1 Cos[a1] Cos[o1] - q1 d[a1] Sin[a1] Cos[o1]},  
{dq1 Cos[a1] Sin[o1] - q1 d[a1] Sin[a1] Sin[o1]},  
{dq1 Sin[a1] + q1 d[a1] Cos[a1]}};

vp2 = {{dq2 Cos[a2] Cos[o2] - q2 d[a2] Sin[a2] Cos[o2]},  
{dq2 Cos[a2] Sin[o2] - q2 d[a2] Sin[a2] Sin[o2]},  
{dq2 Sin[a2] + q2 d[a2] Cos[a2]}};

vp3 = {{dq3 Cos[a3] Cos[o3] - q3 d[a3] Sin[a3] Cos[o3]},  
{dq3 Cos[a3] Sin[o3] - q3 d[a3] Sin[a3] Sin[o3]},  
{dq3 Sin[a3] + q3 d[a3] Cos[a3]}};

m1 = (vp1 - vp2)

m2 = (p1 - p2)

e = (Transpose[m2]) . (m1);

e1 = Expand[e];

Factor[e1];

k11 = Coefficient[e1, q1 d[a1]]  
k12 = Coefficient[e1, q2 d[a2]]  
k13 = 0

m3 = (vp2 - vp3)

m4 = (p2 - p3)

f = (Transpose[m4]) . (m3);



```

e2 = Expand[f];
Factor[e2];

k21 = 0
k22 = Coefficient[e2, q2 d[a2]]
k23 = Coefficient[e2, q3 d[a3]]

m5 = (vp3 - vp1)

m6 = (p3 - p1)

g = (Transpose[m6]) . (m5);

e3 = Expand[g];

Factor[e3];

k31 = Coefficient[e3, q1 d[a1]]
k32 = 0
k33 = Coefficient[e3, q3 d[a3]]

k= {{k11, k12, k13},
     {k21, k22, k23},
     {k31, k32, k33}}

kk = Flatten[k]

kk1=Partition[kk,3]

dk = Det[kk1]/N

Simplify[dk]

```

\*\*\*\* (5) Output Results of Right Angled Triangular Base \*\*\*\*  
\*\*\*\* Platform in 3 DOF \*\*\*\*

\*\*\*\* r1=r2=r and r3 = Sqrt[0.4] r \*\*\*\*

Out[29]

{{-1.974341649025257\*q1\*r^2\*Cos[a3] - 1.974341649025257\*q2\*r^2\*Cos[a3] -  
(3\*q1\*q3\*r\*Cos[a3]^2)/4 - (3\*q2\*q3\*r\*Cos[a3]^2)/4 -  
4.471708245126285\*r^3\*Sin[a3] - 1.698683298050514\*q3\*r^2\*Cos[a3]\*Sin[a3]}}

Out[30]

{{-4.471708245126285\*(0.4415184401122528\*q1\*r^2\*Cos[a3] +  
0.4415184401122528\*q2\*r^2\*Cos[a3] +  
0.1677211389668423\*q1\*q3\*r\*Cos[a3]^2 +  
0.1677211389668423\*q2\*q3\*r\*Cos[a3]^2 + 1.\*r^3\*Sin[a3] +  
0.3798734633239789\*q3\*r^2\*Cos[a3]\*Sin[a3])}}

(q1 r^2 Cos[a3] + q2 r^2 Cos[a3] + 2.26491 r^3 Sin[a3])  
+ (0.379873 q1 r Cos[a3] + 0.379873 q2 r Cos[a3] + 0.8038 r^2 Sin[a3])  
\* q3 Cos[a3]

(q1 r Cos[a3] + q2 r Cos[a3] + 2.26491 r^2 Sin[a3]) r  
+ (q1 r Cos[a3] + q2 r Cos[a3] + 2.264914 r^2 Sin[a3]) q3 Cos[a3]

(q1 Cos[a3] + q2 Cos[a3] + 2.26491 r Sin[a3]) ( r^2 + r q3 Cos[a3] ) = 0

r^2 = r q3 where cos[a3] = -1  
r >= q3

( q1 + q2 ) Cos[a3] = -2.26491 r Sin[a3]

Tan[a3] = - (q1 + q2) / ( 2.26491 r )

Tan[a3] = - ( (q1 + q2) / 2 ) / (1.132455 r)



\*\*\*\* (6) Input Programme of Equilateral Triangular Base \*\*\*\*  
\*\*\*\* Platform in 3 DOF \*\*\*\*

r1 = r2 = r3 = r  
o1 = 0  
o2 = 2 Pi / 3  
o3 = 4 Pi / 3  
a1 = a2 = Pi / 2

p1 = {{r1 Cos[o1] + q1 Cos[a1] Cos[o1]},  
{r1 Sin[o1] + q1 Cos[a1] Sin[o1]},  
{q1 Sin[a1]}}

p2 = {{r2 Cos[o2] + q2 Cos[a2] Cos[o2]},  
{r2 Sin[o2] + q2 Cos[a2] Sin[o2]},  
{q2 Sin[a2]}}

p3 = {{r3 Cos[o3] + q3 Cos[a3] Cos[o3]},  
{r3 Sin[o3] + q3 Cos[a3] Sin[o3]},  
{q3 Sin[a3]}}

vp1 = {{dq1 Cos[a1] Cos[o1] - q1 d[a1] Sin[a1] Cos[o1]},  
{dq1 Cos[a1] Sin[o1] - q1 d[a1] Sin[a1] Sin[o1]},  
{dq1 Sin[a1] + q1 d[a1] Cos[a1]}}

vp2 = {{dq2 Cos[a2] Cos[o2] - q2 d[a2] Sin[a2] Cos[o2]},  
{dq2 Cos[a2] Sin[o2] - q2 d[a2] Sin[a2] Sin[o2]},  
{dq2 Sin[a2] + q2 d[a2] Cos[a2]}}

vp3 = {{dq3 Cos[a3] Cos[o3] - q3 d[a3] Sin[a3] Cos[o3]},  
{dq3 Cos[a3] Sin[o3] - q3 d[a3] Sin[a3] Sin[o3]},  
{dq3 Sin[a3] + q3 d[a3] Cos[a3]}}

v0 = ( vp1 + vp2 + vp3 ) / 3

z2 = vp2[[3]]

x3 = vp3[[1]]

y1 = vp1[[2]]

z0 = v0[[3]]

x0 = v0[[1]]

y0 = v0[[2]]

m1 = z2 - z0

e1=Expand[m1]

k11 = Coefficient[e1, q1 d[a1]]

k12 = Coefficient[e1, q2 d[a2]]

k13 = Coefficient[e1, q3 d[a3]]

m2 = x3 - x0

```
e2=Expand[m2]
k21 = Coefficient[e2, q1 d[a1]]
k22 = Coefficient[e2, q2 d[a2]]
k23 = Coefficient[e2, q3 d[a3]]

m3 = y1 - y0
e3=Expand[m3]
k31 = Coefficient[e3, q1 d[a1]]
k32 = Coefficient[e3, q2 d[a2]]
k33 = Coefficient[e3, q3 d[a3]]

k= {{k11, k12, k13},
    {k21, k22, k23},
    {k31, k32, k33}}

kk = Flatten[k]

kk1=Partition[kk,3]

dk = Det[kk1]//N

Simplify[dk]
```



\*\*\*\* (7) Output Results of Equilateral Triangular Base \*\*\*\*  
 \*\*\*\* Platform in 3 DOF \*\*\*\*

In[30] :=

$$\text{Out}[30] = \left\{ \frac{dq3 \cos[a3]}{2 \sqrt{3}} + \frac{\frac{\pi}{2} q2 d[--]}{2 \sqrt{3}} - \frac{q3 d[a3] \sin[a3]}{2 \sqrt{3}} \right\}$$

In[31] :=

Out[31] = {0}

In[32] :=

$$\text{Out}[32] = \left\{ \frac{1}{2 \sqrt{3}} \right\}$$

In[33] :=

$$\text{Out}[33] = \left\{ \frac{-\sin[a3]}{2 \sqrt{3}} \right\}$$

In[34] :=

In[34] :=

$$\text{Out}[34] = \left\{ \left\{ \{0\}, \{0\}, \left\{ \frac{-\cos[a3]}{3} \right\} \right\}, \left\{ \left\{ \frac{1}{3} \right\}, \left\{ \frac{1}{6} \right\}, \left\{ \frac{\sin[a3]}{3} \right\} \right\} \right\}$$

$$> \left\{ \left\{ \{0\}, \left\{ \frac{1}{2 \sqrt{3}} \right\}, \left\{ \frac{-\sin[a3]}{2 \sqrt{3}} \right\} \right\} \right\}$$

In[35] :=

In[35] :=

$$\text{Out}[35] = \left\{ \frac{-\cos[a3]}{18 \sqrt{3}} \right\}$$

In[36] :=

In[37] :=

In[37] :=

$$\text{Out}[37] = \left\{ \frac{-\cos[a3]}{18 \sqrt{3}} \right\}$$

In[38] :=

In[38] :=

$$\text{Out}[38] = \left\{ \frac{-\cos[a3]}{18 \sqrt{3}} \right\}$$

In[39] :=

\*\*\*\* (8) Input Programme of Equilateral Triangular Base \*\*\*\*  
 \*\*\*\* Platform with different parameters in 3 DOF \*\*\*\*

r1 = r2 = r3 = r  
 o1 = 0  
 o2 = 2 Pi / 3  
 o3 = 4 Pi / 3  
 a1 = Pi / 2  
 a2 = a3  
 q2 = q3

p1 = {{r1 Cos[o1] + q1 Cos[a1] Cos[o1]},  
 {r1 Sin[o1] + q1 Cos[a1] Sin[o1]},  
 {q1 Sin[a1]}}

p2 = {{r2 Cos[o2] + q2 Cos[a2] Cos[o2]},  
 {r2 Sin[o2] + q2 Cos[a2] Sin[o2]},  
 {q2 Sin[a2]}}

p3 = {{r3 Cos[o3] + q3 Cos[a3] Cos[o3]},  
 {r3 Sin[o3] + q3 Cos[a3] Sin[o3]},  
 {q3 Sin[a3]}}

vp1 = {{dq1 Cos[a1] Cos[o1] - q1 d[a1] Sin[a1] Cos[o1]},  
 {dq1 Cos[a1] Sin[o1] - q1 d[a1] Sin[a1] Sin[o1]},  
 {dq1 Sin[a1] + q1 d[a1] Cos[a1]}}

vp2 = {{dq2 Cos[a2] Cos[o2] - q2 d[a2] Sin[a2] Cos[o2]},  
 {dq2 Cos[a2] Sin[o2] - q2 d[a2] Sin[a2] Sin[o2]},  
 {dq2 Sin[a2] + q2 d[a2] Cos[a2]}}

vp3 = {{dq3 Cos[a3] Cos[o3] - q3 d[a3] Sin[a3] Cos[o3]},  
 {dq3 Cos[a3] Sin[o3] - q3 d[a3] Sin[a3] Sin[o3]},  
 {dq3 Sin[a3] + q3 d[a3] Cos[a3]}}

m1 = (vp1 - vp2)

m2 = (p1 - p2)

e = (Transpose[m2]) . (m1);

e1 = Expand[e];

Factor[e1];

k11 = Coefficient[e1, q1 d[a1]]  
 k12 = Coefficient[e1, q2 d[a2]]  
 k13 = 0

m3 = (vp2 - vp3)

m4 = (p2 - p3)

f = (Transpose[m4]) . (m3);



```
e2 = Expand[f];
Factor[e2];

k21 = 0
k22 = Coefficient[e2, q2 d[a2]]
k23 = Coefficient[e2, q3 d[a3]]

m5 = (vp3 - vp1)
m6 = (p3 - p1)
g = (Transpose[m6]) . (m5);
e3 = Expand[g];
Factor[e3];

k31 = Coefficient[e3, q1 d[a1]]
k32 = 0
k33 = Coefficient[e3, q3 d[a3]]

k= {{k11, k12, k13},
     {k21, k22, k23},
     {k31, k32, k33}}

kk = Flatten[k]
kk1=Partition[kk,3]
dk = Det[kk1]//N
Simplify[dk]
```

\*\*\*\* (9) Output Results of Equilateral Triangular Base \*\*\*\*  
\*\*\*\* Platform with different parameters in 3 DOF \*\*\*\*

\*\*\*\* Result of 3 DOF  $a_1=\pi$ ,  $r_1=r_2=r_3=r$  &  $a_2=a_3$  &  $q_2=q_3$  \*\*\*\*

$$\text{Out}[42] = -3. q_1 q_3 r \cos^2[a_3] \sin^3[a_3] - 13.5 r^3 \sin^2[a_3] -$$

$$> 4.5 q_3 r^2 \cos[a_3] \sin^2[a_3] - 4.5 q_1 r^2 \sin[2 a_3]$$

In[43] :=



\*\*\*\* (10) This is an Input Data and Equation File for \*\*\*\*  
\*\*\*\* Formulate the General Form Equation of 3 DOF \*\*\*\*

Out[1]>>>3dof

p1 = {{r1 Cos[o1] + q1 Cos[a1] Cos[o1]},  
{r1 Sin[o1] + q1 Cos[a1] Sin[o1]},  
{q1 Sin[a1]}}>>>3dof

Out[2]>>>3dof

p2 = {{r2 Cos[o2] + q2 Cos[a2] Cos[o2]},  
{r2 Sin[o2] + q2 Cos[a2] Sin[o2]},  
{q2 Sin[a2]}}>>>3dof

Out[3]>>>3dof

p3 = {{r3 Cos[o3] + q3 Cos[a3] Cos[o3]},  
{r3 Sin[o3] + q3 Cos[a3] Sin[o3]},  
{q3 Sin[a3]}}>>>3dof

Out[4]>>>3dof

vp1 = {{dq1 Cos[a1] Cos[o1] - q1 d[a1] Sin[a1] Cos[o1]},  
{dq1 Cos[a1] Sin[o1] - q1 d[a1] Sin[a1] Sin[o1]},  
{dq1 Sin[a1] + q1 d[a1] Cos[a1]}}>>>3dof

Out[5]>>>3dof

vp2 = {{dq2 Cos[a2] Cos[o2] - q2 d[a2] Sin[a2] Cos[o2]},  
{dq2 Cos[a2] Sin[o2] - q2 d[a2] Sin[a2] Sin[o2]},  
{dq2 Sin[a2] + q2 d[a2] Cos[a2]}}>>>3dof

Out[6]>>>3dof

vp3 = {{dq3 Cos[a3] Cos[o3] - q3 d[a3] Sin[a3] Cos[o3]},  
{dq3 Cos[a3] Sin[o3] - q3 d[a3] Sin[a3] Sin[o3]},  
{dq3 Sin[a3] + q3 d[a3] Cos[a3]}}>>>3dof

Out[7]>>>3dof

m1 = (vp1 - vp2)>>>3dof

Out[8]>>>3dof

m2 = (p1 - p2)>>>3dof

Out[9]>>>3dof

e = (Transpose[m2]) . (m1)>>>3dof

Out[10]>>>3dof

e1 = Expand[e]>>>3dof

Out[11]>>>3dof

Factor[e1]>>>3dof

Out[12]>>>3dof

k11 = Coefficient[e1, q1 d[a1]]>>>3dof

```

Out[13]>>>3dofo
k12 = Coefficient[e1, q2 d[a2]]>>>3dofo
Out[14]>>>3dofo
m3 = (vp2 - vp3)>>>3dofo
Out[15]>>>3dofo
m4 = (p2 - p3)>>>3dofo
Out[16]>>>3dofo
f = (Transpose[m4]) . (m3)>>>3dofo
Out[17]>>>3dofo
e2 = Expand[f]>>>3dofo
Out[18]>>>3dofo
Factor[e2]>>>3dofo
Out[19]>>>3dofo
k22 = Coefficient[e2, q2 d[a2]]>>>3dofo
Out[20]>>>3dofo
k23 = Coefficient[e2, q3 d[a3]]>>>3dofo
Out[21]>>>3dofo
m5 = (vp3 - vp1)>>>3dofo
Out[22]>>>3dofo
m6 = (p3 - p1)>>>3dofo
Out[23]>>>3dofo
g = (Transpose[m6]) . (m5)>>>3dofo
Out[24]>>>3dofo
e3 = Expand[g]>>>3dofo
Out[25]>>>3dofo
Factor[e3]>>>3dofo
Out[26]>>>3dofo
k31 = Coefficient[e3, q1 d[a1]]>>>3dofo
Out[27]>>>3dofo
k33 = Coefficient[e3, q3 d[a3]]>>>3dofo
Out [28]>>>3dofo
gf = (( k11 k22 k33 ) + ( k31 k12 k23))>>>3dofo

```



Out[29] >>>3dof0

Expand[*gf*] >>>3dof0

Out[30] >>>3dof0

Factor[*gf*] >>>3dof0

\*\*\*\* (11) This is an Output Data and Equation File for \*\*\*\*  
\*\*\*\* Formulate the General Form Equation of 3 DOF \*\*\*\*

$$\begin{aligned} & \{ \{ (- (r1 \cdot \cos[o1]^2 \cdot \sin[a1]) + r2 \cdot \cos[o1] \cdot \cos[o2] \cdot \sin[a1] + \\ & \quad q2 \cdot \cos[a2] \cdot \cos[o1] \cdot \cos[o2] \cdot \sin[a1] - q2 \cdot \cos[a1] \cdot \sin[a2] - \\ & \quad r1 \cdot \sin[a1] \cdot \sin[o1]^2 + r2 \cdot \sin[a1] \cdot \sin[o1] \cdot \sin[o2] + \\ & \quad q2 \cdot \cos[a2] \cdot \sin[a1] \cdot \sin[o1] \cdot \sin[o2]) \cdot \\ & (- (r2 \cdot \cos[o2]^2 \cdot \sin[a2]) + r3 \cdot \cos[o2] \cdot \cos[o3] \cdot \sin[a2] + \\ & \quad q3 \cdot \cos[a3] \cdot \cos[o2] \cdot \cos[o3] \cdot \sin[a2] - q3 \cdot \cos[a2] \cdot \sin[a3] - \\ & \quad r2 \cdot \sin[a2] \cdot \sin[o2]^2 + r3 \cdot \sin[a2] \cdot \sin[o2] \cdot \sin[o3] + \\ & \quad q3 \cdot \cos[a3] \cdot \sin[a2] \cdot \sin[o2] \cdot \sin[o3]) \cdot \\ & (- (q1 \cdot \cos[a3] \cdot \sin[a1]) + r1 \cdot \cos[o1] \cdot \cos[o3] \cdot \sin[a3] + \\ & \quad q1 \cdot \cos[a1] \cdot \cos[o1] \cdot \cos[o3] \cdot \sin[a3] - r3 \cdot \cos[o3]^2 \cdot \sin[a3] + \\ & \quad r1 \cdot \sin[a3] \cdot \sin[o1] \cdot \sin[o3] + q1 \cdot \cos[a1] \cdot \sin[a3] \cdot \sin[o1] \cdot \sin[o3] - \\ & \quad r3 \cdot \sin[a3] \cdot \sin[o3]^2) + (- (q1 \cdot \cos[a2] \cdot \sin[a1]) + \\ & \quad r1 \cdot \cos[o1] \cdot \cos[o2] \cdot \sin[a2] + q1 \cdot \cos[a1] \cdot \cos[o1] \cdot \cos[o2] \cdot \sin[a2] - \\ & \quad r2 \cdot \cos[o2]^2 \cdot \sin[a2] + r1 \cdot \sin[a2] \cdot \sin[o1] \cdot \sin[o2] + \\ & \quad q1 \cdot \cos[a1] \cdot \sin[a2] \cdot \sin[o1] \cdot \sin[o2] - r2 \cdot \sin[a2] \cdot \sin[o2]^2) \cdot \\ & (- (r1 \cdot \cos[o1]^2 \cdot \sin[a1]) + r3 \cdot \cos[o1] \cdot \cos[o3] \cdot \sin[a1] + \\ & \quad q3 \cdot \cos[a3] \cdot \cos[o1] \cdot \cos[o3] \cdot \sin[a1] - q3 \cdot \cos[a1] \cdot \sin[a3] - \\ & \quad r1 \cdot \sin[a1] \cdot \sin[o1]^2 + r3 \cdot \sin[a1] \cdot \sin[o1] \cdot \sin[o3] + \\ & \quad q3 \cdot \cos[a3] \cdot \sin[a1] \cdot \sin[o1] \cdot \sin[o3]) \cdot \\ & (- (q2 \cdot \cos[a3] \cdot \sin[a2]) + r2 \cdot \cos[o2] \cdot \cos[o3] \cdot \sin[a3] + \\ & \quad q2 \cdot \cos[a2] \cdot \cos[o2] \cdot \cos[o3] \cdot \sin[a3] - r3 \cdot \cos[o3]^2 \cdot \sin[a3] + \\ & \quad r2 \cdot \sin[a3] \cdot \sin[o2] \cdot \sin[o3] + q2 \cdot \cos[a2] \cdot \sin[a3] \cdot \sin[o2] \cdot \sin[o3] - \\ & \quad r3 \cdot \sin[a3] \cdot \sin[o3]^2) \} \} \end{aligned}$$

\*\*\*\* (12) Input Programme of a New Model of 6-SPS \*\*\*\*  
\*\*\*\* which is defined by Kong et. al. \*\*\*\*

r1 = 8 Pi / 9;  
rr1 = 25 Pi / 18;  
r2 = Pi / 2;  
r3 = Pi / 2;  
o1 = 5 Pi / 18;  
o2 = 7 Pi / 6;  
o3 = 65 Pi / 36;

b1 = 0.68405s;  
b2 = b3 = 0.74 s;  
qq1 = q1;  
qq2 = q2;  
qq3 = q3;

xq1 = dq1;  
xq2 = dq2;  
xq3 = dq3;

t3 = t2 = Pi / 2 ;

f11 = ( q1^2 + b1^2 - qq1^2 ) / ( 2 b1 q1 );

f21 = Sqrt[1 - (( q1^2 + b1^2 - qq1^2 ) / ( 2 b1 q1 ) )^2];

p1 = {{s Cos[o1] - q1 f11 Cos[r1] - q1 f21 Sin[r1] Cos[t1]},  
{s Sin[o1] - q1 f11 Sin[r1] + q1 f21 Cos[r1] Cos[t1]},  
{q1 f21 Sin[t1]}};

f12 = ( q2^2 + b2^2 - qq2^2 ) / ( 2 b2 q2 );

f22 = Sqrt[1 - (( q2^2 + b2^2 - qq2^2 ) / ( 2 b2 q2 ) )^2];

p2 = {{2.07 s Cos[o2] + q2 f12 Cos[r2] + q2 f22 Sin[r2] Cos[t2]},  
{2.07 s Sin[o2] + q2 f12 Sin[r2] - q2 f22 Cos[r2] Cos[t2]},  
{q2 f22 Sin[t2]}};

f13 = ( q3^2 + b3^2 - qq3^2 ) / ( 2 b3 q3 );

f23 = Sqrt[1 - (( q3^2 + b3^2 - qq3^2 ) / ( 2 b3 q3 ) )^2];

p3 = {{2.07 s Cos[o3] - q3 f13 Sin[r3] + q3 f23 Cos[r3] Cos[t3]},  
{2.07 s Sin[o3] + q3 f13 Cos[r3] + q3 f23 Sin[r3] Cos[t3]},  
{q3 f23 Sin[t3]}};

w11 = ( 2 q1 ( q1 dq1 - qq1 xq1 ) - dq1 ( q1^2 + b1^2 - qq1^2 ) ) / ( 2 b1 q1^2 );

w21 = ((dq1 ( q1^2 + b1^2 - qq1^2 ) - ( 2 q1 ( q1 dq1 - qq1 xq1 ) ) ) ( q1^2 +  
b1^2 - qq1^2 ) ) / ( 2 b1 q1^2 Sqrt[4 b1^2 q1^2 - ( q1^2 + b1^2 -  
qq1^2 )^2] );

vp1 = {{-Cos[r1] ( dq1 f11 + q1 w11 ) - Sin[r1] ( dq1 f21 Cos[t1] + q1 w21 Cos[t1] - q1 f2  
1 d[t1] Sin[t1] ) },  
{-Sin[r1] ( dq1 f11 + q1 w11 ) + Cos[r1] ( dq1 f21 Cos[t1] + q1 w21 Cos[t1] -  
q1 f21 d[t1] Sin[t1] ) },  
{dq1 f21 Sin[t1] + q1 w21 Sin[t1] + q1 f21 d[t1] Cos[t1]}};

w12 = ( 2 q2 ( q2 dq2 - qq2 xq2 ) - dq2 ( q2^2 + b2^2 - qq2^2 ) ) / ( 2 b2 q2^2 );

w22 = ((dq2 ( q2^2 + b2^2 - qq2^2 ) - ( 2 q2 ( q2 dq2 - qq2 xq2 ) ) ) ( q2^2 +  
b2^2 - qq2^2 ) ) / ( 2 b2 q2^2 Sqrt[4 b2^2 q2^2 - ( q2^2 + b2^2 -  
qq2^2 )^2] );



```
qq2^2)^2]);
```

```
vp2 = {{Cos[r2] (dq2 f12 + q2 w12) + Sin[r2] (dq2 f22 Cos[t2] + q2 w22 Cos[t2] - q2 f22  
d[t2] Sin[t2]) },  
{Sin[r2] (dq2 f12 + q2 w12) - Cos[r2] (dq2 f22 Cos[t2] + q2 w22 Cos[t2] -  
q2 f22 d[t2] Sin[t2])},  
{dq2 f22 Sin[t2] + q2 w22 Sin[t2] + q2 f22 d[t2] Cos[t2]}};
```

```
w13 = (2 q3 (q3 dq3 - qq3 xq3) - dq3 (q3^2 + b3^2 - qq3^2)) / (2 b3 q3^2);
```

```
w23 = ((dq3 (q3^2 + b3^2 - qq3^2) - (2 q3 (q3 dq3 - qq3 xq3))) (q3^2 +  
b3^2 - qq3^2)) / (2 b3 q3^2 Sqrt[4 b3^2 q3^2 - (q3^2 + b3^2 -  
qq3^2)^2]);
```

```
vp3 = {{-(Sin[r3]) (dq3 f13 + q3 w13) + Cos[r3] (dq3 f23 Cos[t3] + q3 w23 Cos[t3] - q3  
f23 d[t3] Sin[t3]) },  
{Cos[r3] (dq3 f13 + q3 w13) + Sin[r3] (dq3 f23 Cos[t3] + q3 w23 Cos[t3] -  
q3 f23 d[t3] Sin[t3])},  
{dq3 f23 Sin[t3] + q3 w23 Sin[t3] + q3 f23 d[t3] Cos[t3]}};
```

```
m1 = (vp1 - vp2);  
Simplify[%]//N
```

```
m2 = (p1 - p2);  
Simplify[%]//N
```

```
e = (Transpose[m2]) . (m1);
```

```
e1 = Expand[e];
```

```
Factor[e1];
```

```
k11 = Coefficient[e1, q1 d[t1]];  
Simplify[%]//N
```

```
k12 = Coefficient[e1, q2 d[t2]];  
Simplify[%]//N
```

```
m3 = (vp2 - vp3);  
Simplify[%]//N
```

```
m4 = (p2 - p3);  
Simplify[%]//N
```

```
f = (Transpose[m4]) . (m3);
```

```
e2 = Expand[f];
```

```
Factor[e2];
```

```
k22 = Coefficient[e2, q2 d[t2]];  
Simplify[%]//N
```

```
k23 = Coefficient[e2, q3 d[t3]];  
Simplify[%]//N
```

```
m5 = (vp3 - vp1);  
Simplify[%]//N
```

```
m6 = (p3 - p1);  
Simplify[%]//N
```

```
g = (Transpose[m6]) . (m5);  
e3 = Expand[g];  
Factor[e3];  
k31 = Coefficient[e3, q1 d[t1]];  
Simplify[%]//N  
k33 = Coefficient[e3, q3 d[t3]];  
Simplify[%]//N  
gf = (( k11 k22 k33 ) + ( k31 k12 k23))/N;  
Simplify[%]//N
```

\*\*\*\* (13) Output Results of a New Model of 6 SPS \*\*\*\*  
 \*\*\*\* which is defined by Kong et. al. \*\*\*\*

In[69] :=

In[69] :=

$$\begin{aligned}
 \text{Out[69]} = & \left\{ \left\{ 0.522303 \, s \, \text{Sqrt}\left[1. - \frac{0.1369 \, s^2}{q^3}\right] \right. \right. \\
 & > \left. \left( 2.75686 \, s \, \text{Sqrt}\left[1. - \frac{0.1369 \, s^2}{q^2}\right] - \right. \right. \\
 & > \left. \left. 0.34202 \, q_1 \, \text{Sqrt}\left[1. - \frac{0.116981 \, s^2}{q_1}\right] \, \text{Sqrt}\left[1. - \frac{0.1369 \, s^2}{q_2}\right] \, \text{Cos}[t_1] \right) \right. \\
 & > \left. \left( -1. \, q_3 \, \text{Sqrt}\left[1. - \frac{0.116981 \, s^2}{q_1}\right] \, \text{Sqrt}\left[1. - \frac{0.1369 \, s^2}{q_3}\right] \, \text{Cos}[t_1] + \right. \right. \\
 & > \left. \left. 1.602 \, s \, \text{Sqrt}\left[1. - \frac{0.116981 \, s^2}{q_1}\right] \, \text{Sin}[t_1] \right) + \right. \\
 & > \left. 3.11832 \, s \, \text{Sqrt}\left[1. - \frac{0.1369 \, s^2}{q_2}\right] \right. \\
 & > \left. \left( 1.83637 \, s \, \text{Sqrt}\left[1. - \frac{0.1369 \, s^2}{q_3}\right] - \right. \right. \\
 & > \left. \left. 0.939693 \, q_1 \, \text{Sqrt}\left[1. - \frac{0.116981 \, s^2}{q_1}\right] \, \text{Sqrt}\left[1. - \frac{0.1369 \, s^2}{q_3}\right] \, \text{Cos}[t_1] \right) \right. \\
 & > \left. \left( -1. \, q_2 \, \text{Sqrt}\left[1. - \frac{0.116981 \, s^2}{q_1}\right] \, \text{Sqrt}\left[1. - \frac{0.1369 \, s^2}{q_2}\right] \, \text{Cos}[t_1] + \right. \right. \\
 & > \left. \left. 2.17772 \, s \, \text{Sqrt}\left[1. - \frac{0.116981 \, s^2}{q_1}\right] \, \text{Sin}[t_1] \right) \right\}
 \end{aligned}$$



\*\*\*\* (14) Input Programme of a New Class of 6-SPS Platform \*\*\*\*  
 \*\*\*\* Type Parallel Manipulator with a Hexagonal Base \*\*\*\*

```

r1 = Pi / 2;
r2 = Pi / 6;
r3 = Pi / 3;
o1 = Pi / 4;
o2 = 11 Pi / 12;
o3 = 19 Pi / 12;

b1 = b2 = b3 = 70.71

qq1 = q1
qq2 = q2
qq3 = q3

xq1 = dq1;
xq2 = dq2;
xq3 = dq3;

t1 = t2 = Pi / 2;

f11 = ( q1^2 + b1^2 - qq1^2 ) / ( 2 b1 q1 );
f21 = Sqrt[1 - (( q1^2 + b1^2 - qq1^2 ) / ( 2 b1 q1 ) )^2];

p1 = {{s Cos[o1] - q1 f11 Cos[r1] - q1 f21 Sin[r1] Cos[t1]},
      {s Sin[o1] - q1 f11 Sin[r1] + q1 f21 Cos[r1] Cos[t1]},
      {q1 f21 Sin[t1]}};

f12 = ( q2^2 + b2^2 - qq2^2 ) / ( 2 b2 q2 );
f22 = Sqrt[1 - (( q2^2 + b2^2 - qq2^2 ) / ( 2 b2 q2 ) )^2];

p2 = {{2.07 s Cos[o2] + q2 f12 Cos[r2] + q2 f22 Sin[r2] Cos[t2]},
      {2.07 s Sin[o2] + q2 f12 Sin[r2] - q2 f22 Cos[r2] Cos[t2]},
      {q2 f22 Sin[t2]}};

f13 = ( q3^2 + b3^2 - qq3^2 ) / ( 2 b3 q3 );
f23 = Sqrt[1 - (( q3^2 + b3^2 - qq3^2 ) / ( 2 b3 q3 ) )^2];

p3 = {{2.07 s Cos[o3] - q3 f13 Sin[r3] + q3 f23 Cos[r3] Cos[t3]},
      {2.07 s Sin[o3] + q3 f13 Cos[r3] + q3 f23 Sin[r3] Cos[t3]},
      {q3 f23 Sin[t3]}};

w11 = ( 2 q1 (q1 dq1 - qq1 xq1) - dq1 (q1^2 + b1^2 - qq1^2) ) / ( 2 b1 q1^2 );
w21 = ((dq1 (q1^2 + b1^2 - qq1^2) - (2 q1 (q1 dq1 - qq1 xq1))) (q1^2 +
b1^2 - qq1^2) ) / ( 2 b1 q1^2 Sqrt[4 b1^2 q1^2 - (q1^2 + b1^2 -
qq1^2)^2]);

vp1 = {{-Cos[r1] (dq1 f11 + q1 w11) - Sin[r1] (dq1 f21 Cos[t1] + q1 w21 Cos[t1] - q1 f2
1 d[t1] Sin[t1]) },
      {-Sin[r1] (dq1 f11 + q1 w11) + Cos[r1] (dq1 f21 Cos[t1] + q1 w21 Cos[t1] -
q1 f21 d[t1] Sin[t1])},
      {dq1 f21 Sin[t1] + q1 w21 Sin[t1] + q1 f21 d[t1] Cos[t1]}};

w12 = ( 2 q2 (q2 dq2 - qq2 xq2) - dq2 (q2^2 + b2^2 - qq2^2) ) / ( 2 b2 q2^2 );
w22 = ((dq2 (q2^2 + b2^2 - qq2^2) - (2 q2 (q2 dq2 - qq2 xq2))) (q2^2 +
b2^2 - qq2^2) ) / ( 2 b2 q2^2 Sqrt[4 b2^2 q2^2 - (q2^2 + b2^2 -
qq2^2)^2]);

```

```

vp2 = {{Cos[r2] (dq2 f12 + q2 w12) + Sin[r2] (dq2 f22 Cos[t2] + q2 w22 Cos[t2] - q2 f22
d[t2] Sin[t2]) },
      {Sin[r2] (dq2 f12 + q2 w12) - Cos[r2] (dq2 f22 Cos[t2] + q2 w22 Cos[t2] -
q2 f22 d[t2] Sin[t2])}},
      {dq2 f22 Sin[t2] + q2 w22 Sin[t2] + q2 f22 d[t2] Cos[t2]}}};

w13 = (2 q3 (q3 dq3 - qq3 xq3) - dq3 (q3^2 + b3^2 - qq3^2)) / (2 b3 q3^2);

w23 = ((dq3 (q3^2 + b3^2 - qq3^2) - (2 q3 (q3 dq3 - qq3 xq3))) (q3^2 +
b3^2 - qq3^2)) / (2 b3 q3^2 Sqrt[4 b3^2 q3^2 - (q3^2 + b3^2 -
qq3^2)^2]);

vp3 = {{-(Sin[r3]) (dq3 f13 + q3 w13) + Cos[r3] (dq3 f23 Cos[t3] + q3 w23 Cos[t3] - q3
f23 d[t3] Sin[t3]) },
      {Cos[r3] (dq3 f13 + q3 w13) + Sin[r3] (dq3 f23 Cos[t3] + q3 w23 Cos[t3] -
q3 f23 d[t3] Sin[t3])}},
      {dq3 f23 Sin[t3] + q3 w23 Sin[t3] + q3 f23 d[t3] Cos[t3]}}};

m1 = (vp1 - vp2);
Simplify[%]//N

m2 = (p1 - p2);
Simplify[%]//N

e = (Transpose[m2]) . (m1);

e1 = Expand[e];

Factor[e1];

k11 = Coefficient[e1, q1 d[t1]];
Simplify[%]//N

k12 = Coefficient[e1, q2 d[t2]];
Simplify[%]//N

m3 = (vp2 - vp3);
Simplify[%]//N

m4 = (p2 - p3);
Simplify[%]//N

f = (Transpose[m4]) . (m3);

e2 = Expand[f];

Factor[e2];

k22 = Coefficient[e2, q2 d[t2]];
Simplify[%]//N

k23 = Coefficient[e2, q3 d[t3]];
Simplify[%]//N

m5 = (vp3 - vp1);
Simplify[%]//N

m6 = (p3 - p1);
Simplify[%]//N

g = (Transpose[m6]) . (m5);

```

```
e3 = Expand[g];
Factor[e3];
k31 = Coefficient[e3, q1 d[t1]];
Simplify[%]/N
k33 = Coefficient[e3, q3 d[t3]];
Simplify[%]/N
gf = (( k11 k22 k33 ) + ( k31 k12 k23))/N;
Simplify[%]/N
```



\*\*\*\* (15) Output Results of a New Class of 6-SPS Platform \*\*\*\*  
 \*\*\*\* Type Parallel Manipulator with a Hexagonal Base \*\*\*\*

In[67] :=

$$\begin{aligned}
 \text{Result} = & \left\{ \left\{ \left( 30.6183 \sqrt{\frac{1249.98}{q_2^2}} + 1.20489 \sqrt{\frac{1249.98}{q_2^2}} \right) s \right. \right. \\
 & > \left( 30.6183 \sqrt{\frac{1249.98}{q_1^2}} + 0.171351 \sqrt{\frac{1249.98}{q_1^2}} \right) s - \\
 & > 0.5 \sqrt{\frac{1249.98}{q_1^2}} \sqrt{\frac{1249.98}{q_3^2}} q_3 \cos[t_3] \\
 & > (-1. \sqrt{\frac{1249.98}{q_2^2}} q_2 \sqrt{\frac{1249.98}{q_3^2}} \cos[t_3] + \\
 & > 30.6183 \sqrt{\frac{1249.98}{q_3^2}} \sin[t_3] + \\
 & > 0.927956 \sqrt{\frac{1249.98}{q_3^2}} s \sin[t_3] \left. \right\} + \\
 & > \left( -30.6183 \sqrt{\frac{1249.98}{q_1^2}} + 2.70657 \sqrt{\frac{1249.98}{q_1^2}} \right) s \\
 & > \left( -30.6183 \sqrt{\frac{1249.98}{q_2^2}} + 3.46318 \sqrt{\frac{1249.98}{q_2^2}} \right) s - \\
 & > 0.5 \sqrt{\frac{1249.98}{q_2^2}} \sqrt{\frac{1249.98}{q_3^2}} q_3 \cos[t_3] \\
 & > (-1. \sqrt{\frac{1249.98}{q_1^2}} q_1 \sqrt{\frac{1249.98}{q_3^2}} \cos[t_3] - \\
 & > 30.6183 \sqrt{\frac{1249.98}{q_3^2}} \sin[t_3] + \\
 & > 2.42964 \sqrt{\frac{1249.98}{q_3^2}} s \sin[t_3] \left. \right\}
 \end{aligned}$$

\*\*\*\* (16) Input Programme of a New Class of 6-SPS Platform \*\*\*\*  
 \*\*\*\* Type Parallel Manipulator with a Pentagonal Base \*\*\*\*

r1 = Pi / 2;

r2 = 0;

r3 = Pi / 4;

o1 = Pi / 4;

o2 = 3 Pi / 4;

o3 = 3 Pi / 2;

b1 = b2 = 1.414 s;

b3 = 2 s;

qq1 = q1;

qq2 = q2;

qq3 = q3;

xq1 = dq1;

xq2 = dq2;

xq3 = dq3;

t1 = t2 = Pi / 2;

f11 = ( q1^2 + b1^2 - qq1^2 ) / ( 2 b1 q1 );

f21 = Sqrt[1 - (( q1^2 + b1^2 - qq1^2 ) / ( 2 b1 q1 ) )^2];

p1 = {{s Cos[o1] - q1 f11 Cos[r1] - q1 f21 Sin[r1] Cos[t1]},  
 {s Sin[o1] - q1 f11 Sin[r1] + q1 f21 Cos[r1] Cos[t1]},  
 {q1 f21 Sin[t1]}};

f12 = ( q2^2 + b2^2 - qq2^2 ) / ( 2 b2 q2 );

f22 = Sqrt[1 - (( q2^2 + b2^2 - qq2^2 ) / ( 2 b2 q2 ) )^2];

p2 = {{2.07 s Cos[o2] + q2 f12 Cos[r2] + q2 f22 Sin[r2] Cos[t2]},  
 {2.07 s Sin[o2] + q2 f12 Sin[r2] - q2 f22 Cos[r2] Cos[t2]},  
 {q2 f22 Sin[t2]}};

f13 = ( q3^2 + b3^2 - qq3^2 ) / ( 2 b3 q3 );

f23 = Sqrt[1 - (( q3^2 + b3^2 - qq3^2 ) / ( 2 b3 q3 ) )^2];

p3 = {{2.07 s Cos[o3] - q3 f13 Sin[r3] + q3 f23 Cos[r3] Cos[t3]},  
 {2.07 s Sin[o3] + q3 f13 Cos[r3] + q3 f23 Sin[r3] Cos[t3]},  
 {q3 f23 Sin[t3]}};

w11 = ( 2 q1 (q1 dq1 - qq1 xq1) - dq1 (q1^2 + b1^2 - qq1^2) ) / ( 2 b1 q1^2 );

w21 = ((dq1 (q1^2 + b1^2 - qq1^2) - (2 q1 (q1 dq1 - qq1 xq1))) (q1^2 +  
 b1^2 - qq1^2) ) / ( 2 b1 q1^2 Sqrt[4 b1^2 q1^2 - (q1^2 + b1^2 -  
 qq1^2)^2] );

vp1 = {{-Cos[r1] (dq1 f11 + q1 w11) - Sin[r1] (dq1 f21 Cos[t1] + q1 w21 Cos[t1] - q1 f2  
 1 d[t1] Sin[t1]) },  
 {-Sin[r1] (dq1 f11 + q1 w11) + Cos[r1] (dq1 f21 Cos[t1] + q1 w21 Cos[t1] -  
 q1 f21 d[t1] Sin[t1])},  
 {dq1 f21 Sin[t1] + q1 w21 Sin[t1] + q1 f21 d[t1] Cos[t1]}};

w12 = ( 2 q2 (q2 dq2 - qq2 xq2) - dq2 (q2^2 + b2^2 - qq2^2) ) / ( 2 b2 q2^2 );

w22 = ((dq2 (q2^2 + b2^2 - qq2^2) - (2 q2 (q2 dq2 - qq2 xq2))) (q2^2 +  
 b2^2 - qq2^2) ) / ( 2 b2 q2^2 Sqrt[4 b2^2 q2^2 - (q2^2 + b2^2 -  
 qq2^2)^2] );

```

qq2^2)^2]);

vp2 = {{Cos[r2] (dq2 f12 + q2 w12) + Sin[r2] (dq2 f22 Cos[t2] + q2 w22 Cos[t2] - q2 f22
d[t2] Sin[t2]) },
      {Sin[r2] (dq2 f12 + q2 w12) - Cos[r2] (dq2 f22 Cos[t2] + q2 w22 Cos[t2] -
q2 f22 d[t2] Sin[t2])},
      {dq2 f22 Sin[t2] + q2 w22 Sin[t2] + q2 f22 d[t2] Cos[t2]}};

w13 = (2 q3 (q3 dq3 - qq3 xq3) - dq3 (q3^2 + b3^2 - qq3^2)) / (2 b3 q3^2);

w23 = ((dq3 (q3^2 + b3^2 - qq3^2) - (2 q3 (q3 dq3 - qq3 xq3))) (q3^2 +
b3^2 - qq3^2)) / (2 b3 q3^2 Sqrt[4 b3^2 q3^2 - (q3^2 + b3^2 -
qq3^2)^2]);

vp3 = {{-(Sin[r3]) (dq3 f13 + q3 w13) + Cos[r3] (dq3 f23 Cos[t3] + q3 w23 Cos[t3] - q3
f23 d[t3] Sin[t3]) },
      {Cos[r3] (dq3 f13 + q3 w13) + Sin[r3] (dq3 f23 Cos[t3] + q3 w23 Cos[t3] -
q3 f23 d[t3] Sin[t3])},
      {dq3 f23 Sin[t3] + q3 w23 Sin[t3] + q3 f23 d[t3] Cos[t3]}};

m1 = (vp1 - vp2);
Simplify[%]//N

m2 = (p1 - p2);
Simplify[%]//N

e = (Transpose[m2]) . (m1);

e1 = Expand[e];

Factor[e1];

k11 = Coefficient[e1, q1 d[t1]];
Simplify[%]//N

k12 = Coefficient[e1, q2 d[t2]];
Simplify[%]//N

m3 = (vp2 - vp3);
Simplify[%]//N

m4 = (p2 - p3);
Simplify[%]//N

f = (Transpose[m4]) . (m3);

e2 = Expand[f];

Factor[e2];

k22 = Coefficient[e2, q2 d[t2]];
Simplify[%]//N

k23 = Coefficient[e2, q3 d[t3]];
Simplify[%]//N

m5 = (vp3 - vp1);
Simplify[%]//N

m6 = (p3 - p1);
Simplify[%]//N

```



```
g = (Transpose[m6]) . (m5);
```

```
e3 = Expand[g];
```

```
Factor[e3];
```

```
k31 = Coefficient[e3, q1 d[t1]];
```

```
Simplify[%]//N
```

```
k33 = Coefficient[e3, q3 d[t3]];
```

```
Simplify[%]//N
```

```
gf = (( k11 k22 k33 ) + ( k31 k12 k23 ))//N;
```

```
Simplify[%]//N
```

\*\*\*\* (17) Output Results of a New Class of 6-SPS Platform \*\*\*\*  
 \*\*\*\* Type Parallel Manipulator with a Pentagonal Base \*\*\*\*

In[68] :=

$$\text{Out[68]} = \left\{ \left\{ 1.4636 s \sqrt{1 - \frac{0.499849 s^2}{q_2^2}} \right. \right.$$

$$> \left. \left( 1.41421 s \sqrt{1 - \frac{0.499849 s^2}{q_1^2}} - \right. \right.$$

$$> \left. 0.707107 q_3 \sqrt{1 - \frac{0.499849 s^2}{q_1^2}} \sqrt{1 - \frac{1. s^2}{q_3^2}} \cos[t_3] \right)$$

$$> \left. \left( -1. q_2 \sqrt{1 - \frac{0.499849 s^2}{q_2^2}} \sqrt{1 - \frac{1. s^2}{q_3^2}} \cos[t_3] + \right. \right.$$

$$> \left. 1.96364 s \sqrt{1 - \frac{1. s^2}{q_3^2}} \sin[t_3] \right) +$$

$$> \left. 1.46382 s \sqrt{1 - \frac{0.499849 s^2}{q_1^2}} \right.$$

$$> \left. \left( 2.8266 s \sqrt{1 - \frac{0.499849 s^2}{q_2^2}} - \right. \right.$$

$$> \left. 0.707107 q_3 \sqrt{1 - \frac{0.499849 s^2}{q_2^2}} \sqrt{1 - \frac{1. s^2}{q_3^2}} \cos[t_3] \right)$$

$$> \left. \left( -1. q_1 \sqrt{1 - \frac{0.499849 s^2}{q_1^2}} \sqrt{1 - \frac{1. s^2}{q_3^2}} \cos[t_3] + \right. \right.$$

$$> \left. 1.96379 s \sqrt{1 - \frac{1. s^2}{q_3^2}} \sin[t_3] \right) \left. \right\}$$

\*\*\*\* (18) Input Programme of a New Class of 6-SPS Platform \*\*\*\*  
 \*\*\*\* Type Parallel Manipulator with a Tetragonal Base \*\*\*\*

r1 = Pi / 2;  
 r2 = 0;  
 r3 = 0;  
 o1 = Pi / 4;  
 o2 = 3 Pi / 4;  
 o3 = 5 Pi / 4;

b1 = b2 = 1.414 s;  
 b3 = 1.414 s;  
 qq1 = q1;  
 qq2 = q2;  
 qq3 = q3;

xq1 = dq1;  
 xq2 = dq2;  
 xq3 = dq3;

t1 = Pi / 2;  
 t2 = Pi / 2;

f11 = ( q1^2 + b1^2 - qq1^2 ) / ( 2 b1 q1 );

f21 = Sqrt[1 - (( q1^2 + b1^2 - qq1^2 ) / ( 2 b1 q1 ) )^2];

p1 = {{s Cos[o1] - q1 f11 Cos[r1] - q1 f21 Sin[r1] Cos[t1]},  
 {s Sin[o1] - q1 f11 Sin[r1] + q1 f21 Cos[r1] Cos[t1]},  
 {q1 f21 Sin[t1]}};

f12 = ( q2^2 + b2^2 - qq2^2 ) / ( 2 b2 q2 );

f22 = Sqrt[1 - (( q2^2 + b2^2 - qq2^2 ) / ( 2 b2 q2 ) )^2];

p2 = {{2.07 s Cos[o2] + q2 f12 Cos[r2] + q2 f22 Sin[r2] Cos[t2]},  
 {2.07 s Sin[o2] + q2 f12 Sin[r2] - q2 f22 Cos[r2] Cos[t2]},  
 {q2 f22 Sin[t2]}};

f13 = ( q3^2 + b3^2 - qq3^2 ) / ( 2 b3 q3 );

f23 = Sqrt[1 - (( q3^2 + b3^2 - qq3^2 ) / ( 2 b3 q3 ) )^2];

p3 = {{2.07 s Cos[o3] - q3 f13 Sin[r3] + q3 f23 Cos[r3] Cos[t3]},  
 {2.07 s Sin[o3] + q3 f13 Cos[r3] + q3 f23 Sin[r3] Cos[t3]},  
 {q3 f23 Sin[t3]}};

w11 = ( 2 q1 (q1 dq1 - qq1 xq1) - dq1 (q1^2 + b1^2 - qq1^2) ) / ( 2 b1 q1^2 );

w21 = ((dq1 (q1^2 + b1^2 - qq1^2) - (2 q1 (q1 dq1 - qq1 xq1))) (q1^2 + b1^2 - qq1^2) / ( 2 b1 q1^2 Sqrt[4 b1^2 q1^2 - (q1^2 + b1^2 - qq1^2)^2]);

vp1 = {{-Cos[r1] (dq1 f11 + q1 w11) - Sin[r1] (dq1 f21 Cos[t1] + q1 w21 Cos[t1] - q1 f21 d[t1] Sin[t1]) },  
 {-Sin[r1] (dq1 f11 + q1 w11) + Cos[r1] (dq1 f21 Cos[t1] + q1 w21 Cos[t1] - q1 f21 d[t1] Sin[t1])},  
 {dq1 f21 Sin[t1] + q1 w21 Sin[t1] + q1 f21 d[t1] Cos[t1]}};

w12 = ( 2 q2 (q2 dq2 - qq2 xq2) - dq2 (q2^2 + b2^2 - qq2^2) ) / ( 2 b2 q2^2 );

w22 = ((dq2 (q2^2 + b2^2 - qq2^2) - (2 q2 (q2 dq2 - qq2 xq2))) (q2^2 + b2^2 - qq2^2) / ( 2 b2 q2^2 Sqrt[4 b2^2 q2^2 - (q2^2 + b2^2 - qq2^2)^2]);



```

vp2 = {{Cos[r2] (dq2 f12 + q2 w12) + Sin[r2] (dq2 f22 Cos[t2] + q2 w22 Cos[t2] - q2 f22
d[t2] Sin[t2]) },
      {Sin[r2] (dq2 f12 + q2 w12) - Cos[r2] (dq2 f22 Cos[t2] + q2 w22 Cos[t2] -
q2 f22 d[t2] Sin[t2])},
      {dq2 f22 Sin[t2] + q2 w22 Sin[t2] + q2 f22 d[t2] Cos[t2]}}};

w13 = (2 q3 (q3 dq3 - qq3 xq3) - dq3 (q3^2 + b3^2 - qq3^2)) / (2 b3 q3^2);

w23 = ((dq3 (q3^2 + b3^2 - qq3^2) - (2 q3 (q3 dq3 - qq3 xq3))) (q3^2 +
b3^2 - qq3^2)) / (2 b3 q3^2 Sqrt[4 b3^2 q3^2 - (q3^2 + b3^2 -
qq3^2)^2]);

vp3 = {{-(Sin[r3]) (dq3 f13 + q3 w13) + Cos[r3] (dq3 f23 Cos[t3] + q3 w23 Cos[t3] - q3
f23 d[t3] Sin[t3]) },
      {Cos[r3] (dq3 f13 + q3 w13) + Sin[r3] (dq3 f23 Cos[t3] + q3 w23 Cos[t3] -
q3 f23 d[t3] Sin[t3])},
      {dq3 f23 Sin[t3] + q3 w23 Sin[t3] + q3 f23 d[t3] Cos[t3]}}};

m1 = (vp1 - vp2);
Simplify[%]//N

m2 = (p1 - p2);
Simplify[%]//N

e = (Transpose[m2]) . (m1);

e1 = Expand[e];

Factor[e1];

k11 = Coefficient[e1, q1 d[t1]];
Simplify[%]//N

k12 = Coefficient[e1, q2 d[t2]];
Simplify[%]//N

m3 = (vp2 - vp3);
Simplify[%]//N

m4 = (p2 - p3);
Simplify[%]//N

f = (Transpose[m4]) . (m3);

e2 = Expand[f];

Factor[e2];

k22 = Coefficient[e2, q2 d[t2]];
Simplify[%]//N

k23 = Coefficient[e2, q3 d[t3]];
Simplify[%]//N

m5 = (vp3 - vp1);
Simplify[%]//N

m6 = (p3 - p1);
Simplify[%]//N

g = (Transpose[m6]) . (m5);

```

```
e3 = Expand[g];
Factor[e3];
k31 = Coefficient[e3, q1 d[t1]];
Simplify[%]//N
k33 = Coefficient[e3, q3 d[t3]];
Simplify[%]//N
gf = (( k11 k22 k33 ) + ( k31 k12 k23 ))//N;
Simplify[%]//N
```

\*\*\*\* (19) Output Results of a New Class of 6-SPS Platform \*\*\*\*  
 \*\*\*\* Type Parallel Manipulator with a Tetragonal Base \*\*\*\*

In[69] :=

$$\begin{aligned}
 \text{Out}[69] = & \left\{ \left\{ 1.4636 s \sqrt{1. - \frac{0.499849 s^2}{q_2^2}} \right. \right. \\
 & > \left. \left( 2.17082 s \sqrt{1. - \frac{0.499849 s^2}{q_1^2}} - \right. \right. \\
 & > \left. \left. 1. q_3 \sqrt{1. - \frac{0.499849 s^2}{q_1^2}} \sqrt{1. - \frac{0.499849 s^2}{q_3^2}} \cos[t_3] \right) \right. \\
 & > \left. \left( -1. q_2 \sqrt{1. - \frac{0.499849 s^2}{q_2^2}} \sqrt{1. - \frac{0.499849 s^2}{q_3^2}} \cos[t_3] + \right. \right. \\
 & > \left. \left. 0.707 s \sqrt{1. - \frac{0.499849 s^2}{q_3^2}} \sin[t_3] \right) + \right. \\
 & > \left. \left. 3.25029 s \sqrt{1. - \frac{0.499849 s^2}{q_1^2}} \sqrt{1. - \frac{0.499849 s^2}{q_2^2}} \right. \right. \\
 & > \left. \left. \left( -1. q_1 \sqrt{1. - \frac{0.499849 s^2}{q_1^2}} \sqrt{1. - \frac{0.499849 s^2}{q_3^2}} \cos[t_3] + \right. \right. \\
 & > \left. \left. \left. \left. 2.17082 s \sqrt{1. - \frac{0.499849 s^2}{q_3^2}} \sin[t_3] \right) \right] \right\} \right\}
 \end{aligned}$$



\*\*\*\* (20) Input Programme of a New Class of 6-SPS Platform \*\*\*\*  
 \*\*\*\* Type Parallel Manipulator with a Triangular Base \*\*\*\*

r1 = Pi / 2;  
 r2 = 0;  
 r3 = Pi / 4;  
 o1 = Pi / 4;  
 o2 = 8 Pi / 9;  
 o3 = 29 Pi / 18;

b1 = b2 = 2.65 s;  
 b3 = 3.75 s;  
 qq1 = q1;  
 qq2 = q2;  
 qq3 = q3;

xq1 = dq1;  
 xq2 = dq2;  
 xq3 = dq3;

t1 = Pi / 2;  
 t2 = Pi / 2;

f11 = ( q1^2 + b1^2 - qq1^2 ) / ( 2 b1 q1 );  
 f21 = Sqrt[1 - (( q1^2 + b1^2 - qq1^2 ) / ( 2 b1 q1 ) )^2];

p1 = {{s Cos[o1] - q1 f11 Cos[r1] - q1 f21 Sin[r1] Cos[t1]},  
 {s Sin[o1] - q1 f11 Sin[r1] + q1 f21 Cos[r1] Cos[t1]},  
 {q1 f21 Sin[t1]}};

f12 = ( q2^2 + b2^2 - qq2^2 ) / ( 2 b2 q2 );  
 f22 = Sqrt[1 - (( q2^2 + b2^2 - qq2^2 ) / ( 2 b2 q2 ) )^2];

p2 = {{2.07 s Cos[o2] + q2 f12 Cos[r2] + q2 f22 Sin[r2] Cos[t2]},  
 {2.07 s Sin[o2] + q2 f12 Sin[r2] - q2 f22 Cos[r2] Cos[t2]},  
 {q2 f22 Sin[t2]}};

f13 = ( q3^2 + b3^2 - qq3^2 ) / ( 2 b3 q3 );  
 f23 = Sqrt[1 - (( q3^2 + b3^2 - qq3^2 ) / ( 2 b3 q3 ) )^2];

p3 = {{2.07 s Cos[o3] - q3 f13 Sin[r3] + q3 f23 Cos[r3] Cos[t3]},  
 {2.07 s Sin[o3] + q3 f13 Cos[r3] + q3 f23 Sin[r3] Cos[t3]},  
 {q3 f23 Sin[t3]}};

w11 = ( 2 q1 ( q1 dq1 - qq1 xq1 ) - dq1 ( q1^2 + b1^2 - qq1^2 ) ) / ( 2 b1 q1^2 );

w21 = ((dq1 ( q1^2 + b1^2 - qq1^2 ) - ( 2 q1 ( q1 dq1 - qq1 xq1 ) ) ) ( q1^2 + b1^2 - qq1^2 ) / ( 2 b1 q1^2 Sqrt[4 b1^2 q1^2 - ( q1^2 + b1^2 - qq1^2 )^2] );

vp1 = {{-Cos[r1] ( dq1 f11 + q1 w11 ) - Sin[r1] ( dq1 f21 Cos[t1] + q1 w21 Cos[t1] - q1 f21 d[t1] Sin[t1] ) },  
 {-Sin[r1] ( dq1 f11 + q1 w11 ) + Cos[r1] ( dq1 f21 Cos[t1] + q1 w21 Cos[t1] - q1 f21 d[t1] Sin[t1] ) },  
 {dq1 f21 Sin[t1] + q1 w21 Sin[t1] + q1 f21 d[t1] Cos[t1]}};

w12 = ( 2 q2 ( q2 dq2 - qq2 xq2 ) - dq2 ( q2^2 + b2^2 - qq2^2 ) ) / ( 2 b2 q2^2 );

w22 = ((dq2 ( q2^2 + b2^2 - qq2^2 ) - ( 2 q2 ( q2 dq2 - qq2 xq2 ) ) ) ( q2^2 + b2^2 - qq2^2 ) / ( 2 b2 q2^2 Sqrt[4 b2^2 q2^2 - ( q2^2 + b2^2 - qq2^2 )^2] );

```

vp2 = {{Cos[r2] (dq2 f12 + q2 w12) + Sin[r2] (dq2 f22 Cos[t2] + q2 w22 Cos[t2] - q2 f22
d[t2] Sin[t2]) },
      {Sin[r2] (dq2 f12 + q2 w12) - Cos[r2] (dq2 f22 Cos[t2] + q2 w22 Cos[t2] -
q2 f22 d[t2] Sin[t2])}},
      {dq2 f22 Sin[t2] + q2 w22 Sin[t2] + q2 f22 d[t2] Cos[t2]}};

w13 = (2 q3 (q3 dq3 - qq3 xq3) - dq3 (q3^2 + b3^2 - qq3^2)) / (2 b3 q3^2);

w23 = ((dq3 (q3^2 + b3^2 - qq3^2) - (2 q3 (q3 dq3 - qq3 xq3))) (q3^2 +
b3^2 - qq3^2)) / (2 b3 q3^2 Sqrt[4 b3^2 q3^2 - (q3^2 + b3^2 -
qq3^2)^2]);

vp3 = {{-(Sin[r3]) (dq3 f13 + q3 w13) + Cos[r3] (dq3 f23 Cos[t3] + q3 w23 Cos[t3] - q3
f23 d[t3] Sin[t3]) },
      {Cos[r3] (dq3 f13 + q3 w13) + Sin[r3] (dq3 f23 Cos[t3] + q3 w23 Cos[t3] -
q3 f23 d[t3] Sin[t3])}},
      {dq3 f23 Sin[t3] + q3 w23 Sin[t3] + q3 f23 d[t3] Cos[t3]}};

m1 = (vp1 - vp2);
Simplify[%]//N

m2 = (p1 - p2);
Simplify[%]//N

e = (Transpose[m2]) . (m1);

e1 = Expand[e];

Factor[e1];

k11 = Coefficient[e1, q1 d[t1]];
Simplify[%]//N

k12 = Coefficient[e1, q2 d[t2]];
Simplify[%]//N

m3 = (vp2 - vp3);
Simplify[%]//N

m4 = (p2 - p3);
Simplify[%]//N

f = (Transpose[m4]) . (m3);

e2 = Expand[f];

Factor[e2];

k22 = Coefficient[e2, q2 d[t2]];
Simplify[%]//N

k23 = Coefficient[e2, q3 d[t3]];
Simplify[%]//N

m5 = (vp3 - vp1);
Simplify[%]//N

m6 = (p3 - p1);
Simplify[%]//N

g = (Transpose[m6]) . (m5);

```

```
e3 = Expand[g];  
Factor[e3];  
k31 = Coefficient[e3, q1 d[t1]];  
Simplify[%]//N  
k33 = Coefficient[e3, q3 d[t3]];  
Simplify[%]//N  
gf = (( k11 k22 k33 ) + ( k31 k12 k23 ))//N;  
Simplify[%]//N
```



\*\*\*\* (21) Output Results of a New Class of 6-SPS Platform \*\*\*\*  
 \*\*\*\* Type Parallel Manipulator with a Triangular Base \*\*\*\*

In[69] :=

$$\begin{aligned}
 \text{Out}[69] = & \left\{ \left\{ 1.32587 s \sqrt{1. - \frac{1.75563 s^2}{q_2^2}} \right\} \right. \\
 & > \left( 1.32495 s \sqrt{1. - \frac{1.75563 s^2}{q_1^2}} - \right. \\
 & > 0.707107 q_3 \sqrt{1. - \frac{1.75563 s^2}{q_1^2}} \sqrt{1. - \frac{3.51562 s^2}{q_3^2}} \cos[t_3] \\
 & > (-1. q_2 \sqrt{1. - \frac{1.75563 s^2}{q_2^2}} \sqrt{1. - \frac{3.51562 s^2}{q_3^2}} \cos[t_3] + \\
 & > 0.936916 s \sqrt{1. - \frac{3.51562 s^2}{q_3^2}} \sin[t_3] \left. \right) + \\
 & > 1.32727 s \sqrt{1. - \frac{1.75563 s^2}{q_1^2}} \\
 & > (1.32732 s \sqrt{1. - \frac{1.75563 s^2}{q_2^2}} - \\
 & > 0.707107 q_3 \sqrt{1. - \frac{1.75563 s^2}{q_2^2}} \sqrt{1. - \frac{3.51562 s^2}{q_3^2}} \cos[t_3] \\
 & > (-1. q_1 \sqrt{1. - \frac{1.75563 s^2}{q_1^2}} \sqrt{1. - \frac{3.51562 s^2}{q_3^2}} \cos[t_3] + \\
 & > 0.937903 s \sqrt{1. - \frac{3.51562 s^2}{q_3^2}} \sin[t_3] \left. \right\} \left. \right\}
 \end{aligned}$$

\*\*\*\* (22) Input Programme in Chapter 4 for Case 1 to 5 \*\*\*\*  
 \*\*\*\* Theta 1 and 2 can be changed from 0 to 180 Degree \*\*\*\*

r1 = Pi / 2;  
 r2 = Pi / 6;  
 r3 = Pi / 3;  
 o1 = Pi / 4;  
 o2 = 11 Pi / 12;  
 o3 = 19 Pi / 12;

t1 = Pi / 2  
 t2 = Pi / 2

f11 = ( q1^2 + b1^2 - qq1^2 ) / ( 2 b1 q1 );

f21 = Sqrt[1 - (( q1^2 + b1^2 - qq1^2 ) / ( 2 b1 q1 ) )^2];

p1 = {{s Cos[o1] - q1 f11 Cos[r1] - q1 f21 Sin[r1] Cos[t1]},  
 {s Sin[o1] - q1 f11 Sin[r1] + q1 f21 Cos[r1] Cos[t1]},  
 {q1 f21 Sin[t1]}};

f12 = ( q2^2 + b2^2 - qq2^2 ) / ( 2 b2 q2 );

f22 = Sqrt[1 - (( q2^2 + b2^2 - qq2^2 ) / ( 2 b2 q2 ) )^2];

p2 = {{s Cos[o2] + q2 f12 Cos[r2] + q2 f22 Sin[r2] Cos[t2]},  
 {s Sin[o2] + q2 f12 Sin[r2] - q2 f22 Cos[r2] Cos[t2]},  
 {q2 f22 Sin[t2]}};

f13 = ( q3^2 + b3^2 - qq3^2 ) / ( 2 b3 q3 );

f23 = Sqrt[1 - (( q3^2 + b3^2 - qq3^2 ) / ( 2 b3 q3 ) )^2];

p3 = {{s Cos[o3] - q3 f13 Sin[r3] + q3 f23 Cos[r3] Cos[t3]},  
 {s Sin[o3] + q3 f13 Cos[r3] + q3 f23 Sin[r3] Cos[t3]},  
 {q3 f23 Sin[t3]}};

w11 = ( 2 q1 (q1 dq1 - qq1 xq1) - dq1 (q1^2 + b1^2 - qq1^2) ) / ( 2 b1 q1^2 );

w21 = ((dq1 (q1^2 + b1^2 - qq1^2) - (2 q1 (q1 dq1 - qq1 xq1))) (q1^2 +  
 b1^2 - qq1^2) ) / ( 2 b1 q1^2 Sqrt[4 b1^2 q1^2 - (q1^2 + b1^2 -  
 qq1^2)^2] );

vp1 = {{-Cos[r1] (dq1 f11 + q1 w11) - Sin[r1] (dq1 f21 Cos[t1] + q1 w21 Cos[t1] - q1 f2  
 1 d[t1] Sin[t1]) },  
 {-Sin[r1] (dq1 f11 + q1 w11) + Cos[r1] (dq1 f21 Cos[t1] + q1 w21 Cos[t1] -  
 q1 f21 d[t1] Sin[t1]) },  
 {dq1 f21 Sin[t1] + q1 w21 Sin[t1] + q1 f21 d[t1] Cos[t1]}};

w12 = ( 2 q2 (q2 dq2 - qq2 xq2) - dq2 (q2^2 + b2^2 - qq2^2) ) / ( 2 b2 q2^2 );

w22 = ((dq2 (q2^2 + b2^2 - qq2^2) - (2 q2 (q2 dq2 - qq2 xq2))) (q2^2 +  
 b2^2 - qq2^2) ) / ( 2 b2 q2^2 Sqrt[4 b2^2 q2^2 - (q2^2 + b2^2 -  
 qq2^2)^2] );

vp2 = {{Cos[r2] (dq2 f12 + q2 w12) + Sin[r2] (dq2 f22 Cos[t2] + q2 w22 Cos[t2] - q2 f22  
 d[t2] Sin[t2]) },  
 {Sin[r2] (dq2 f12 + q2 w12) - Cos[r2] (dq2 f22 Cos[t2] + q2 w22 Cos[t2] -  
 q2 f22 d[t2] Sin[t2]) },  
 {dq2 f22 Sin[t2] + q2 w22 Sin[t2] + q2 f22 d[t2] Cos[t2]}};

w13 = ( 2 q3 (q3 dq3 - qq3 xq3) - dq3 (q3^2 + b3^2 - qq3^2) ) / ( 2 b3 q3^2 );

```

w23 = ((dq3 (q3^2 + b3^2 - qq3^2) - (2 q3 (q3 dq3 - qq3 xq3))) (q3^2 +
b3^2 - qq3^2)) / (2 b3 q3^2 Sqrt[4 b3^2 q3^2 - (q3^2 + b3^2 -
qq3^2)^2]);

vp3 = {{-(Sin[r3]) (dq3 f13 + q3 w13) + Cos[r3] (dq3 f23 Cos[t3] + q3 w23 Cos[t3] - q3
f23 d[t3] Sin[t3]) },
{Cos[r3] (dq3 f13 + q3 w13) + Sin[r3] (dq3 f23 Cos[t3] + q3 w23 Cos[t3] -
q3 f23 d[t3] Sin[t3])},
{dq3 f23 Sin[t3] + q3 w23 Sin[t3] + q3 f23 d[t3] Cos[t3]}};

m1 = (vp1 - vp2);

m2 = (p1 - p2);

e = (Transpose[m2]) . (m1);

e1 = Expand[e];

Factor[e1];

k11 = Coefficient[e1, q1 d[t1]];

k12 = Coefficient[e1, q2 d[t2]];

m3 = (vp2 - vp3);

m4 = (p2 - p3);

f = (Transpose[m4]) . (m3);

e2 = Expand[f];

Factor[e2];

k22 = Coefficient[e2, q2 d[t2]];

k23 = Coefficient[e2, q3 d[t3]];

m5 = (vp3 - vp1);

m6 = (p3 - p1);

g = (Transpose[m6]) . (m5);

e3 = Expand[g];

Factor[e3];

k31 = Coefficient[e3, q1 d[t1]];

k33 = Coefficient[e3, q3 d[t3]];

gf = (( k11 k22 k33 ) + ( k31 k12 k23))/N;

Simplify[%]

```



\*\*\*\* (23) Output Results of Case 1 in Chapter 4 \*\*\*\*  
 \*\*\*\* (General Form Solutions) \*\*\*\*  
 \*\*\*\* Theta 1 is 90 Degree and theta 2 is 90 Degree \*\*\*\*

$$\text{Out}[48] = \left\{ \left( \text{Sqrt} \left[ \frac{-b_1^4 + 2 b_1^2 q_1^2 - q_1^4 + 2 b_1^2 q_1^2 + 2 q_1^2 q_1^2 - q_1^4}{b_1^2 q_1^2} \right] \right. \right.$$

$$\left. \text{Sqrt} \left[ \frac{-b_2^4 + 2 b_2^2 q_2^2 - q_2^4 + 2 b_2^2 q_2^2 + 2 q_2^2 q_2^2 - q_2^4}{b_2^2 q_2^2} \right] \right.$$

$$\left. \text{Sqrt} \left[ \frac{-b_3^4 + 2 b_3^2 q_3^2 - q_3^4 + 2 b_3^2 q_3^2 + 2 q_3^2 q_3^2 - q_3^4}{b_3^2 q_3^2} \right] \right.$$

$$\left. \left( \text{Sqrt}[3] b_2^2 - \text{Sqrt}[3] q_2^2 + \text{Sqrt}[3] q_2^2 - 3 \text{Sqrt}[2] b_2 s - \right. \right.$$

$$\left. \text{Sqrt}[6] b_2 s \right) \left( -\left( \text{Sqrt}[3] b_3 \right) + \text{Sqrt}[3] q_3^2 - \text{Sqrt}[3] q_3^2 + \right.$$

$$\left. 3 \text{Sqrt}[2] b_3 s + \text{Sqrt}[6] b_3 s - \right.$$

$$\left. b_3 q_3 \text{Sqrt} \left[ \frac{-b_3^4 + 2 b_3^2 q_3^2 - q_3^4 + 2 b_3^2 q_3^2 + 2 q_3^2 q_3^2 - q_3^4}{b_3^2 q_3^2} \right] \right.$$

$$\left. \text{Cos}[t_3] \right) \left( 2 b_1 q_1 \text{Sqrt} \left[ \frac{-b_1^4 + 2 b_1^2 q_1^2 - q_1^4 + 2 b_1^2 q_1^2 + 2 q_1^2 q_1^2 - q_1^4}{b_1^2 q_1^2} \right] \right.$$

$$\left. \text{Cos}[t_3] + \text{Sqrt}[3] b_1^2 \text{Sin}[t_3] - \text{Sqrt}[3] q_1^2 \text{Sin}[t_3] + \right.$$

$$\left. \text{Sqrt}[3] q_1^2 \text{Sin}[t_3] - 3 \text{Sqrt}[2] b_1 s \text{Sin}[t_3] - \right.$$

$$\left. \text{Sqrt}[6] b_1 s \text{Sin}[t_3] \right) / (512 b_1 b_2 b_3) +$$

$$\left( \text{Sqrt} \left[ \frac{-b_1^4 + 2 b_1^2 q_1^2 - q_1^4 + 2 b_1^2 q_1^2 + 2 q_1^2 q_1^2 - q_1^4}{b_1^2 q_1^2} \right] \right.$$

$$\left. \text{Sqrt} \left[ \frac{-b_2^4 + 2 b_2^2 q_2^2 - q_2^4 + 2 b_2^2 q_2^2 + 2 q_2^2 q_2^2 - q_2^4}{b_2^2 q_2^2} \right] \right)$$

$$\text{Sqrt}\left[\frac{-b_3^4 + 2 b_3^2 q q_3^2 - q q_3^4 + 2 b_3^2 q_3^2 + 2 q q_3^2 q_3^2 - q_3^4}{b_3^2 q_3^2}\right]$$

$$\begin{aligned} & (\text{Sqrt}[3] b_1^2 - \text{Sqrt}[3] q q_1^2 + \text{Sqrt}[3] q_1^2 + 3 \text{Sqrt}[2] b_1 s - \\ & \text{Sqrt}[6] b_1 s) (- (\text{Sqrt}[3] b_3^2) + \text{Sqrt}[3] q q_3^2 - \text{Sqrt}[3] q_3^2 - \\ & 3 \text{Sqrt}[2] b_3 s + \text{Sqrt}[6] b_3 s + \\ & b_3 q_3 \text{Sqrt}[ \end{aligned}$$

$$\frac{-b_3^4 + 2 b_3^2 q q_3^2 - q q_3^4 + 2 b_3^2 q_3^2 + 2 q q_3^2 q_3^2 - q_3^4}{b_3^2 q_3^2}$$

$$\text{Cos}[t_3]) (2 b_2 q_2 \text{Sqrt}[$$

$$\frac{-b_2^4 + 2 b_2^2 q q_2^2 - q q_2^4 + 2 b_2^2 q_2^2 + 2 q q_2^2 q_2^2 - q_2^4}{b_2^2 q_2^2}$$

$$\text{Cos}[t_3] - \text{Sqrt}[3] b_2^2 \text{Sin}[t_3] + \text{Sqrt}[3] q q_2^2 \text{Sin}[t_3] -$$

$$\text{Sqrt}[3] q_2^2 \text{Sin}[t_3] - 3 \text{Sqrt}[2] b_2 s \text{Sin}[t_3] +$$

$$\text{Sqrt}[6] b_2 s \text{Sin}[t_3]) / (512 b_1 b_2 b_3)}$$

\*\*\*\* (24) Output Results of Case 2 in Chapter 4 \*\*\*\*  
 \*\*\*\* (General Form Solutions) \*\*\*\*  
 \*\*\*\* Theta 1 is 90 Degree and theta 2 is 60 Degree \*\*\*\*

$$\text{Out}[49] = \left\{ \left( \sqrt{\frac{-b_1^4 + 2 b_1^2 q_1^2 - q_1^4 + 2 b_1^2 q_1^2 + 2 q_1^2 q_1^2 - q_1^4}{b_1^2 q_1^2}} \right) \right\}$$

$$> \sqrt{\frac{-b_2^4 + 2 b_2^2 q_2^2 - q_2^4 + 2 b_2^2 q_2^2 + 2 q_2^2 q_2^2 - q_2^4}{b_2^2 q_2^2}}$$

$$> \sqrt{\frac{-b_3^4 + 2 b_3^2 q_3^2 - q_3^4 + 2 b_3^2 q_3^2 + 2 q_3^2 q_3^2 - q_3^4}{b_3^2 q_3^2}}$$

$$> (2 \sqrt{3} b_2^2 - 2 \sqrt{3} q_2^2 + 2 \sqrt{3} q_2^2 + b_2 q_2 \sqrt{\dots})$$

$$> \frac{-b_2^4 + 2 b_2^2 q_2^2 - q_2^4 + 2 b_2^2 q_2^2 + 2 q_2^2 q_2^2 - q_2^4}{b_2^2 q_2^2}$$

$$> 6 \sqrt{2} b_2 s - 2 \sqrt{6} b_2 s$$

$$> (-3 b_3^2 + 3 q_3^2 - 3 q_3^2 + 3 \sqrt{2} b_3 s + 3 \sqrt{6} b_3 s - \sqrt{3} b_3 q_3 \sqrt{\dots})$$

$$> \frac{-b_3^4 + 2 b_3^2 q_3^2 - q_3^4 + 2 b_3^2 q_3^2 + 2 q_3^2 q_3^2 - q_3^4}{b_3^2 q_3^2}$$

$$> \text{Cos}[t_3] - 2 b_3 q_3 \sqrt{\dots}$$

$$> \frac{-b_3^4 + 2 b_3^2 q_3^2 - q_3^4 + 2 b_3^2 q_3^2 + 2 q_3^2 q_3^2 - q_3^4}{b_3^2 q_3^2}$$

$$> \text{Sin}[t_3] (2 b_1 q_1 \sqrt{\dots})$$

$$> \frac{-b_1^4 + 2 b_1^2 q_1^2 - q_1^4 + 2 b_1^2 q_1^2 + 2 q_1^2 q_1^2 - q_1^4}{b_1^2 q_1^2}$$



$$\begin{aligned} & \cos[t_3] + \sqrt{3} b_1 \sin[t_3] - \sqrt{3} q_1 \sin[t_3] + \\ & \sqrt{3} q_1^2 \sin[t_3] - 3 \sqrt{2} b_1 s \sin[t_3] - \\ & \sqrt{6} b_1 s \sin[t_3]) / (2048 b_1 b_2 b_3) - \\ & \sqrt{\frac{-b_1^4 + 2 b_1^2 q_1^2 - q_1^4 + 2 b_1^2 q_1^2 + 2 q_1^2 q_1^2 - q_1^4}{b_1^2 q_1^2}} \end{aligned}$$

$$\sqrt{\frac{-b_2^4 + 2 b_2^2 q_2^2 - q_2^4 + 2 b_2^2 q_2^2 + 2 q_2^2 q_2^2 - q_2^4}{b_2^2 q_2^2}}$$

$$\sqrt{\frac{-b_3^4 + 2 b_3^2 q_3^2 - q_3^4 + 2 b_3^2 q_3^2 + 2 q_3^2 q_3^2 - q_3^4}{b_3^2 q_3^2}}$$

$$(3 b_1^2 - 3 q_1^2 + 3 q_1^2 -$$

$$2 b_1 q_1 \sqrt{[$$

$$\frac{-b_1^4 + 2 b_1^2 q_1^2 - q_1^4 + 2 b_1^2 q_1^2 + 2 q_1^2 q_1^2 - q_1^4}{b_1^2 q_1^2}] -$$

$$3 \sqrt{2} b_1 s + 3 \sqrt{6} b_1 s)$$

$$\begin{aligned} & (\sqrt{3} b_3^2 - \sqrt{3} q_3^2 + \sqrt{3} q_3^2 + 3 \sqrt{2} b_3 s - \\ & \sqrt{6} b_3 s - b_3 q_3 \end{aligned}$$

$$\sqrt{\frac{-b_3^4 + 2 b_3^2 q_3^2 - q_3^4 + 2 b_3^2 q_3^2 + 2 q_3^2 q_3^2 - q_3^4}{b_3^2 q_3^2}}$$

$$\cos[t_3]) (2 \sqrt{3} b_2 q_2$$

$$\sqrt{\frac{-b_2^4 + 2 b_2^2 q_2^2 - q_2^4 + 2 b_2^2 q_2^2 + 2 q_2^2 q_2^2 - q_2^4}{b_2^2 q_2^2}}$$

$$\cos[t_3] - 2 \sqrt{3} b_2^2 \sin[t_3] + 2 \sqrt{3} q_2^2 \sin[t_3] -$$

$$2 \sqrt{3} q_2^2 \sin[t_3] +$$

$$b_2 q_2 \sqrt{[$$



\*\*\*\* (25) Output Results of Case 3 in Chapter 4 \*\*\*\*  
 \*\*\*\* (General Form Solutions) \*\*\*\*  
 \*\*\*\* Theta 1 is 90 Degree and theta 2 is 45 Degree \*\*\*\*

$$\begin{aligned}
 & \text{Out[49]} = \left\{ \left( \text{Sqrt} \left[ \frac{-b_1^4 + 2 b_1^2 q_1^2 - q_1^4 + 2 b_1^2 q_1^2 + 2 q_1^2 q_1^2 - q_1^4}{b_1^2 q_1^2} \right] \right) \right. \\
 & \text{Sqrt} \left[ \frac{-b_2^4 + 2 b_2^2 q_2^2 - q_2^4 + 2 b_2^2 q_2^2 + 2 q_2^2 q_2^2 - q_2^4}{b_2^2 q_2^2} \right] \\
 & \text{Sqrt} \left[ \frac{-b_3^4 + 2 b_3^2 q_3^2 - q_3^4 + 2 b_3^2 q_3^2 + 2 q_3^2 q_3^2 - q_3^4}{b_3^2 q_3^2} \right] \\
 & (2 \text{ Sqrt}[3] b_2^2 - 2 \text{ Sqrt}[3] q_2^2 + 2 \text{ Sqrt}[3] q_2^2 + \\
 & \text{Sqrt}[2] b_2 q_2 \text{ Sqrt} \left[ \frac{-b_2^4 + 2 b_2^2 q_2^2 - q_2^4 + 2 b_2^2 q_2^2 + 2 q_2^2 q_2^2 - q_2^4}{b_2^2 q_2^2} \right] - \\
 & 6 \text{ Sqrt}[2] b_2 s - 2 \text{ Sqrt}[6] b_2 s) \\
 & (- (\text{Sqrt}[6] b_3^2) + \text{Sqrt}[6] q_3^2 - \text{Sqrt}[6] q_3^2 + 6 b_3 s + \\
 & 2 \text{ Sqrt}[3] b_3 s - \text{Sqrt}[2] b_3 q_3 \\
 & \text{Sqrt} \left[ \frac{-b_3^4 + 2 b_3^2 q_3^2 - q_3^4 + 2 b_3^2 q_3^2 + 2 q_3^2 q_3^2 - q_3^4}{b_3^2 q_3^2} \right] \\
 & \text{Cos}[t_3] - 2 \text{ Sqrt}[2] b_3 q_3 \\
 & \text{Sqrt} \left[ \frac{-b_3^4 + 2 b_3^2 q_3^2 - q_3^4 + 2 b_3^2 q_3^2 + 2 q_3^2 q_3^2 - q_3^4}{b_3^2 q_3^2} \right] \\
 & \text{sin}[t_3]) (2 b_1 q_1 \text{ Sqrt} \left[ \frac{-b_1^4 + 2 b_1^2 q_1^2 - q_1^4 + 2 b_1^2 q_1^2 + 2 q_1^2 q_1^2 - q_1^4}{b_1^2 q_1^2} \right]
 \end{aligned}$$



$$\text{Cos}[t3] + \text{Sqrt}[3] b1 \text{ Sin}[t3] - \text{Sqrt}[3] qq1 \text{ Sin}[t3] +$$

$$\text{Sqrt}[3] q1^2 \text{ Sin}[t3] - 3 \text{Sqrt}[2] b1 s \text{ Sin}[t3] -$$

$$\text{Sqrt}[6] b1 s \text{ Sin}[t3]) / (2048 b1 b2 b3) -$$

$$\text{Sqrt}\left[\frac{-b1^4 + 2 b1^2 qq1^2 - qq1^4 + 2 b1^2 q1^2 + 2 qq1^2 q1^2 - q1^4}{b1^2 q1^2}\right]$$

$$\text{Sqrt}\left[\frac{-b2^4 + 2 b2^2 qq2^2 - qq2^4 + 2 b2^2 q2^2 + 2 qq2^2 q2^2 - q2^4}{b2^2 q2^2}\right]$$

$$\text{Sqrt}\left[\frac{-b3^4 + 2 b3^2 qq3^2 - qq3^4 + 2 b3^2 q3^2 + 2 qq3^2 q3^2 - q3^4}{b3^2 q3^2}\right]$$

$$(\text{Sqrt}[6] b1^2 - \text{Sqrt}[6] qq1^2 + \text{Sqrt}[6] q1^2 -$$

$$2 \text{Sqrt}[2] b1 q1 \text{Sqrt}[$$

$$\frac{-b1^4 + 2 b1^2 qq1^2 - qq1^4 + 2 b1^2 q1^2 + 2 qq1^2 q1^2 - q1^4}{b1^2 q1^2}] +$$

$$6 b1 s - 2 \text{Sqrt}[3] b1 s)$$

$$(\text{Sqrt}[3] b3^2 - \text{Sqrt}[3] qq3^2 + \text{Sqrt}[3] q3^2 + 3 \text{Sqrt}[2] b3 s -$$

$$\text{Sqrt}[6] b3 s - b3 q3$$

$$\text{Sqrt}\left[\frac{-b3^4 + 2 b3^2 qq3^2 - qq3^4 + 2 b3^2 q3^2 + 2 qq3^2 q3^2 - q3^4}{b3^2 q3^2}\right]$$

$$\text{Cos}[t3]) (2 \text{Sqrt}[2] b2 q2$$

$$\text{Sqrt}\left[\frac{-b2^4 + 2 b2^2 qq2^2 - qq2^4 + 2 b2^2 q2^2 + 2 qq2^2 q2^2 - q2^4}{b2^2 q2^2}\right]$$

$$\text{Cos}[t3] - 2 \text{Sqrt}[3] b2^2 \text{Sin}[t3] + 2 \text{Sqrt}[3] qq2^2 \text{Sin}[t3] -$$

$$2 \text{Sqrt}[3] q2^2 \text{Sin}[t3] +$$

$$\text{Sqrt}[2] b2 q2 \text{Sqrt}[$$



\*\*\*\* (26) Output Results of Case 4 in Chapter 4 \*\*\*\*  
 \*\*\*\* (General Form Solutions) \*\*\*\*  
 \*\*\*\* Theta 1 is 90 Degree and theta 2 is 15 Degree \*\*\*\*

$$\begin{aligned}
 & \text{Out}[49] = \left\{ \left( \text{Sqrt} \left[ \frac{-b_1^4 + 2 b_1^2 q_1^2 - q_1^4 + 2 b_1^2 q_1^2 + 2 q_1^2 q_1^2 - q_1^4}{b_1^2 q_1^2} \right] \right) \right. \\
 & > \left. \text{Sqrt} \left[ \frac{-b_2^4 + 2 b_2^2 q_2^2 - q_2^4 + 2 b_2^2 q_2^2 + 2 q_2^2 q_2^2 - q_2^4}{b_2^2 q_2^2} \right] \right. \\
 & > \left. \text{Sqrt} \left[ \frac{-b_3^4 + 2 b_3^2 q_3^2 - q_3^4 + 2 b_3^2 q_3^2 + 2 q_3^2 q_3^2 - q_3^4}{b_3^2 q_3^2} \right] \right. \\
 & > (4 \text{ Sqrt}[3] b_2^2 - 4 \text{ Sqrt}[3] q_2^2 + 4 \text{ Sqrt}[3] q_2^2 + \\
 & > \text{Sqrt}[2] b_2 q_2 \text{ Sqrt}[ \\
 & > \left. \frac{-b_2^4 + 2 b_2^2 q_2^2 - q_2^4 + 2 b_2^2 q_2^2 + 2 q_2^2 q_2^2 - q_2^4}{b_2^2 q_2^2} \right] + \\
 & > \text{Sqrt}[6] b_2 q_2 \text{ Sqrt}[ \\
 & > \left. \frac{-b_2^4 + 2 b_2^2 q_2^2 - q_2^4 + 2 b_2^2 q_2^2 + 2 q_2^2 q_2^2 - q_2^4}{b_2^2 q_2^2} \right] - \\
 & > 12 \text{ Sqrt}[2] b_2 s - 4 \text{ Sqrt}[6] b_2 s) \\
 & > (-3 \text{ Sqrt}[2] b_3^2 + \text{Sqrt}[6] b_3^2 + 3 \text{ Sqrt}[2] q_3^2 - \text{Sqrt}[6] q_3^2 - \\
 & > 3 \text{ Sqrt}[2] q_3^2 + \text{Sqrt}[6] q_3^2 + 4 \text{ Sqrt}[3] b_3 s + \\
 & > \text{Sqrt}[2] b_3 q_3 \text{ Sqrt}[ \\
 & > \left. \frac{-b_3^4 + 2 b_3^2 q_3^2 - q_3^4 + 2 b_3^2 q_3^2 + 2 q_3^2 q_3^2 - q_3^4}{b_3^2 q_3^2} \right] \\
 & > \text{Cos}[t_3] - \text{Sqrt}[6] b_3 q_3 \\
 & > \left. \text{Sqrt} \left[ \frac{-b_3^4 + 2 b_3^2 q_3^2 - q_3^4 + 2 b_3^2 q_3^2 + 2 q_3^2 q_3^2 - q_3^4}{b_3^2 q_3^2} \right] \right\}
 \end{aligned}$$



b3 q3

Cos[t3] - 2 Sqrt[2] b3 q3

$$\text{Sqrt}\left[\frac{-b_3^4 + 2 b_3^2 q_3^2 - q_3^4 + 2 b_3^2 q_3^2 + 2 q_3^2 q_3^2 - q_3^4}{b_3^2 q_3^2}\right]$$

Sin[t3] - 2 Sqrt[6] b3 q3

$$\text{Sqrt}\left[\frac{-b_3^4 + 2 b_3^2 q_3^2 - q_3^4 + 2 b_3^2 q_3^2 + 2 q_3^2 q_3^2 - q_3^4}{b_3^2 q_3^2}\right]$$

Sin[t3]) (2 b1 q1 Sqrt[

$$\frac{-b_1^4 + 2 b_1^2 q_1^2 - q_1^4 + 2 b_1^2 q_1^2 + 2 q_1^2 q_1^2 - q_1^4}{b_1^2 q_1^2}$$

Cos[t3] + Sqrt[3] b1 Sin[t3] - Sqrt[3] q1 Sin[t3] +

Sqrt[3] q1 Sin[t3] - 3 Sqrt[2] b1 s Sin[t3] -

Sqrt[6] b1 s Sin[t3])) / (8192 b1 b2 b3) +

$$\left(\text{Sqrt}\left[\frac{-b_1^4 + 2 b_1^2 q_1^2 - q_1^4 + 2 b_1^2 q_1^2 + 2 q_1^2 q_1^2 - q_1^4}{b_1^2 q_1^2}\right]\right)$$

$$\text{Sqrt}\left[\frac{-b_2^4 + 2 b_2^2 q_2^2 - q_2^4 + 2 b_2^2 q_2^2 + 2 q_2^2 q_2^2 - q_2^4}{b_2^2 q_2^2}\right]$$

$$\text{Sqrt}\left[\frac{-b_3^4 + 2 b_3^2 q_3^2 - q_3^4 + 2 b_3^2 q_3^2 + 2 q_3^2 q_3^2 - q_3^4}{b_3^2 q_3^2}\right]$$

(-3 Sqrt[2] b1 + Sqrt[6] b1 + 3 Sqrt[2] q1 - Sqrt[6] q1 -

3 Sqrt[2] q1 + Sqrt[6] q1 +

2 Sqrt[2] b1 q1 Sqrt[

$$\frac{-b_1^4 + 2 b_1^2 q_1^2 - q_1^4 + 2 b_1^2 q_1^2 + 2 q_1^2 q_1^2 - q_1^4}{b_1^2 q_1^2} +$$

b1 q1

2 Sqrt[6] b1 q1 Sqrt[

$$\frac{-b_1^4 + 2 b_1^2 q_1^2 - q_1^4 + 2 b_1^2 q_1^2 + 2 q_1^2 q_1^2 - q_1^4}{b_1^2 q_1^2}] +$$

12 b1 s - 8 Sqrt[3] b1 s)

$$(Sqrt[3] b_3^2 - Sqrt[3] q_3^2 + Sqrt[3] q_3^2 + 3 Sqrt[2] b_3 s - Sqrt[6] b_3 s - b_3 q_3$$

$$Sqrt[-\frac{-b_3^4 + 2 b_3^2 q_3^2 - q_3^4 + 2 b_3^2 q_3^2 + 2 q_3^2 q_3^2 - q_3^4}{b_3^2 q_3^2}])$$

Cos[t3]) (-2 Sqrt[2] b2 q2

$$Sqrt[-\frac{-b_2^4 + 2 b_2^2 q_2^2 - q_2^4 + 2 b_2^2 q_2^2 + 2 q_2^2 q_2^2 - q_2^4}{b_2^2 q_2^2}])$$

Cos[t3] + 2 Sqrt[6] b2 q2

$$Sqrt[-\frac{-b_2^4 + 2 b_2^2 q_2^2 - q_2^4 + 2 b_2^2 q_2^2 + 2 q_2^2 q_2^2 - q_2^4}{b_2^2 q_2^2}])$$

Cos[t3] - 4 Sqrt[3] b2 Sin[t3] + 4 Sqrt[3] q\_2^2 Sin[t3] -

4 Sqrt[3] q\_2^2 Sin[t3] +

Sqrt[2] b2 q2 Sqrt[

$$\frac{-b_2^4 + 2 b_2^2 q_2^2 - q_2^4 + 2 b_2^2 q_2^2 + 2 q_2^2 q_2^2 - q_2^4}{b_2^2 q_2^2}]$$

Sin[t3] + Sqrt[6] b2 q2

$$Sqrt[-\frac{-b_2^4 + 2 b_2^2 q_2^2 - q_2^4 + 2 b_2^2 q_2^2 + 2 q_2^2 q_2^2 - q_2^4}{b_2^2 q_2^2}])$$

Sin[t3] - 12 Sqrt[2] b2 s Sin[t3] + 4 Sqrt[6] b2 s Sin[t3])) /

(8192 b1 b2 b3)}}}





$$\text{Sqrt}\left[\frac{-b_3^4 + 2 b_3^2 q_3^2 - q_3^4 + 2 b_3^2 q_3^2 + 2 q_3^2 q_3^2 - q_3^4}{b_3^2 q_3^2}\right]$$

$$\text{Sin}[t_3] - 2 \text{Sqrt}[6] b_3 q_3$$

$$\text{Sqrt}\left[\frac{-b_3^4 + 2 b_3^2 q_3^2 - q_3^4 + 2 b_3^2 q_3^2 + 2 q_3^2 q_3^2 - q_3^4}{b_3^2 q_3^2}\right]$$

$$\text{Sin}[t_3]) (2 \text{Sqrt}[2] b_1 q_1$$

$$\text{Sqrt}\left[\frac{-b_1^4 + 2 b_1^2 q_1^2 - q_1^4 + 2 b_1^2 q_1^2 + 2 q_1^2 q_1^2 - q_1^4}{b_1^2 q_1^2}\right]$$

$$\text{Cos}[t_3] + 2 \text{Sqrt}[6] b_1 q_1$$

$$\text{Sqrt}\left[\frac{-b_1^4 + 2 b_1^2 q_1^2 - q_1^4 + 2 b_1^2 q_1^2 + 2 q_1^2 q_1^2 - q_1^4}{b_1^2 q_1^2}\right]$$

$$\text{Cos}[t_3] + 4 \text{Sqrt}[3] b_1^2 \text{Sin}[t_3] - 4 \text{Sqrt}[3] q_1^2 \text{Sin}[t_3] +$$

$$4 \text{Sqrt}[3] q_1^2 \text{Sin}[t_3] -$$

$$\text{Sqrt}[2] b_1 q_1 \text{Sqrt}[$$

$$\frac{-b_1^4 + 2 b_1^2 q_1^2 - q_1^4 + 2 b_1^2 q_1^2 + 2 q_1^2 q_1^2 - q_1^4}{b_1^2 q_1^2}$$

$$\text{Sin}[t_3] + \text{Sqrt}[6] b_1 q_1$$

$$\text{Sqrt}\left[\frac{-b_1^4 + 2 b_1^2 q_1^2 - q_1^4 + 2 b_1^2 q_1^2 + 2 q_1^2 q_1^2 - q_1^4}{b_1^2 q_1^2}\right]$$

$$\text{Sin}[t_3] - 12 \text{Sqrt}[2] b_1 s \text{Sin}[t_3] - 4 \text{Sqrt}[6] b_1 s \text{Sin}[t_3])) /$$

$$(32768 b_1 b_2 b_3) - (\text{Sqrt}[$$

$$\frac{-b_1^4 + 2 b_1^2 q_1^2 - q_1^4 + 2 b_1^2 q_1^2 + 2 q_1^2 q_1^2 - q_1^4}{b_1^2 q_1^2}$$

$$\text{Sqrt}\left[\frac{-b_2^4 + 2 b_2^2 q_2^2 - q_2^4 + 2 b_2^2 q_2^2 + 2 q_2^2 q_2^2 - q_2^4}{b_2^2 q_2^2}\right]$$

$$b_2^2 q_2^2$$

$$\text{Sqrt}\left[\frac{-b_3^4 + 2 b_3^2 q_3^2 - q_3^4 + 2 b_3^2 q_3^2 + 2 q_3^2 q_3^2 - q_3^4}{b_3^2 q_3^2}\right]$$

$$(3 \text{Sqrt}[2] b_1^2 + \text{Sqrt}[6] b_1^2 - 3 \text{Sqrt}[2] q_1^2 - \text{Sqrt}[6] q_1^2 + 3 \text{Sqrt}[2] q_1^2 + \text{Sqrt}[6] q_1^2 - 6 b_1 q_1 \text{Sqrt}[$$

$$\frac{-b_1^4 + 2 b_1^2 q_1^2 - q_1^4 + 2 b_1^2 q_1^2 + 2 q_1^2 q_1^2 - q_1^4}{b_1^2 q_1^2}] +$$

$$4 \text{Sqrt}[3] b_1 s) (3 \text{Sqrt}[2] b_3^2 + \text{Sqrt}[6] b_3^2 - 3 \text{Sqrt}[2] q_3^2 - \text{Sqrt}[6] q_3^2 + 3 \text{Sqrt}[2] q_3^2 + \text{Sqrt}[6] q_3^2 + 4 \text{Sqrt}[3] b_3 s - \text{Sqrt}[2] b_3 q_3 \text{Sqrt}[$$

$$\frac{-b_3^4 + 2 b_3^2 q_3^2 - q_3^4 + 2 b_3^2 q_3^2 + 2 q_3^2 q_3^2 - q_3^4}{b_3^2 q_3^2}]$$

$$\text{Cos}[t_3] - \text{Sqrt}[6] b_3 q_3$$

$$\text{Sqrt}\left[\frac{-b_3^4 + 2 b_3^2 q_3^2 - q_3^4 + 2 b_3^2 q_3^2 + 2 q_3^2 q_3^2 - q_3^4}{b_3^2 q_3^2}\right]$$

$$\text{Cos}[t_3] + 2 \text{Sqrt}[2] b_3 q_3$$

$$\text{Sqrt}\left[\frac{-b_3^4 + 2 b_3^2 q_3^2 - q_3^4 + 2 b_3^2 q_3^2 + 2 q_3^2 q_3^2 - q_3^4}{b_3^2 q_3^2}\right]$$

$$\text{Sin}[t_3] - 2 \text{Sqrt}[6] b_3 q_3$$

$$\text{Sqrt}\left[\frac{-b_3^4 + 2 b_3^2 q_3^2 - q_3^4 + 2 b_3^2 q_3^2 + 2 q_3^2 q_3^2 - q_3^4}{b_3^2 q_3^2}\right]$$

$$\text{Sin}[t_3]) (2 \text{Sqrt}[2] b_2 q_2$$

$$b_2^2 q_2^2$$

$$\text{Sqrt}\left[\frac{-b^2 + 2 b^2 q q^2 - q q^2 + 2 b^2 q^2 + 2 q q^2 q^2 - q^2}{b^2 q^2}\right]$$

$$\text{Cos}[t_3] + 2 \text{Sqrt}[6] b^2 q^2$$

$$\text{Sqrt}\left[\frac{-b^4 + 2 b^2 q q^2 - q q^2 + 2 b^2 q^2 + 2 q q^2 q^2 - q^4}{b^2 q^2}\right]$$

$$\text{Cos}[t_3] - 4 \text{Sqrt}[3] b^2 \text{Sin}[t_3] + 4 \text{Sqrt}[3] q q^2 \text{Sin}[t_3] -$$

$$4 \text{Sqrt}[3] q^2 \text{Sin}[t_3] -$$

$$\text{Sqrt}[2] b^2 q^2 \text{Sqrt}[$$

$$\frac{-b^4 + 2 b^2 q q^2 - q q^2 + 2 b^2 q^2 + 2 q q^2 q^2 - q^4}{b^2 q^2}]$$

$$\text{Sin}[t_3] + \text{Sqrt}[6] b^2 q^2$$

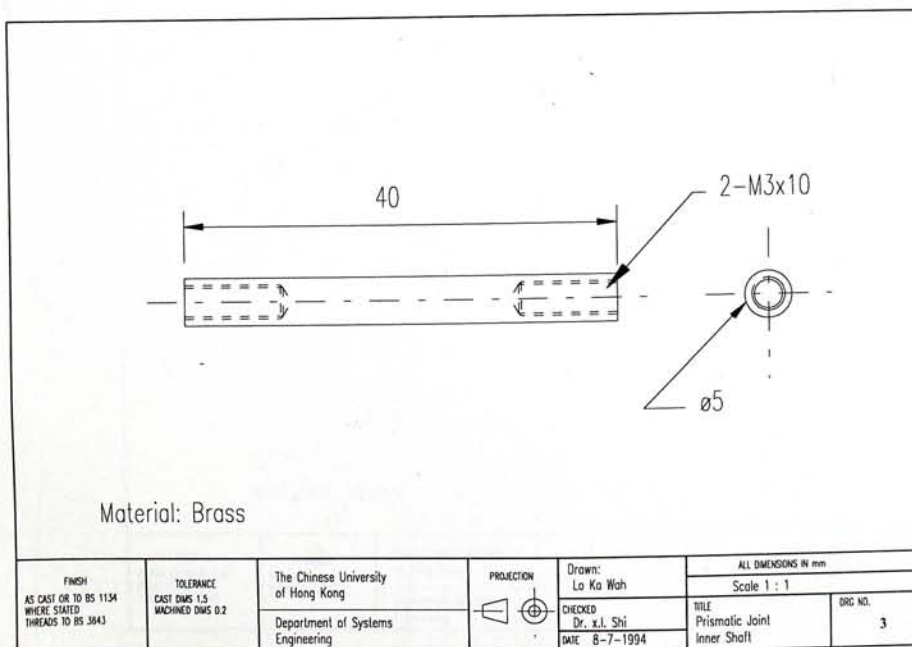
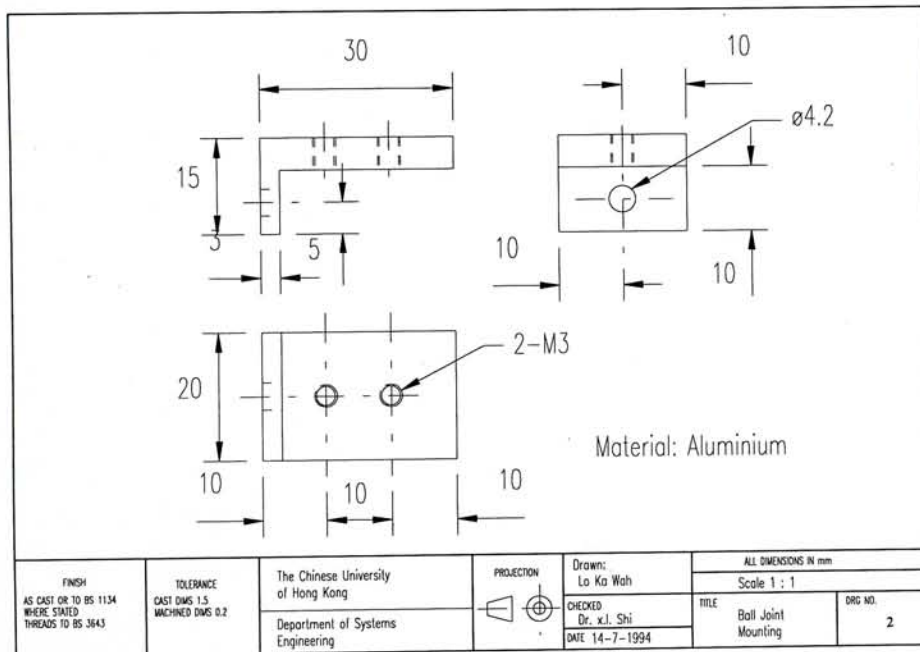
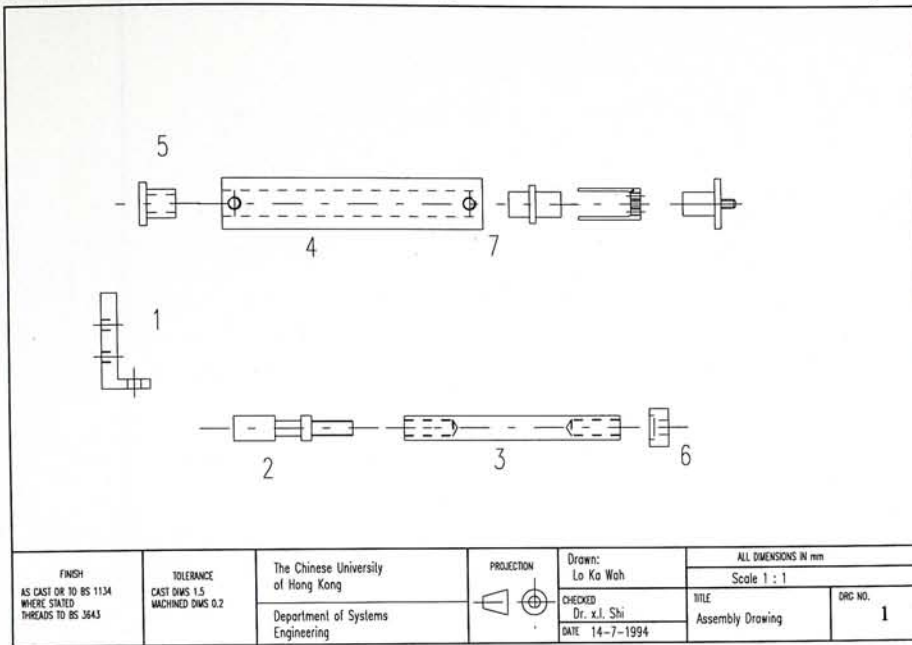
$$\text{Sqrt}\left[\frac{-b^4 + 2 b^2 q q^2 - q q^2 + 2 b^2 q^2 + 2 q q^2 q^2 - q^4}{b^2 q^2}\right]$$

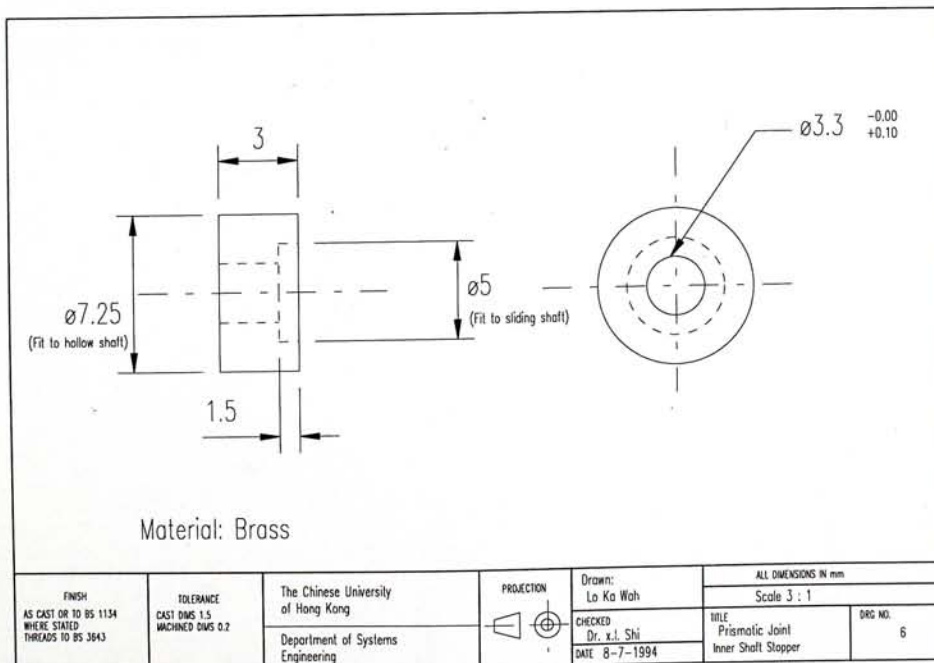
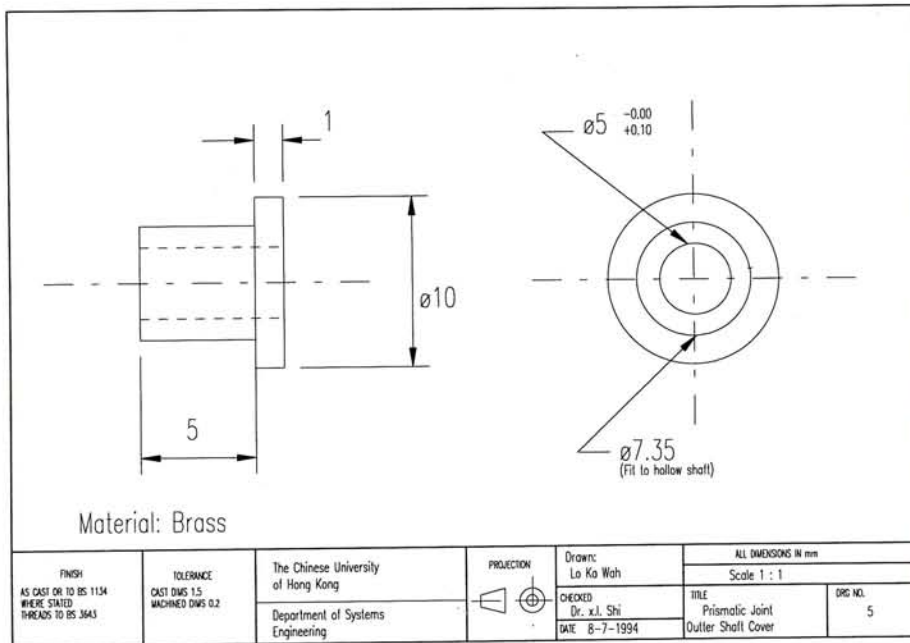
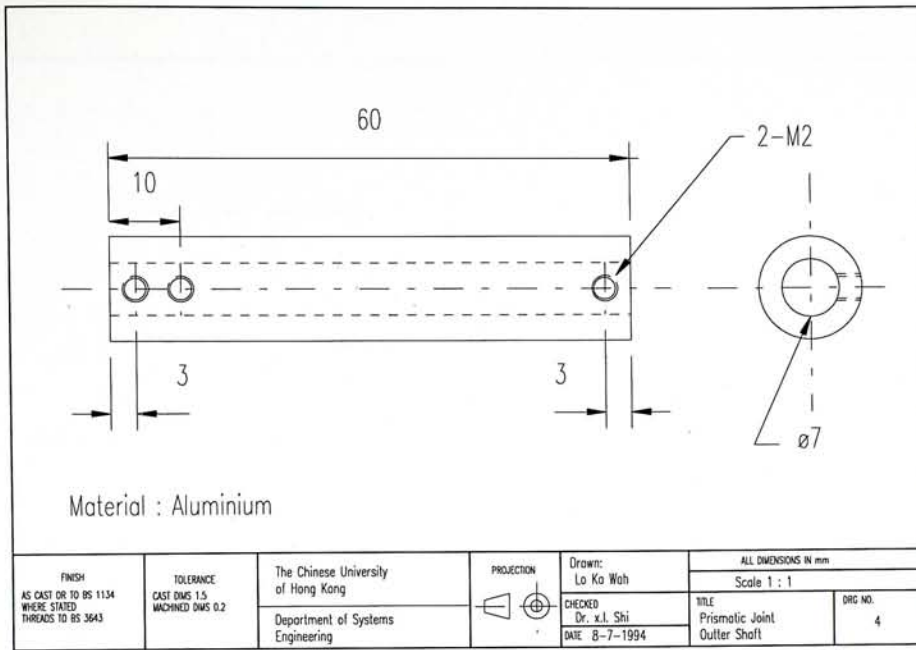
$$\text{Sin}[t_3] - 12 \text{Sqrt}[2] b^2 s \text{Sin}[t_3] + 4 \text{Sqrt}[6] b^2 s \text{Sin}[t_3])) /$$

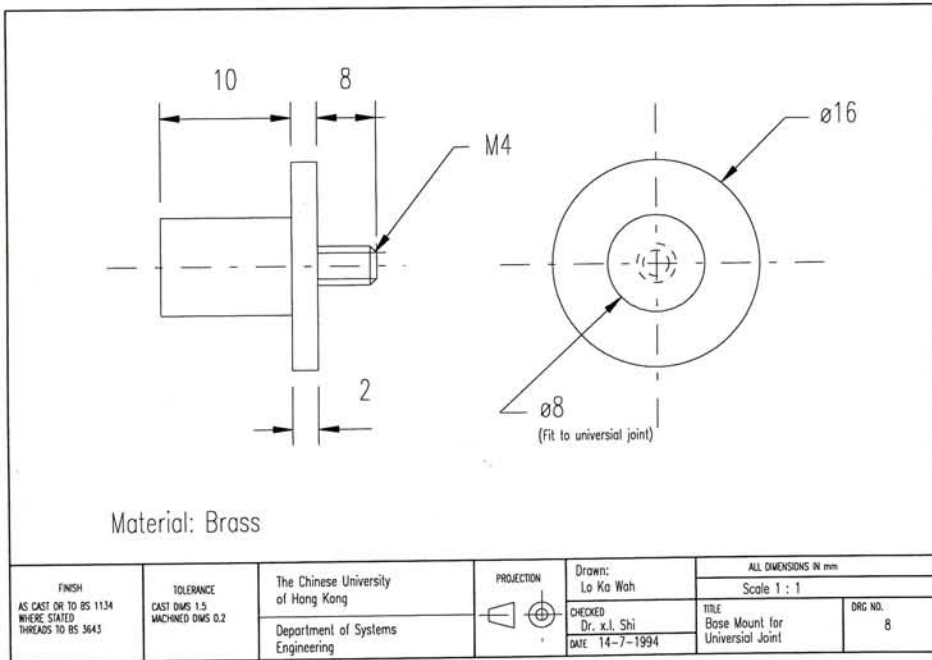
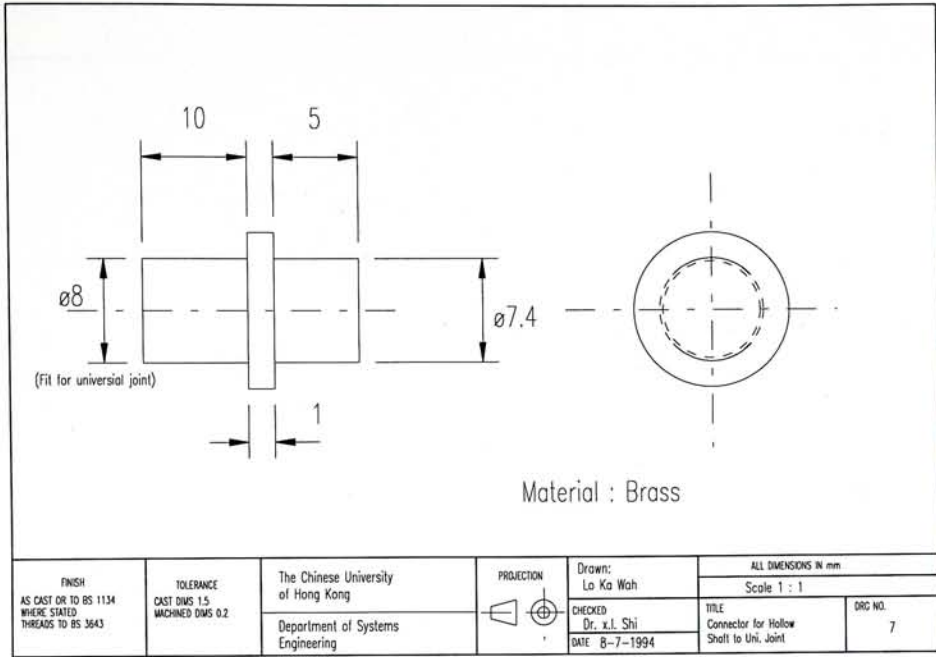
(32768 b1 b2 b3)}}}



## (28) Components Drawing of the Mechanical Model (Stewart Platform)













CUHK Libraries



000733956